NOTE TO USERS

Page(s) not included in the original manuscript and are
unavailable from the author or university. The manuscript
was scanned as received.

pp. 63, 131

This reproduction is the best copy available.

UMI®

University of Alberta

Argon Laser versus Conventional Visible Light cured Orthodontic Bracket Bonding:
An *in vivo* and *in vitro* Study

by

Dr. Nadja K.S Hildebrand

A thesis submitted to the Faculty of Graduate Studies and Research in partial

fulfillment of requirements for the degree of Master of Science in

Orthodontics

Department of Dentistry

Edmonton, Alberta

Spring 2004

Canadä

Abstract

Many advantages of using argon laser have been reported, including reduction of enamel demineralization. The purpose of the study was to compare the bond strength after curing with the argon laser versus the conventional curing light *in vivo* and *in vitro*, and to investigate the effect of argon laser irradiation on the enamel surface.

Four premolars from forty-eight volunteers were randomly assigned to either the argon laser or the conventional light group. *In vivo* and *in vitro* bond strengths were measured using custom designed debonding pliers. No significant differences were found in bond strength according to curing method, dental arch or gender. *In vivo* results were significantly lower ($P > 0.001$) than *in vitro* results.

Three different surface scans (XPS, AFM, Nanoindentation) of argon laser irradiated enamel and control, showed no major changes in the chemical composition, a significant increase in hardness ($P > 0.001$), and decrease in roughness of the enamel surface.

Acknowledgement

My sincere appreciation and gratitude to the following individuals:

Dr. Daron Stevens, my classmate, for his flexibility and unconditional support without whom the consistency in the debonding procedure could not have been accomplished.

Dr. Paul Major, my supervisor, for his immediate responses, guidance and faith.

Dr. Alan Nelson for his support in investigating the surface changes on the enamel surface.

Dr. Don Raboud for his assistance in inventing the in vivo debonding pliers.

Dr. Giseon Heo for her time and effort while helping to analyze the statistical data.

Mr. Anthony Noronah and Bob Gleich, our 3M Unitek representatives, for the generous supply of materials.

My fellow classmates, orthodontic graduate clinic staff, and our instructors who assisted in patient recruitment and the conduction of the *in vivo* study.

The oral surgery department, especially Dr. Saranjeev Lalh and Jacylyn Dietz, for providing the environment for the second half of the *in vivo* part.

The mechanical engineering department, in particular Berni, for loaning the necessary measuring devices, and for their flexibility in time over the last 12 months.

To my parents for offering their long-lasting support, their constant encouragement, and unrestricted love. Thank you for understanding why we moved far away from home and why we chose this path of life.

And last but for sure not least, my lovely husband and best friend Chris, for his emotional and financial support, for his understanding, for being extremely patient throughout the last couple of years, and for cheering me up in stressful times.

Table of Contents

Table of Contents (continued)

Table of Contents (continued)

Table of Contents (continued)

Table of Contents (continued)

Table of Contents (continued)

Table of Contents (continued)

Table of Contents (continued)

Table of Contents (continued)

Table of Contents (continued)

List of Figures

List of Figures (continued)

List of Tables

List of Tables (continued)

List of Nomenclature

Absorption: The incorporation of the laser energy by the intended target tissue. This effect is the usual desirable effect, and the amount of energy that is absorbed by the tissue depends on the tissue characteristics, such as pigmentation and water content, and on the laser wavelength and emission mode. Certain wavelengths are preferentially absorbed by certain tissue components and by water.

Auger effect: A sample bombarded by electrons or x-rays will eject core electrons from a level in atoms in a region of the sample up to 1 μm deep. The core hole is then filled by an internal process in the atom whereby an electron from an other level falls into the core hole with the energy balance taken by a **third electron** from a third level. This last electron, called an **Auger electron** after **Pierre Auger** is then ejected from the atom.

Birefingence: The resolution or splitting of a light wave into two unequally reflected or transmitted waves by an optically anisotropic medium such as calcite or quartz, also referred to as double refraction.

Coherency: A property unique to lasers. The light waves produced by a laser are a specific form of electromagnetic energy. A laser produces light waves that are physically identical. They are all in phase with one another and have identical amplitude, that is, all the peaks and valleys are same size.

Collimation: Refers to the beam having specific spatial boundaries. These boundaries insure that there is a constant beam size and shape that is emitted from the laser cavity. An X-ray beam has the identical property.

Fluence: The energy incident on a surface expressed in Joules per centimeter squared (Joules/cm²) = energy density. To calculate the energy density (J/cm²), the output of the curing source (in mW/cm²) and the duration of the exposure (in seconds) are used.

$$\text{Energy density} = (\text{Watts x seconds}) / cm^2 = \text{Joules} / cm^2 = J / cm^2$$

Monochromatic: In contrast to ordinary light produced by a table lamp, laser produce a monochromatic not a polychromatic light. It only has one specific wavelength.

Chapter One

Introduction

And

Literature Review

1.1.Introduction

Direct bonding of orthodontic attachments has become a routine clinical procedure. *Newman (1965)*[1] introduced the concept of using epoxy resin and the acid-etch technique to bond orthodontic attachments directly to teeth. Bonded orthodontic brackets have advantages over bands in that they have no inter-proximal contact, are both easier to place and to remove, are more esthetic, hygienic and less irritating to the gingiva.[2] However, the use of composite resins as the bonding medium in orthodontics has disadvantages. Enamel can be lost during the debonding procedures as well as during the cleanup process of residual resin removal. This is of clinical significance since the concentration of fluoride is greatest at the surface of the enamel.[3] The bond strength of adhesive and attachments should be sufficient to withstand the forces of mastication, the stresses exerted by the archwires, and patient abuse as well as allow for control of tooth movement in all 3 planes of space. At the same time, the bond strength should be low enough to allow for bracket debonding without causing damage to the enamel surface. Various studies have suggested bond strengths ranging from 2.8 MPa to 10 MPa as being adequate for clinical situations.[4][5]

Today's orthodontic practices are focusing on efficiency. Time saving during the bonding procedure and ideally no bond failures during treatment, are part of an effective plan. Multiple high speed curing lights (Xenon Plasma Arc, LED, high-speed Halogen Curing Light, Argon Laser), which can save the operator minutes of valuable time per initial bonding, were introduced in the last couple of years. Compared to the conventional curing light, the argon laser seems to be the only curing light which results in less curing time, similar or better bond strength and decalcification protection to a certain degree.

2

Enamel decalcification is a significant problem in orthodontics due to poor oral hygiene and lack of patient compliance. In previous studies, the percentage of patients who experience some degree of white spot formation during orthodontic treatment ranged from 49.6% to 64%.[6][7][8] Orthodontic brackets bonded to the surface of the enamel trap plaque around the bracket bases, allowing bacterial acids long periods of time to dissolve the inorganic portion of the enamel. Several studies have found an increased amount of plaques around orthodontic appliances [9][10] and an increase in the number of *Streptococcus mutans* and *Lactobacillus* species in the oral cavity following the placement of fixed orthodontic appliances.[9] Higher concentrations of these bacteria produce more organic acids, which cause the dissolution of calcium and phosphate ions from the enamel surface and therefore an increased risk of decalcification. As the enamel loses its mineral content, it appears chalky white, which is esthetically displeasing and may eventually progress to caries lesions.

An interesting application of the argon laser in orthodontics involves its ability to alter enamel, rendering it less susceptible to demineralization.[11][12][13] As early as 1965, investigators showed that exposure of enamel to laser irradiation imparts some degree of protection against demineralization under acid attack.[14] Argon laser irradiation of enamel reduces the amount of demineralization by 30–50% [15][16][17] and reduces, by about a factor of five, the threshold pH at which dissolution occurs.[18] In addition, argon laser treatment at low fluences alters the surface morphology considerably while maintaining an intact enamel surface.[19] A number of studies have also shown that combining laser irradiation with fluoride treatment can have a synergistic effect on acid resistance.[20][21][22][23][24]

In summary, lasing the enamel surface at the time of bracket placement may not

3

just significantly reduce the prevalence of decalcification associated with poor oral hygiene during orthodontic treatment but may also cure composite resins used in bonding orthodontic appliances faster [25] [26] and with enhanced physical properties.[27]

The objective of the present study was to compare the bond strength of orthodontic brackets cured with the argon laser compared to the conventional curing light *in vitro* and *in vivo*. Custom debonding pliers connected to a strain gauge were used to measure the bond strength *in vivo* and *in vitro* with the same appliance to allow for direct comparison. The hypothesis is that bond strengths following argon laser curing (10s) are comparable to bond strength with the conventional light (40s). In addition enamel surface scan were performed to find evidence and further insight regarding the potential protective effect against demineralization resulting from argon laser irradiation.

1.2 Literature Review

1.2.1 Laser

The word LASER is an acronym for Light Amplification by Stimulated Emission of Radiation. Dental lasers are named for the chemical elements, molecules or compounds that comprise the core, or active medium, that is stimulated. This active medium can be a container of gas, a solid crystal rod, or a solid state electronic device. Since the development of the ruby laser by *Maiman* in 1960, there has been great interest among dental practitioners, scientists, and patients to use this tool to make dental treatment more pleasant. The first lasers approved for dental uses procedures involved soft tissue surgery and procedures including gingivectomy, frenectomy, curettage, crown lengthening, biopsy, and other gingival procedures. These lasers included the carbon dioxide lasers,

4

Nd:YAG, argon lasers, and diode lasers. Today the argon laser has been FDA cleared for curing of commonly used tooth colored fillings in the mouth and bleaching.

1.2.2 Curing Devices

1.2.2.1 Differences in Curing Devices

The Argon Laser (AL) was invented in 1964 by William Bridges. The active medium in the AL is a gas of excited ions. A high voltage discharger (8kV) activates the argon gas, resulting in a reduction in voltage. The electric discharge is created in a narrow tube filled with gaseous argon. The argon atoms are first ionized and then excited into their upper energy levels by multiple collisions with electrons. Because of the existence of closely spaced upper levels, several laser transitions occur simultaneously in the blue and green region of the spectrum. The emission spectrum consists of a number of sharp emission lines, with those at 488 nm (blue) and 514 nm (green) being the most intense. The 488 nm spectrum presents the ideal wavelength to activate camphorquinone, the activator of most light-cured adhesives.[27]The 514 nm line is filtered out for dental purposes. Due to the high energy required to ionize and excite the argon atoms, very high current densities are needed in the order of 1 A mm^{-2}. A magnetic field surrounds the laser tube to help constrict the gas discharge and keep the current density high. This longitudinal field increases the electron density in the plasma by constraining the electrons to move in a helical path around the field lines. This prevents loss of electrons to the walls. The discharge tube is normally made of a material with a low thermal conductivity such as berrylium oxide, graphite or a metal-ceramic tube construction. To keep operating temperatures low, metal discs are inserted inside the tube to act as heat exchangers. A laser produces a monochromatic, collimated and coherent beam of light

5

energy.

The Conventional (quartz halogen-tungsten) Curing Light (CCL) has a broad emission spectrum, which is that of the incandescent tungsten filament. It is a band spectrum containing UV radiation and heat. Only a small portion of this band can be absorbed by the initiator/accelerator of light-cured adhesives (camphorquinone).[27] These unwanted frequencies are not useful for polymerization and must be filtered out. Thus, only a proportion of the total output of the lamp is useful for curing. The heat component is frequently removed by reflection from a paraboloid dichroic filter (cold mirror), which preferentially absorbs heat. This device may be integral with the bulb. Further filtration occurs via the removal of the UV component by glass and, often a blue filter is included to remove non-curing visible wavelength. The light is then transmitted through a suitable guiding device to the irradiation tip.

Although CCL are most commonly used to cure dental composites, this technology has inherent drawbacks. Halogen bulbs have a limited effective lifetime of around 50 hours. The bulb, reflector and filter degrade over time due to the high temperatures produced, leading to a reduction in light output. The result is a reduction of the CCLs effectiveness to cure dental composites. The clinical implication of this for the dentist is a negative effect on the physical properties of composites with an increased risk of premature failure of restorations. *Martin*[28] has shown that many CCLs used by dental practitioners do not produce their optimum power output. A reduced output of CCLs is due to a lack of maintenance, such as changing the filter and/or the halogen bulb from time to time, and checking the CCLs irradiance. The lower effective limit of irradiance for halogen technology based CCLs used in dental practice has been suggested to be 300

6

mW/cm^2. Some halogen CCLs available presently exceed an irradiance of 1000 mW/cm^2.[29]

Recently, the Xenon Plasma Arc (XPAC) curing system has been introduced for use in dentistry. XPAC has a light intensity of 1650 mW/cm^2. This XPAC is filtered to provide an intense light focus at a wavelength of 470 nm to activate the initiator/activator (camphorquinone).[30] A high energy, high pressure ionized gas in the presence of an electric current is used to create a light source strong enough to increase the curing rate of dental adhesives.[30] Filters narrow the spectrum of visible light to a band centered on the 470 nm wavelength. Plasma is sometimes described as the "fourth state of matter", together with solid, liquid, and gas. If a high voltage discharge is passed between two electrodes in plasma, the plasma emits a band spectrum, which is dependant on the specimen involved and on the temperature of the plasma

The blue Light Emitting Diode (LED) curing lights based on gallium nitride technology were developed in 1995. The spectral output falls mainly within the absorption spectrum of the camphorquinone of most dental composites (95% between 400 and 500 nm) with a peak wavelength of 470 nm.[29] LEDs do not require a fan due to its minimal heat generation during operation. In addition the LED requires less than 10 percent of the electrical power consumed by CCL. Because LED light is fully utilized in the polymerization process, it is an extremely efficient form of curing.

1.2.2.2 Comparison of Curing Devices

Theoretically, the AL should be more efficient than a CCL source for the photoinitiation of resin polymerization, because a greater proportion of its wavelengths are selectively absorbed by camphorquinone.[31] Because AL emits light over a narrow

7

band of wavelengths in the blue green spectrum (457.9 to 514.5 nm), it is ideally suited to polymerize composite resins.[25] Although CCL curing units also emit energy centered around 480 nm, the energy is emitted over a much broader range. Furthermore, the power density of light reaching the composite from a CCL decreases dramatically over distance, due to divergence of light from the source. Light from the AL is collimated, resulting in more consistent power density over distance.[32]The collimated beam of the AL is a factor that might contribute to its efficiency by producing higher peak intensity than the divergent and attenuated light from the CCL. [33] Another interesting point is that CCL bulbs, reflector and filters degrade frequently and decrease curing efficiency.[34]The reduction in polymerization times provided by AL compared to the CCL might prove beneficial in reducing chair-side time and achieving patient satisfaction, especially with restless children. It could also be helpful in situations where maintenance of a dry field is difficult.[35] In addition, the 0.5 mm-diameter fiber optic tip of the laser is easy to manipulate and provides ready access to posterior teeth (second molar bonds). This aspect is based on the size of the hand-piece and fiber-optic tip.[36] The fiber-optic cable delivers the coherent, collimated beam of the laser light to the target tissue in a manner that is both ergonomic and precise. The glass fiber optic cable is usually small in diameter, with sizes ranging from 200 to 600 microns. Although the glass fiber is encased in a resilient sheath, it can be somewhat fragile and cannot be bent into a sharp angle. The fiber fits snugly into a handpiece with either the bare end protruding or in some cases with an attached glass-like tip. This fiber system can be used in either contact or non-contact mode. Finally, AL cured brackets showed less than half the frequency of enamel fracture during the debonding procedure.[26] *Retief*[37] demonstrated enamel fractures on *in*

8

vitro CCL cured specimens with bond strengths as low as 9.7 MPa. All these factors might contribute to the increased efficiency of AL curing of composite resin compared with the CCL.[25]

Several *in vitro* studies have tested the physical properties of resin composites activated using different light-curing units. *Kelsey et al.*[27] and *Blankenau et al.*[32] concluded that polymerization of composite resin with an AL results in physical properties superior to those cured using a conventional CCL. Recently, *James et al.*[38] summarized that the XPAC (5s) produced shear peel bond strength that is comparable with or greater than that produced by the CCL (40s) or the AL (10s) depending on the adhesive used (APC or Transbond). *Cobb et al.*[31], *Eldiwany et al.*[39], *Vargas et al.*[40], and *Peutzfeldt et al.*[41] report no significant differences in physical properties such as diametral tensile strength, compressive strength, flexural strength, and hardness, regardless of the light source used. *Kurchak et al.*[36] and *Lalani et al.*[26] demonstrated that 5 to 10 seconds of curing with the AL produces bond strengths comparable to those achieved with 20 to 40 seconds of curing with a CCL. *Eldiwany et al.*[39], *Burgess et al.*[42], and *Peutzfeldt et al.*[41] state inconsistent values for properties such as flexural modulus and hardness when an AL or a XPAC curing light is used.

The LED is advocated as a promising light cure unit and it has been compared with the CCL by several authors. *Mills et al.*[29] presented results that demonstrate the capability of LED to cure in a significantly greater depth for three different types of composite than a CCL. *Jandt et al.*[43] found that the compressive strengths of dental composites cured under laboratory conditions with a LED were not statistically different to those cured with a CCL with its inherent advantages, such as a constant power output

9

over the lifetime of the diodes. *Dunn et al.*[44] demonstrated inferior performance of the LED compared with the CCL in term of composite hardness after curing. The specimens were indented on their top and bottom surfaces with a Knoop hardness tester and measured for hardness. Bottom : top hardness ratios determined the percentage of cure. The superior performance of the CCL was significant (P < .0001), regardless of composite type, with the two CCLs producing harder top and bottom composite surfaces than the two LEDs. They came to the conclusion, that the light output of commercially available diodes for resin-based composite polymerization still requires improvement to rival the adequacy of cure of CCLs. LED curing seems to be 2 - 3 times more efficient than CCL, and more than 10 times more energy efficient, since no cooling fan is needed. A CCL unit of the same output intensity unit will perform at a lower level than an LED curing unit. This means that an LED curing light with an intensity of 350 mW/cm^2 is as effective as a 700-1050 mW/cm^2 halogen light.[29] To the author's knowledge, there is no comparative study between the AL and LED to date.

In general, from the results of the studies found in the literature, there is no clear consensus regarding the effects of high-intensity lights on the mechanical properties of resin composites. *St-Georges et al.*[45] examined a potential problem with high-intensity lights, that is, that the polymer chains might fail to grow and cross-link in a desired fashion, thereby affecting the structure and properties of the polymers formed. The purpose of their study was to evaluate mechanical properties of resin composites polymerized using four different light-curing units (CCL, AL, XPAC and a 'soft start' CCL). Part of their conclusion was that AL, which has the second shortest curing time with the second highest power density, produced an energy density (9–11 J/cm^2) lower

10

than the 'soft-start' (19 J/cm^2) and the CCL (22 J/cm^2) units. However, the results show that the AL produced higher mean bond strength values.[45]

In summary, the argon laser seems to perform *in vitro* as well as the other high-intensity lights in terms of the faster curing time and adequate bond strength. *In vivo* testing must be performed ultimately to determine if clinically significant differences exist between the different lights and polymerization methods.[45]

1.2.3 Demineralization Prevention

Demineralization around orthodontic appliances is a problem. Suboptimal oral hygiene, long intervals between appointments and potentially poor patient cooperation with using fluoride dentifrices and mouth rinses necessitate a compliance-free means of preventing tooth decay.[46] The AL is the only curing light which seems to have the potential to reduce or even prevent demineralization. Early studies with the AL were focused on prevention of dental caries. *Goodman et al.*[21] found that AL radiation in combination with NaF treatment markedly reduces the rate of dissolution of tooth enamel in acid when compared with the effects of NaF alone. Subsequently other investigators have shown that exposing enamel to laser irradiation imparts some degree of protection against demineralization under acid attack. *Yamamoto et al.*[47] for example, embedded small pieces of lased enamel into human dentures. After 8 months, the non-lased area of the enamel showed a chalk white lesion, whereas no noticeable change was observed in the lased area. More recently, *Hicks et al.*[48] have shown that AL irradiation of enamel reduces the susceptibility of enamel to demineralization by up to 50%.

Westerman et al.[49] realized that AL treatment at low energy could considerably alter surface morphology while maintaining an intact enamel surface. The purpose of his

11

study was to determine the effect of low fluence AL irradiation delivered from two different AL systems on enamel caries-like lesion initiation and progression. Twenty extracted human molars were selected, and 10 teeth were assigned to the first AL group (Model 8, HGM, Salt Lake City, UT) and 10 were assigned to the second AL group (AccuCure 3000, Lasermed, Salt Lake City, UT). The exposed buccal windows of sound enamel were exposed to low fluence irradiation, while the lingual windows of enamel were not exposed to laser irradiation and served as the no-treatment (control) group. Enamel caries-like lesions were created using an acidified gel. Two longitudinal sections were taken per sample (n = 20 lesions per group) and evaluated by polarized light microscopy for body of the lesion depths after lesion initiation (8 weeks) and progression (12 weeks) periods. After lesion initiation and progression, the body of lesion depths was similar for both AL-irradiated groups ($p > 0.05$). With the no-treatment (control) group, there were significant increases in lesion depth with a 61-78% increase for the lesion initiation period and a 50-69% increase for the lesion progression period when compared with the AL-treated groups. The authors concluded that AL irradiation provides a certain degree of protection against *in vitro* enamel caries initiation and progression and that it may prove to be beneficial in reducing the caries susceptibility of sound enamel and white spot lesions in the clinical environment.[49] Another *in vitro* study by *Hicks et al.*[22] came to the same conclusion. The latter proposed that the most likely mechanism would be alteration in the pore structure of lased enamel with entrapment and re-precipitation of mineral phases released during demineralization.

Talbot et al.[25] applied these principles to orthodontics. The authors lased enamel before bracket placement and did not find any significant effect on bond strength. It is not

12

known however, whether the acid-etch procedure obliterates all micro-structural changes in the enamel imparted by laser treatment. It might be that the laser does impart some structural changes to the enamel surfaces, but that these changes are eliminated by the acid-etch procedure. If this were the case, any demineralization resistance imparted to the enamel by the laser would also be eliminated. Another possibility is that laser treatment alters the enamel surface, but not by any amount sufficient to affect bond strength, regardless whether the acid-etch procedure obliterates these surface changes. If not completely countered by acid-etching, the effect of laser treatment might still impart some degree of demineralization resistance without affecting bond strength. Therefore the authors concluded that laser irradiation has promising potential in that it might reduce the enamel decalcification that is often seen during fixed appliance treatment. An AL could be substituted for the CCL during bracket placement. The adjacent enamel would be simultaneously irradiated, which might confer demineralization resistance.

A recent study by *Monseau Anderson et al.*[50] investigated the *in vivo* effect of AL irradiation on enamel decalcification during orthodontic treatment. A specially designed orthodontic band with a wide (1.5 mm) buccal "gap" to create a pocket for plaque and therefore demineralization was placed on premolars to be extracted of 9 volunteers (n=36). The results showed that AL irradiation is effective in reducing enamel decalcification during orthodontic treatment.

1.2.4 Surface Scan Methods

It is not yet completely understood how and why AL converts the enamel into a surface which is less prone to demineralization. To get a better understanding it is necessary to examine the enamel surface more closely.

13

<u>1.2.4.1 Scanning electron microscopy (SEM)</u>

Scanning electron microscopy (SEM) has been the traditional method for studying the microscopic "surface structure" of tooth tissues such as enamel. While allowing visualization and chemical analysis of the specimen, SEM is not a surface-specific technique in the strictest sense. Imaging is generally achieved by detection of either the electrons, which are backscattered from the sample, or the secondary electrons generated on impaction of the primary beam with the specimen. The detected beam thus has two components: one of high resolution originating from a shallow sampling depth, and one of low resolution which retains the lateral and the depth characteristics of the backscattered electrons. Consequently, neither mechanism gives images that are solely representative of the surface structure.

Westerman et al. [19] used the SEM surface scanning method to compare the effects of AL irradiation at relatively low fluences (11.5 Joules/cm² and 100 Joules/cm²) on enamel surface morphology. Enamel surface morphology was compared among the two AL irradiation groups and matched non-treated control enamel surfaces. AL treatment resulted in considerable alterations in the surface morphology compared with matched controls. Control enamel surfaces showed relatively smooth contours with occasional termination of enamel prisms at the surface. Both AL treatment groups had intact enamel surfaces lacking prism end markings and cratering of the enamel surface. Surface coatings composed of a confluence of globular material of 0.5 to 2 μm in diameter and microporosities of less than 1μm (considerable smaller than with acid etching) were present with the low fluence (11.5 J/cm²) AL irradiation.

In contrast, *El-Din et al.*[51] examined thirty-two human posterior teeth in their

14

study to investigate the effect of pulsed AL of different densities (40 J/cm², 50 J/cm², 60 J/cm²) on the surface topography of human enamel. The SEM results showed apparent alterations on the surface topography of both tissues. Increasing the energy density from 40 to 60 J/cm² showed worse, destructive changes. The present study used an energy density of 2.5 and 15 J/cm², therefore "destructive" changes with these low fluence energies are unlikely.

Palamara et al.[52] examined the effect on the surface of enamel with AL and other lasers. The authors recorded that AL irradiation produced a changed non-cratered surface with inter-crystalline porosity and a mixture of small and some large irregularly packed recrystallized enamel crystals. *Westerman et al.*[53] described their SEM results on sound human root surfaces as follows: "AL irradiation (11.5 J/cm²) alone produced irregular textured surfaces with adherent globular material and fine microporosities in the background".

Featherstone et al.[54] reviewed further SEM studies to investigate subsurface demineralization of dental enamel. The authors came to the conclusion that lasing conditions can be chosen so that they produce surface fusion of the apatite which inhibits caries-like lesion progression. SEM examination of crystals formed on and in enamel during high concentration fluoride treatments implies in their opinion that calcium fluoride-like crystals are formed which may act as a slow-release fluoride reservoir in the mouth.

1.2.4.2 X-ray photoelectron spectroscopy (XPS)

X-ray photoelectron spectroscopy (XPS) exploits the photoelectric effect to obtain information about the chemical composition and structure of a surface. This technique

15

relies on the phenomenon first explained by Einstein that electrons in matter may become energetically excited in interaction with quanta of light (photons). If the photons supply sufficient energy (hv), electrons are ejected out of their orbitals within an atom or molecule.

XPS runs into the same problem as the SEM in terms of the reflected information representing two components. High energy x-rays are used to excite electrons from the core-level orbitals of the atoms. The kinetic energies (E_K) of the emitted photoelectrons are characteristic of the element and atomic orbital from which they originate, being related to the binding energy (E_B) through the relationship: $E_B = hv - E_K$. When a photoelectron is emitted from an atomic orbital, a "hole" is left behind. The core-hole state created by the XPS process is energetically unstable and may be filled by an electron from a higher orbital with the concurrent emission of a second Auger electron.[55]

In the dental literature XPS was utilized to investigate the chemical interaction of synthesized polyalkenoic acid with enamel and synthetic hydroxyapatite,[56] to monitor the adsorption of active agents from six commercially available mouthrinses,[57] to provide evidence of chemical bonding of glass-polyalkenoate cement to enamel,[58] and to examine resin-modified glass-ionomer cements, specifically to indicate that resistance to water displacement decreases as hydrophobicity increases.[59] *Yoshioka et al.*[60] studied adhesion/decalcification mechanisms of acid interactions with human hard tissues such as bones and teeth, and analyzed the chemical interaction of five carboxylic acids (acetic, citric, lactic, maleic, and oxalic) and two inorganic acids (hydrochloric and nitric) with enamel and two synthetic hydroxyapatite (HAp) powders using XPS. No study was found that used XPS to investigate the changes on the enamel surface caused by AL irradiation.

16

1.2.4.3 Atomic force microscopy (AFM)

Atomic force microscopy (AFM), also known as scanning force microscopy (SPM), is used to study well defined surfaces on the atomic scale. The AFM, invented in 1986, is a new instrument which provides three-dimensional surface images of samples by scanning with a sharp probing tip over the sample surface. Unlike SEM, the AFM has the advantage of obtaining high-resolution pictures not only in a vacuous but also in a non-vacuous (i.e., air or liquid) environment.[61] The theory and operation of an atomic force microscope is similar to a stylus profiler. The primary difference is that in the atomic force microscope, the probe forces on the surface are much smaller than those in a stylus profiler. Because the forces in such a microscope are much smaller, smaller probes can be used, and the resolution is much higher than can be achieved with a stylus profiler. In this kind of microscope a constant force is maintained between the probe and sample while the probe is scanned across the surface. By monitoring the motion of the probe a three dimensional image of the surface is constructed. The strongest forces between the probe and surface are mechanical, which are forces that occur when the atoms on the probe physically interact with the atoms on a surface. However, other forces between the probe and surface can have an impact on an AFM image. These other forces include surface contamination, electrostatic forces, and surface material properties.

Surface contamination: In ambient air, all surfaces are covered with a very thin layer (< 50 nm) of contamination. This contamination can be comprised of water and hydrocarbons and depends on the environment the microscope is located in. When the AFM probe comes into contact with the surface contamination, capillary forces can pull the probe towards the surface.

17

Electrostatic forces: Insulating surfaces can store charges on their surface. These charges can interact with charges on the AFM probe or cantilever. Such forces can be so strong that they "bend" the cantilever when scanning a surface.

Surface material properties: Heterogeneous surfaces can have regions of different hardness and friction. As the probe is scanned across a surface, the interaction of the probe with the surface can change when moving from one region to another. Such changes in forces can give a contrast that is useful for differentiating between materials on a heterogeneous surface.

No dental literature was found that used AFM to examine the effects of AL on the enamel surface. It has been utilized to study the ultrastructure of human enamel afflicted with hypoplasia,[62] with amelogenesis imperfecta,[63] and the effect of acid agents,[64] of bleaching agents,[65] of Carisolv agent,[66] and of different fluoride compounds[67] on the enamel surface.

Untreated human dental enamel was observed by AFM to inspect the features from individual crystals up to prisms, [68] to reveal the structure of the enamel of third molars,[69] and to study tooth surfaces in order to compare the pattern of particle distribution in the outermost layer of the tooth surfaces. Human teeth and teeth from a rodent (Golden hamster), from a fish (piranha), and from a grazing mollusk (chiton) with distinct feeding habits were analyzed in terms of particle arrangement, packing, and size distribution.[70]

1.2.4.4 Nano-Indentation (NI)

Nano-Indentation (NI) is utilized to measure nanomechanical properties (hardness). It consists of the application of controlled load to a surface, which causes

18

local surface deformation. In contrast to AFM, this technique is able to provide perfectly normal force, and is less susceptible to van der Waals (intermolecular bonding) forces because of the larger mass of the indenter. With a computer-controlled nanoindentation technique, minute triangular indentations are made within a small area of a few micrometers diameter at a load of a few milli-newtons. The load and displacement of the indenter are continuously monitored during the loading-unloading sequence, so the hardness can be computed as a function of the indenter geometry and the applied load.

Habelitz et al.[71] used nanoindentations (size<500 nm) in the cusp area of third molars to measure the mechanical properties of single enamel rods at different orientations. One year later, he utilized this method to determine changes in nanomechanical properties of enamel during storage in de-ionized water, calcium chloride buffered saline solution and Hank's balanced salts solution (HBSS). The NI results showed that storing teeth in de-ionized water or $CaCl^{2-}$solution resulted in a large decrease in elastic modulus and hardness. At 1 day a decrease in the mechanical properties values of up to 20% was observed for enamel. After 1 week, mechanical properties dropped below 50% of its starting values, which is attributed to a demineralization process during storage. In contrast, storing teeth in HBSS did not significantly alter the mechanical properties for a time interval of 2 weeks. The use of HBSS for storage of samples from teeth is recommended. No NI study was found for 0.1% thymol solution, which was used in the present study. No study was found in the dental literature using the NI method to evaluate the hardness of the enamel surface after AL irradiation.

19

1.2.5 Laser Safety

Patient perception towards lasers in general seems to be positive. *Wigdor*[72] conducted a survey with patients to whom no information about laser was previously given. In the eyes of the patient, it appears that the use of laser technology in the health profession implies an advanced, up-to-date treatment philosophy. Patients presumably feel confident that the provider has researched the laser being used, so that the patient risk would be non-existent.

It is the responsibility of every practitioner to ensure that proper training and safety parameters are in place. All laser devices have comprehensive instructions on the safe use of the machine. There are certain fundamentals that all laser practitioners should know. One of them is mandatory eye protection.

Appropriate protective eyewear for the patient and the entire operating team must be worn when the laser is used so that any reflected energy does no damage to the eyes. The cornea, lens, and vitreous fluid are transparent to the electromagnetic radiation of the 400-700 nm band of wavelength, including the AL spectrum. Damage to the retinal tissue occurs by absorption of light and its conversion to heat by melanin granules in the pigmented epithelium or by photochemical action of the photoreceptor. The focusing effect of the cornea and lens will increase the irradiance on the retina by up to 100 000 times. The aversion reflex, which takes 0.25 seconds, may reduce exposure causing the subject to turn away from a bright light source.[73]

The two wavelengths emitted by the AL are visible to the human eye. Both AL wavelengths are not well absorbed in dental hard tissues and are very poorly absorbed in water. The poor absorption into enamel and dentin is advantageous. According to Boehm

20

et al.[74] wavelengths lower than 1.25 μm are reflected more than 40% by dental enamel. *Kurchak et al.*[36] used AL for light-curing adhesives in their *in vitro* study. The authors reported that ALs demonstrated no damage to pulp or enamel at energy levels of 1.6 to 6 Watts. The maximum power output of the AccuCure 1000 is 0.25 watts.

Launey et al.[75] examined the thermal effects of AL irradiation on dental tissues and concluded that the AL effects are inconsistent depending on whether the enamel surface is cleaned. After cleaning, the superficial and deep temperatures are low. *Brenneise et al.*[76] investigated the response of associated oral soft tissues when exposed to AL during polymerization of dental resins. It has been shown that extended curing times can have deleterious effects on the parakeratinized gingiva of dogs if the fiber-optic tip is pointed towards the gingiva not the tooth. When 10-, 20- and 30-second exposure times were tested, minimal effects were noted following the 10- and 20-second exposure times, whereas necrosis, disruption and vesiculation were noted five days after application of 30-second exposures. The authors demonstrated that clinically relevant AL exposure (10 seconds) of parakeratinized gingiva adjacent to teeth undergoing restoration did not cause lasting damage.

Powell et al.[77]conducted a study to determine the enamel damage, pulp temperature changes, and associated pulpal tissue damage following irradiation at various AL energy levels using 1.6 - 6.0 watts, approximately 1 and 2 mm diameter beam for 0.2-5.0 seconds. To evaluate pulpal damage, selected dogs' teeth were irradiated *in vivo*, extracted 7 days post-lasing, fixed, decalcified, sectioned, stained, and examined for pulpal damage. Pulp temperature and enamel damage tests utilized extracted human and dog teeth. Temperature probes were inserted in the pulp chambers of human teeth and

temperature changes were recorded as the enamel surface was lased. Enamel surface damage was evaluated by visual and microscope examination. Results showed that histologic pulpal damage occurred at > 600 J/cm². Temperature changes were < 6 ° F in human teeth with approximately 900 J/cm². No enamel damage was observed at these energy densities. At energy densities needed for proposed uses (2.5 - 15 J/cm²), no apparent damage would be expected to pulp or enamel.[77]

The decreased temperature rise with the AL irradiation in composite material can also be seen in different tooth layers.[78] *Cobb et al.*[79] measured *in vitro* temperatures at the dentin-pulpal interface upon external light exposure. Independent variables included the dentin thickness, duration and waveform of exposure, and presence of composite resin. In most instances, curing with the AL resulted in less temperature rise on the pulpal-dentin interface when compared with CCL. The authors concluded that the AL should not pose a serious thermal risk to the pulp if used at recommended energies.

Two similar studies were conducted examining the *in vitro* pulp chamber temperature rises associated with the AL curing of composite resin. The first study[80] demonstrated that temperature increases for the AL at recommended curing time were 3 °F or less. The longer the exposure times for either method of curing, the higher the temperature increased. The authors concluded that at recommended curing times, *in vitro* pulp chamber temperature increases from laser units were significantly lower than those of CCLs. The second study[81] presented similar results and "indicated that AL curing might be a method of choice for polymerization of composite resin".

The FDA (US Food and Drug Administration) approved the AL in 1991 for the intra-oral polymerization of composite materials at low fluence levels (1 – 25 J/cm²).[77]

22

1.2.6 Enhancement of Physical Properties and Time-Saving

Blankenau[82] looked at the post-cure physical properties of a composite (Silux Plus, 3M Dental Products) after AL irradiation. The diametral tensile strengths of samples of the composite were tested after they were exposed to a CCL (Caulk Max Light, L.D. Caulk Inc., Milford, DE) (300 mW), a Multi-Line AL (HGM Model 8, HGM Lasers, Salt Lake City, UT) (231 mW), and the AccuCure 3000 (LaserMed, Salt Lake City, UT) at several different output levels: 100, 150, 200, 225, 250 and 300 mW. While the CCL produced the most output power (300 mW) and had the longest exposure time of 40 seconds, it produced the poorest post-cure physical performance from the composite. The Multi-Line AL produced the second highest power output (231 mW), for one quarter of the exposure time (10 s) and produced a 21% stronger post-cure composite. A previous study had shown that an output setting of 231 mW was the 'ideal' power setting for curing Silux Plus (3M Dental Products Division, Irvine, CA) with the Multi-Line AL.[33] In the recent study[82] 200 mW was determined to be the ideal output power setting for curing Silux Plus with the AccuCure 3000. At a power output that was the lowest of the three light sources tested (200 mW) and at an exposure less than or equal to the other light sources, the AccuCure 3000 was able to produce post-cure physical properties 63% stronger than the CCL and 34% stronger than the Multi-Line AL. Reducing the power output level by 23-33% and reducing the exposure time by up to 75% increased the diametral tensile strength of the composite by as much as 63%.[82]

According to *Powell et al.*[83] research supports the use of the AL in dentistry. Used at powers of 250 mW +/- 50 mW for 10 seconds per increment (2 - 3 J/cm²), "the AL provides good curing of light-activated restorative materials in a shorter period of time

with equal or better physical properties as compared to the CCL".

Kelsey et al.[27] examined the enhancement of physical properties of resin restorative materials by laser polymerization. Two restorative materials, a microfill resin and a small particle composite, were compared for the effects of AL and CCL polymerization on their compressive strength, transverse flexural strength, and flexural modulus. The results of this study indicated that the aforementioned properties can be enhanced by AL polymerization and that this can be accomplished with only about one-fourth of the polymerization time required for visible light activation. Thus "the AL appears to be a potentially advantageous method of initiating the polymerization of dental composite resin restorations".

In contrast, the literature suggests a strong divergence of opinion about many aspects of the effectiveness of laser curing compared to CCL curing.[40] Research indicates that the AL offers a greater depth and degree of polymerization, less time required and an enhancement of the physical properties of composite resins polymerized. These advantages would be offset by reports that the increased polymerization caused by the laser results in increased shrinkage, brittleness and marginal leakage.

Addressing this concern, *Oesterle et al.*[84] wrote in their discussion that in restorative dentistry, where a bulk of resin is placed in a cavity restoration, rapid curing might create excess shrinkage and gap formation along the resin-preparation interface. However, in bonding orthodontic brackets there are several factors that vary from those in restorative dentistry applications. First, the adhesive layer is very thin, pressed between the bracket and the tooth. Second, there is usually an excess of resin at the edges of the adhesive area to absorb some of the shrinkage. Third, the bracket is free floating and

24

shrinkage would pull the bracket closer to the enamel, which is probably an advantage, rather than a disadvantage. Thus, in orthodontic applications, resin shrinkage is probably not a concern.[84]

1.2.7 *In vivo* versus *in vitro* Bond Strength

Considerable research has been conducted in evaluating the bond strength of various orthodontic bracket-bonding systems. Traditionally, orthodontic bonding systems have been evaluated by means of *in vitro* shear bond strength tests using a universal testing machine such as the Instron (Instron Corp, Canton, MA). Even though the universal testing machine is considered the gold standard when it comes to assessing bond strength values, the results are, nevertheless, obtained *in vitro*. It would be preferable to record *in vivo* measurements to assess bond strengths, since the bracket-bonding systems being tested are intended to be utilized *in vivo* and not in an *in vitro* environment.[85]

Zachrisson[86] summarized the difference between *in vivo* and *in vitro* results in orthodontic bracket bonding. The clinical results in the author's office have demonstrated differences between clinical and laboratory findings, even as far as being contradictory. In his opinion there are at least three different reasons why it is not possible to draw valid clinical conclusions from laboratory bond strength studies:

1. A continually increasing tensile or shear load applied to bonded brackets in the laboratory is not representative for the force applications that occur clinically

2. The type of debonding force in machines is not the same as the force applied in clinical debonding

3. The complex oral environment with variations in temperature, stresses,

25

humidity, acidity, and plaque is not reproducible in the laboratory.

Results obtained in *in vitro* studies do not always correlate well with those achieved *in vivo*.[25] Clinical studies would be required to substantiate laboratory experiments.[25] Therefore, bond strength values are only meaningful in the context of how closely they correlate with results obtained in a well-designed clinical trial.[25]

Bond study findings are reported as bond strength values, in units of MegaPascals, calculated by dividing the peak load at which an orthodontic bond fails by the surface area of the bracket.[87] *Reynolds*[5] found that minimum bond strength of 6-8 MPa was adequate for most clinical orthodontic needs. Other authors suggest that the bond strength of the adhesive and attachments should be sufficient to withstand the forces of mastication, the stresses exerted by the archwires, and patient abuse, as well as allow for control of tooth movement in all 3 planes of space. At the same time, the bond strength should be at a level to allow for bracket debonding without causing damage to the enamel surface. Bond strengths ranging from 2.8 MPa to 10 MPa are suggested as being adequate for clinical situations.[4 88 89] According to *Newman*[90] the orthodontic force applied to brackets during treatment is approximately 1 MPa, with a maximum of approximately 3 MPa probably occurring under certain clinical conditions.

The use of Weibull analysis as an approach to provide the clinician with more useful information relative to the extrapolation of *in vitro* data to clinical practice.[91] The Weibull analysis is the process of discovering the trends in product or system failure data, and using them to predict future failures in similar situations. It allows for fracture probability to be calculated as a function of applied load or vice versa.[92] For example, in orthodontics, Weibull analysis would allow the researcher to calculate the *in vitro*

26

probabilities of failure of a bonding system under loads encountered in the clinical situation or calculate the *in vitro* bond strengths based on failure rates obtained in the clinical situation. Weibull analysis may offer a better way of interpreting *in vitro* data, however, this is still a system that is based on predictions of bond strength values rather than on actual recordings of *in vivo* bond strength values. Hence, there is a need for a more accurate method of assessing *in vivo* bond strength values.[85]

Pickett et al.[85] compared the shear bond strength results of *in vivo* and *in vitro* bracket debonding. He used similar debonding pliers as seen in the present study and showed significantly different values. The mean bond strength results recorded *in vitro* were 11.02 MPa +/- 4.49 and 12.82 MPa +/- 3.05 respectively, while the mean value obtained *in vivo* was much lower at 5.47MPa +/- 2.18. The results of this study indicated that debonding forces measured *in vivo* were significantly lower (P = .0001) than those measured *in vitro*.

1.2.8 Summary

Patients undergoing orthodontic treatment with fixed appliances are at an increased risk for enamel decalcification. AL, used to cure the bonding material between bracket base and the tooth surface, is suggested to significantly reduce enamel decalcification and the curing time.

"The future looks bright for the use of the AL" not only for enhanced composite curing and demineralization prevention, but also "in other areas, such as decay prevention or pulpal treatments for primary teeth as well as an adjunct to endodontic therapy".[83]

27

1.2.9 Bibliography

1. Newman GV. Epoxy adhesives for orthodontic attachments: progress report. Am J Orthod Dentofac Orthop 1965; 51:901–912

2. Proffit WR. Contemporary Orthodontics. Third edition. St Louis, Mo: CV Mosby; 2000: 392

3. Retief DH, Sadowsky PL. Clinical experience with the acid-etch technique in orthodontics. Am J Orthod Dentofac Orthop 1975; 68:645–54

4. Lopez, JI. Retentive shear strengths of various bonding attachment bases. Am J Orthod Dentofac Orthop. 1980; 77:669–678

5. Reynolds, IR. A review of direct orthodontic bonding. Br J Orthod. 1985; 2:171–178

6. Geiger AM, Gorelick L, Gwinnett AJ, Griswold PF. The effect of a fluoride proved program on white spot formation during orthodontic treatment. Am J Orthod Dentofacial Orthop. 1988; 93:29–38. [PubMed Citation]

7. Geiger AM, Gorelick L, Gwinnett AJ, Benson BJ. Reducing white spot lesions in orthodontic populations with fluoride rinsing. Am J Orthod Dentofacial Orthop. 1992; 101:403–7. [PubMed Citation]

8. Magness WS, Shannon IL, West D. Office applied fluoride treatments for orthodontic patients. J Dent Res 1979; 58:1427 [PubMed Citation]

9. Hallgren A, Oliveby A, Twetman S. Caries associated microflora in plaque from orthodontic appliances retained with glass ionomer cement. Scand J Dent Res. 1992 Jun;100(3):140-3

10. Muller HP, Flores de Jacoby L. [Composition of the oral subgingival flora in wearers of fixed orthodontic appliances] [Article in German] Dtsch Zahnarztl Z. 1982 Oct; 37(10):855-60

11. Wisth PJ, Nord A. Caries experience in orthodontically treated individuals. Angle Orthod. 1977; 47:59–64. [PubMed Citation]

12. Gorelick L, Gieger A, Gwinnett AJ. Incidence of white spot formation after bonding and banding. Am J Orthod. 1982; 81:93–98. [PubMed Citation]

13. Artun J, Brobakken BO. Prevalence of carious white spots after orthodontic treatment with multibonded appliances. Eur J Orthod. 1986; 8:229–234. [PubMed Citation]

14. Sognnaes RF, Stern RH. Laser effect on resistance of human dental enamel to demineralization in vitro. J S Calif Dent Assoc. 1965; 33:328–329

28

15. Powell LG, Duncan Y, Higuchi WI, Fox JL. Comparison of three lasers on demineralization of human enamel. SPIE. 1994; 1880:188–192

16. Powell LG, Higuchi WI, Fox JL: Argon laser effect on demineralization of human enamel. SPIE. 1992; 1643:374–379

17. Duncan Y, Powell GL, Higuchi WI, Fox J. Enhancement of argon laser effect on dissolution and loss of human enamel. J Clin Laser Med Surg. 1993; 11:5259–61

18. Fox JL, Duncan Y, Otsuka M. et al. Initial dissolution rate studies on dental enamel after CO_2 laser irradiation. J Dent Res 1992; 71:71390–8.

19. Westerman GH, Hicks MJ, Flaitz CM, Powell GL, Blankenau RJ. Surface morphology of sound enamel after argon laser irradiation: an in vitro scanning electron microscopic study. J Clin Pediatr Dent. 1996 Fall; 21(1):55-9

20. Flaitz CM, Hicks MJ, Westerman GH. Argon laser irradiation and acidulated phosphate fluoride treatment in caries-like lesion formation in enamel: an in vitro study. Pediatr Dent 1995; 17:131–9

21. Goodman BD, Kaufman HW. Effects of argon laser on the crystalline properties and rate of dissolution in acid of tooth enamel in the presence of sodium fluoride. J Dent Res 1977; 56(10):1201-7

22. Hicks MJ, Flaitz CM, Westerman GH. Caries-like lesion initiation and progression in sound enamel following argon laser irradiation: an in vitro study. *J Dent Child.* 1993; 60:201–206. [PubMed Citation]

23. Hicks MJ, Flaitz CM, Westerman GH. Enamel caries initiation and progression following low fluence (energy) argon laser and fluoride treatment. J Clin Pediatr Dent. 1995; 20:19–23. [PubMed Citation]

24. Hicks MJ, Flaitz CM, Westerman GH. Roots caries in vitro after low fluence argon laser and fluoride treatment. Compendium. 1997; 18:6543–52. [PubMed Citation]

25. Talbot TQ, Blankenau RJ, Zobitz ME, Weaver AL, Lohse CM, Rebellato J. Effect of argon laser irradiation on shear bond strength of orthodontic brackets: An in vitro study. Am J Orthod Dentofacial Orthop 2000;118: 274-9

26. Lalani N, Foley TF, Voth R, Banting D, Mamandras A. Polymerization with the argon laser: curing time and shear bond strength. Angle Orthod 2000 Feb; 70(1):28-33

27. Kelsey WP, Blankenau RJ, Powell GL, Barkmeier WW, Cavel WT, Whisenant BK. Enhancement of Physical Properties of Resin Restorative Materials by Laser

29

Polymerization. Lasers Surg Med 1989; 9:623-7

28. Martin FE. A survey of the efficiency of visible light curing units. J Dent. 1998 Mar;26(3):239-43

29. Mills RW, Jandt KD, Ashworth SH. Dental composite depth of cure with halogen and blue light emitting diode technology. Br Dent J. 1999 Apr 24; 186(8):388-91

30. Cacciafesta V, Sfondrini MF, Klersy C and Sfondrini G. Polymerizartion with a micro-xenon light of a resin-modified glass ionomer: a shear bond strength study 15 minutes after bonding. Europ. J Orthod 2002; 24:689-697

31. Cobb DS, Vargas MA Rundle T. Physical properties of composites cured with conventional light or argon laser. Am J Dent 1996 (9):199–202

32. Blankenau RJ, Kelsey WP, Powell GL, Shearer GO, Barkmeier WW, Cavel WT. Degree of composite resin polymerization with visible light and argon laser. Am J Dent 1991; 4:40-2

33. Kelsey WP, Blankenau RJ, Powell GL, Barkmeier WW, Stormberg EF. Power and time requirements for use of the argon laser to polymerize composite resins. J Clin Laser Med Surg. 1992 Aug; 10(4):273-8

34. Sakaguchi RL, Douglas WH, Peters MC. Curing light performance and polymerization of composite restorative materials. J Dent 1992;20: 183-8

35. Fleming MG, Maillet WA: Photopolymerization of composite resin using the argon laser. J Can Dent Assoc. 1999 Sep; 65(8):447-50

36. Kurchak M, Desantos B, Powers J, Turner D. Argon Laser for Light-Curing Adhesives. J Clin Orthod 1997 June; 31(6):371-4

37. Retief, DH. Failure at the dental adhesive etched enamel interface. J Oral Rehab. 1974; 1:265–284

38. James JW, Miller BH, English JD, Tadlock LP, Buschang PH. Effects of high-speed curing devices on shear bond strength and microleakage of orthodontic brackets. Am J Orthod Dentofacial Orthop 2003(123):555-61

39. Eldiwany M, Komatsu S, Powers JM. Curing light intensity affects mechanical properties of composite. J Dent Res 1997: 73–6 (Abstr. No. 477)

40. Vargas MA, Cobb DS, Schmit JL. Polymerization of Composite Resin. Argon Laser or Conventional Light. Oper Dent 1998;23: 87-93

41. Peutzfeldt A, Sahafi A, Asmussen E. Characterization of resin composites

30

polymerized with plasma arc curing units. Dent Mater 2000 (16): 330–336

42. Burgess JO, DeGoes M,. Walker R, Ripps AH. An evaluation of four light-curing units comparing soft and hard curing. Pract Periodont Aesthet Dent 1999(11): 125–132.

43. Jandt KD, Mills RW, Blackwell GB, Ashworth SH. Depth of cure and compressive strength of dental composites cured with blue light emitting diodes (LEDs). Dent Mater. 2000 Jan; 16(1):41-7

44. Dunn WJ, Taloumis LJ. Polymerization of orthodontic resin cement with light-emitting diode curing units. Am J Orthod Dentofacial Orthop 2002 Sept.; 122:236-41

45. St-Georges AJ, Swift EJ Jr, Thompson JY, Heymann HO. Irradiance effects on the mechanical properties of universal hybrid and flowable hybrid resin composites. Dent Mater. 2003 Jul;19(5):406-13

46. Gorton J, Featherstone JD. In vivo inhibition of demineralization around orthodontic brackets. Am J Orthod Dentofacial Orthop 2003 Jan;123(1):10-4

47. Yamamoto HY, Sato K. Prevention of dental caries by ND:YAG laser irradiation. J Dent Res 1980; 2171-7

48. Hicks MJ. Effects of argon laser irradiation and acidulated phosphate fluoride on root caries. Am J Dent 1995; 8:10-14

49. Westerman GH, Flaitz CM, Powell GL, Hicks MJ. Enamel Caries Initiation and Progression after Argon Laser Irradiation: *In Vitro* Argon Laser Systems Comparison. J Clin Laser Med & Surg 2002 (20); 5: 257-262

50. Monseau Anderson A, Kao E, Gladwin M, Benli O, Ngan P. The effect of argon laser irradiation on enamel decalcification: An in vivo study. Am J Orthod Dentofacial Orthop 2002 Sept.; 122:251-9

51. El-Din IM, Fathy LM. Scanning electron microscopic study of argon laser-induced morphologic changes on human dental enamel and dentin. Egypt Dent J. 1993 Jul;39(3):473-8

52. Palamara J, Phakey PP, Orams HJ, Rachinger WA. The effect on the ultrastructure of dental enamel of excimer-dye, argon-ion and CO2 lasers. Scanning Microsc. 1992 Dec;6(4):1061-70; discussion 1070-1.

53. Westerman GH, Hicks MJ, Flaitz CM, Blankenau RJ, Powell GL. Combined effects of acidulated phosphate fluoride and argon laser on sound root surface morphology: an in vitro scanning electron microscopy study. J Clin Laser Med Surg. 1999 Apr; 17(2):63-8.

54. Featherstone JD, Nelson DG. Recent uses of electron microscopy in the study of physico-chemical processes affecting the reactivity of synthetic and biological apatites. Scanning Microscopy 1989 Sep;3(3):815-27; discussion 827-8

55. Jones FH: Teeth and bones. Applications of surface science to dental materials and related biomaterials. Surface Science Reports 2001 (42) 75-205

56. Spencer P, Wang Y. X-ray photoelectron spectroscopy (XPS) used to investigate the chemical interaction of synthesized polyalkenoic acid with enamel and synthetic hydroxyapatite. J Dent Res. 2001 May;80(5):1400-1

57. Perdok JF, Van Der Mei HC, Buscher HJ, Genet MJ, Rouxhet PG. Surface free energies and elemental surface compositions of human enamel after application of commercially available mouthrinses and adsorption of salivary constituents. J Clin Dent. 1990 Fall;2(2):43-7

58. Yoshida Y, Van Meerbeek B, Nakayama Y, Snauwaert J, Hellemans L, Lambrechts P, Vanherle G, Wakasa K. Evidence of chemical bonding at biomaterial-hard tissue interfaces. J Dent Res. 2000 Feb;79(2):709-14

59. Smith DC. Development of glass-ionomer cement systems. Biomaterials 1998 Mar;19(6):467-78

60. Yoshioka M, Yoshida Y, Inoue S, Lambrechts P, Vanherle G, Nomura Y, Okazaki M, Shintani H, Van Meerbeek B. Adhesion/decalcification mechanisms of acid interactions with human hard tissues. J Biomed Mater Res. 2002 Jan;59(1):56-62

61. Ushiki T. Atomic force microscopy and its related techniques in biomedicine. Ital J Anat Embryol 2001;106(2 Suppl 1):3-8. (abstr.)

62. Batina N, Renugopalakrishnan V, Casillas Lavin PN, Guerrero JC, Morales M, Garduno-Juarez R, Lakka SL. Ultrastructure of Dental Enamel afflicted with Hypoplasia: An Atomic Force Microscopic Study. Calcif Tissue Int. 2003 Nov 3 [Epub ahead of print]

63. Batina N, Renugopalakrishnan V, Lavin PN, Hernandez Guerrero JC, Morales M, Garduno-Juarez R. An atomic force microscopic study of the ultrastructure of dental enamel afflicted with amelogenesis imperfecta. J Biomater Sci Polym Ed. 2002;13(3):337-48

64. Watari F. In-situ etching observation of human teeth in acid agent by atomic force microscopy. J Electron Microsc (Tokyo) abstract 1999;48(5):537

65. Hegedus C, Bistey T, Flora-Nagy E, Keszthelyi G, Jenei A. An atomic force microscopy study on the effect of bleaching agents on enamel surface. J Dent 1999

Sep;27(7):509-15

66. Wennerberg A, Sawase T, Kultje C. The influence of Carisolv on enamel and dentine surface topography. Eur J Oral Sci. 1999 Aug;107(4):297-306

67. Petzold M. The influence of different fluoride compounds and treatment conditions on dental enamel: a descriptive in vitro study of the CaF(2) precipitation and microstructure. Caries Res. 2001;35 Suppl 1:45-51

68. Schaad P, Paris E, Cuisinier FJ, Voegel JC. Atomic force microscopy study of human tooth enamel surfaces. Scanning Microsc. 1993 Dec;7(4):1149-52

69. Habelitz S, Marshall SJ, Marshall GW Jr, Balooch M. Mechanical properties of human dental enamel on the nanometre scale. Arch Oral Biol 2001 Feb;46(2):173-83

70. Farina M, Schemmel A, Weissmuller G, Cruz R, Kachar B, Bisch PM. Atomic force microscopy study of tooth surfaces. J Struct Biol. 1999 Mar;125(1):39-49

71. Habelitz S, Marshall GW Jr, Balooch M, Marshall SJ. Nanoindentation and storage of teeth. J Biomech. 2002 Jul;35(7):995-8

72. Wigdor H. Patients' Perception of Lasers in Dentistry. Lasers Surg Med 1997;20: 47-50

73. University of Florida, Administrative affairs, environmental health & safety, radiation control and radiological services: Laser safety manual. UW safety program (website)

74. Boehm R, Baechl E., Webster J, Janke S. Laser processes in preventive dentistry. Opt Eng 1977; 16:493-6

75. Launay Y, Mordon S, Cornil A, Brunetaud JM, Moschetto Y. Thermal Effects of Lasers on Dental Tissues. Lasers Surg Med 1987; 7:473-7

76. Brenneise CV, Blankenau RJ. Response of Associated Oral Soft Tissues When Exposed to Argon Laser During Polymerization of Dental Resins. Lasers Surg. Med.1997; 20:467-72

77. Powell GL, Morton TH, Whisenant BK. Argon Laser Oral Safety Parameters for Teeth. Lasers Surg Med 1993; 13:548-552

78. Pradhan RD, Melikechi N, Eichmiller F. The effect of irradiation wavelength bandwidth and spot size on the scraping depth and temperature rise in composite exposed to an argon laser or a conventional quartz-tungsten-halogen source. Dent Mater. 2002 May; 18(3):221-6

79. Cobb DS, Dederich DN, Gardner TV. In vitro temperature change at the dentin /

33

pulpal interface by using conventional visible light versus argon laser. Lasers Surg Med 2000; 26(4):386-97

80. Powell GL, Anderson JR, Blankenau RJ. Laser and curing light induced in vitro pulpal temperature changes. J Clin Laser Med Surg 1999 Feb; 17(1):3-5

81. Anic I, Pavelic B, Peric B, Matsumoto K. In vitro pulp chamber temperature rises associated with the argon laser polymerization of composite resin. Lasers Surg Med 1996; 19(4):438-44

82. Blankenau RJ. Post-Cure Physical Properties of Composite after Argon Laser Irradiation. LaserMed website: www.lasermed.com

83. Powell GL, Blankenau RJ. Laser curing of dental materials. Dent Clin North Am. 2000 Oct; 44(4):923-30.

84. Oesterle LJ, Newman SM, Shellhart WC. Rapid curing of bonding composite with a xenon plasma arc light. Am J Orthod Dentofacial Orthop 2001; 119:610- 6

85. Pickett KL, Sadowsky PL Jacobson A, Lacefield W. Orthodontic In Vivo Bond Strength: Comparison with In Vitro Results, Angle Orthod 2001; 71(2):141-8

86. Zachrisson BU: Orthodontic bonding to artificial tooth surfaces. Clinical versus laboratory findings. Am J Orthod 2000 May;5: 592-4

87. Grubisa H, Heo G, Raboud D Glover K, Major P. Bond Strength Study Comparing a Self-Etching Primer System and Traditional Acid Etch for Light Cure Orthodontic Bonding. MSc thesis 2002; Edmonton, AB: University of Alberta

88. Keizer S, Ten Cate JM, Arends J. Direct bonding of orthodontic brackets. Am J Orthod Dentofac Orthop. 1976; 69:318–327

89. Miura, F, K Nakagawa, and E. Masuhara. A new direct bonding system for plastic brackets. Am J Orthod Dentofac Orthop. 1971; 59:350– 361

90. Newman, GV. A posttreatment survey of direct bonding of metal brackets. Am J Orthod Dentofac Orthop. 1978; 74:197–201.

91. Ferreira, A. An Investigation of the Relationship Between *In Vivo* and *In Vitro* Data When Evaluating Orthodontic Bonding Systems. MSc thesis 1997; Birmingham, Ala: Department of Orthodontics, University of Alabama

92. Mc Cabe, JF, Carrick TE. A statistical approach to the mechanical testing of dental materials. Dent Mater. 1986; 2:139–142.

34

1.3 Statement of the Problem

Patients undergoing orthodontic treatment with fixed appliances are at an increased risk for enamel decalcification. AL, used to cure the bonding material between bracket base and the tooth surface, is suggested to significantly reduce enamel decalcification and the curing time. The first part of the study will investigate whether the bond strength of argon laser cured brackets is comparable to the bond strength of CCL cured brackets and whether there is a difference between the study type *(in vivo/ in vivo)* location of the specimen (maxillary/mandibular), and subject's gender. The second part of the study will use three different surface scans to examine the effect caused by AL irradiation on the enamel surface, in terms of the chemical composition, surface morphology, hardness, and roughness. The results might help to explain why argon laser irradiation is diminishing demineralization of human enamel.

1.4 Significance of the Study

The results of the present study will reflect the effectiveness of argon laser irradiation in curing the bonding material four times faster than the conventional curing light *in vivo* and *in vitro* and will help to investigate what kind of changes take place at the enamel surface that could explain the demineralization prevention effect. If the argon laser is effective in curing orthodontic material in less time and if AL irradiation reduces enamel decalcification during orthodontic treatment, it may become a valuable and time saving tool to the orthodontic practice and may improve the esthetic results and satisfaction of the orthodontic patient

35

1.5 Research Questions

Paper #1

1. Are *in vivo* orthodontic bracket bond strengths using argon laser curing (10s) significantly different than those achieved with conventional light curing (40s)?

2. Are *in vivo* bond strength results significantly different than *in vitro* bond strength results?

3. Is there a significant difference in bond strength between mandibular versus maxillary premolar teeth?

4. Is there a significant difference in bond strength between premolars originating from male versus female subjects?

5. Is there a significant difference between the proportions of ARI scores between the curing methods?

6. Does argon laser curing produce significantly more or less enamel fracture at debonding than conventional curing light?

Paper #2

7. Is there a difference in the chemical composition of the enamel surface after argon laser irradiation (60s)?

Paper #3

8. Is there a visual change in surface morphology of the enamel after argon laser irradiation (60s)?

Paper #4

9. Is there a difference in hardness of the enamel surface after argon laser irradiation (60s)?

10. Is there a difference in roughness of the enamel surface after argon laser irradiation (60s)?

36

1.6 Null Hypotheses

Paper #1

1. There is no difference between the bond strength of argon laser curing (10s) compared to the conventional light curing (40s).

2. *In vivo* bond strength results are not different than *in vitro* bond strength results.

3. There is no difference in bond strength between mandibular versus maxillary premolar teeth.

4. There is no difference in bond strength between premolars originating from male versus female subjects.

5. There is no difference in the proportions of ARI scores between the curing methods.

6. There is no difference in the amount of enamel fracture between the curing methods.

Paper #2

7. There is no difference in the chemical composition of the enamel surface after argon laser irradiation (60s).

Paper #3

8. There is a visual change in surface morphology of the enamel after argon laser irradiation (60s).

Paper #4

9. There is no difference in hardness of the enamel surface after argon laser irradiation (60s).

10. There is a difference in roughness after argon laser irradiation (60s).

37

Chapter Two

Research Paper One

Argon Laser versus Conventional Visible Light cured

Orthodontic Bracket Bonding: An *in vivo* and *in vitro* Study

2.1 Introduction

The use of light-cured adhesives has become the most popular way for bracket bonding because of their ease of application and the extended time they allow for bracket placement.[1] Clinicians whose primary focus is efficiency were up until now reluctant to switch to the light-cured adhesives, due to the fact that additional chair time has to be sacrificed for the curing process. The amount of curing time needed to cure orthodontic adhesive with a conventional curing light (CCL) takes 40 seconds per tooth which adds up to 13-14 minutes or more for the upper and lower arch, depending on the number of brackets placed.

The argon laser (AL) is capable of polymerizing a light-cured orthodontic adhesive four times faster with the same or even higher bond strength[2] and with less frequency of enamel fracture at debonding than with the CCL.[3] In addition, at recommended curing times, *in vitro* pulp chamber temperature increases from laser units were significantly lower than those of the CCLs.[4] Therefore the AL should not pose a serious thermal risk to the pulp if used at the recommended energies.[5]

Available published *in vitro* data indicate that AL curing may be a method of choice for polymerization of composite resin.[6] Additional research into applying the technique in the mouth is indicated.[7] A literature review did not identify any *in vivo* studies regarding the comparison of curing orthodontic adhesive with AL versus CCL.

The aim of this in study was to compare *in vivo* and *in vitro* bond strength results and debonding characteristics when an AL is used to bond orthodontic brackets in comparison to the CCL.

39

2.2 Material and Method

This study was approved by the University of Alberta, Health Research Ethics Board (Appendix A).

2.2.1 Pilot study

The purpose of the pilot study was to establish the sample size. Seventy-six extracted premolars from nineteen patients were collected and randomly assigned to be cured with the AL or the CCL. A power analysis was performed, using a power of 0.80 and a clinical significance level of 0.5 MPa. A minimum sample size of 23 x 4 (n=92) was determined with an objective of 23 for each group *in vitro* and *in vivo*.

2.2.2 *In vivo* Study

Twenty-three patients who required four premolar extractions (n=92) as part of their comprehensive orthodontic treatment were included in this study. Participants were recruited from the University of Alberta Orthodontic Graduate Program. The selection criteria for the sample consisted of:

- Patients between the age 12-16 years of age

- Teeth without enamel defect, morphological anomalies or decalcification

- Teeth that were not bonded previously

Informed consent (Appendix B & C) was obtained and each of the premolars were randomly assigned to either the argon laser (AL) or conventional (quartz tungsten halogen) curing light (CCL) group for the maxillary and mandibular arch by computer generated random allocation. A record of the assignment was recorded by the primary investigator (NH).

40

The four groups were named:

MX AL = Maxillary arch, argon laser cured

MX CCL = Maxillary arch, conventional light cured

MN AL = Mandibular arch, argon laser cured

MN CCL = Mandibular arch, conventional light cured

An AL (AccuCure 1000, LaserMed, Salt Lake City, UT) (Appendix D) was used in the present study. This AL is classified as a 3b laser. Safety approval was obtained from the U of A safety officer after a radiation protection lecture was given to the primary investigator (Appendix E). The CCL unit used in the present study was the Ortholux XT (3M Unitek, Monrovia, CA). The AL and CCL output were tested with a Curing Radiometer (Model 100, P/N 10503, Demetron Research Corporation, Danbury, CT) on a regular basis to ensure that the chosen output value (AL: 250 mW/cm^2) and the existing output value (CCL: 480 mW/cm^2) were the actual output values throughout the study. The AL produced an energy density (fluence) of 2.5 J/cm^2 and the CCL produced an energy density of 19.2 J/cm^2.

An AL leakage current test was performed by a specialized technician (AF) at the University of Alberta. The readings of the AL leakage currents were taken with a BK Precision Model 1655 AC Power Supply and leakage Tester U of A # 162679. The AL was well under 500 micro amp hospital standards.

Bracket bonding was completed by the primary investigator. The buccal surface of each tooth was pumiced for 5 seconds, rinsed with water for 5 seconds, and dried with oil-free air for 5 seconds. Transbond Plus Self Etching Primer (3M Unitek, Monrovia, CA) was rubbed onto the surface for 3 seconds and left alone for 30 seconds. A gentle oil

41

and moisture free airburst away from the gingiva was applied following the manufacturer's instructions. Pre-coated 0.022 mil bracket slot size Victory series APC brackets (3M Unitek, Monrovia, CA) for first or second premolar teeth accordingly was pressed firmly onto the tooth, moved to its proper location and the excess bonding material was removed from around the bracket base. After the teeth were randomly assigned (left or right), the interface between enamel surface, bonding material, and bracket base was cured with either the AL (AccuCure 1000, LaserMed, Salt Lake City, UT) for 10 seconds or the CCL (Ortholux XT, 3M Unitek, Monrovia, CA) for 40 seconds. The light tip of both curing devices was held approximately 3 mm away from the tooth surface in a 45 degree angle. The light beam was applied from the occlusal and gingival direction for half of the curing time respectively. After the bonding process was completed, Alastiks were applied around each bracket for patient comfort. Wax strips were handed out for application in case of occurrence of oral mucosa irritation. Oral hygiene and wax application instructions and a copy of the patient and parental consent form were given to the patient before dismissal.

Debonding pliers (Figure 2.1) were designed to measure the force needed to debond a bracket from the enamel surface. The debonding device may be introducing a combination of debonding forces, eg, shear, peel, and tensile forces. A design was chosen to mainly measure shear forces. A metal pad was soldered to the tip of the upper arm of the pliers to serve as a resting platform for the premolar cusps. A groove for the wire sling was created on the lower arm perpendicular to the end of the resting pad to apply a force parallel to the long axis of the tooth. A strain gauge (#CEA-06-062UW-350, Micro-Measurements Group Inc., NC) was attached to the lower arm of the pliers and measured

42

the strain in the arm, which was related to the force that was applied to the handles during the debonding procedure. At bracket bond failure, the peak voltage from the circuit was recorded and converted into MPa (see calibration formula below). Before any measurements were taken, the pliers had to be calibrated. A known load (N) was applied to the wire sling and the measurements in volts were recorded. A linear least-squares regression was used to fit the data ($R^2 = 0.9998$) (Figure 2.2). The resulting formula was used to convert the readings from volts into MPa:

MPa = (35.113 x Strain gauge measurement (V) − 0.158) / 12.8 mm^2 (bracket base area)

After 14 days, the Alastiks were removed, and dental floss was attached to each bracket to prevent loss of the bracket during debonding. Following calibration of the debonding device, a second investigator (DS), who was blinded regarding the curing device, debonded each bracket. The wire loop was hooked around the gingival tie wings near the base of the bracket as close to the tooth as possible and the platform of the debonding plier was placed occlusal to the cusp tips (Figure 2.3). The handles of the pliers were squeezed together in a slow but steady manner, the frontal arms separated and the wire sling applied a force until the bracket detached from the tooth. At bracket bond failure, a volt meter, monitoring the strain gauge circuit, digitally displayed a peak voltage which was recorded by the principal investigator. The debonded brackets were disinfected and placed in labeled bags. Following debonding all four premolars were extracted.

2.2.3 *In vitro* Study

Four premolar teeth of 25 patients (n=100), who were not enrolled in the *in vivo* part of this study, were collected. Selection criteria were the same as for the *in vivo* study and informed consent was obtained. Teeth with cracks due to the pressure of the

43

extraction forceps were not included. After extraction, the teeth were stored separately in 0.1 % thymol solution (one labeled jar per patient). When all of the teeth had been collected, the teeth were rinsed with distilled water. The premolars were randomly assigned by computer generated random allocation to the AL group or the CCL group. A code was applied to root of the tooth. The brackets were bonded using the same protocol described in the *in vivo* part of this study. The teeth were stored in distilled water for 14 days after thermal cycling the teeth for 1000 cycles between water baths of 5°C and 55°C (30-second dwell time in each bath) to imitate the oral environment. The teeth were embedded in chemically cured dental acrylic (acrylic resin powder (#0911104) & pink acrylic liquid (#010410), Dentsply Chaulk) to approximately the level of the cemento-enamel junction and it was ensured that all brackets were mounted in the same orientation relative to the acrylic cylinder. The code was transferred to the backside of the acrylic square for blinding before the teeth were embedded. The *in vivo* debonding pliers (Figure 2.4) utilized in the *in vivo* part, were also used to debond *in vitro*.

2.2.4 Adhesive Remnant Index Scoring

An adhesive remnant index (ARI) [8] was used to determine the type of bond failure. A visual inspection was conducted on the bracket base and not on the tooth under the assumption that the adhesive remained either on the tooth or the bracket. A light stereomicroscope (Bausch & Lomb, U of A # 0047503, magnification: 10x) was utilized to evaluate the ARI on the debonded brackets after the debonding procedure was conducted. The criteria for scoring are as follows:

44

- 0 = No adhesive on the tooth　　　　– All adhesive on the bracket base
- 1 = Less than half of the adh. on the tooth　– More than half of the adhesive on bracket base
- 2 = More than half of the adh. on the tooth　– Less than half of the adhesive on bracket base
- 3 = All of the adhesive on the tooth　　– No adhesive on the bracket base

The score is used to determine if the bond failure is of adhesive (between the adhesive and the enamel), of cohesive (within the adhesive layer) or of adhesive/cohesive (areas of both types of failure) origin. Detected enamel fractures were also recorded.

2.2.5 Statistical Analysis

The data obtained was grouped by Curing Method (AL/CCL), Location (MX / MN), Study Type (*in vitro / in vivo*), and Gender (M/F). Descriptive statistics, including mean, standard deviation, and minimum and maximum bond strength values were calculated (SPSS software, Chicago, IL) for each of the experimental groups. Multivariate analysis of variance (MANOVA) was used to determine whether significant differences of mean bond strength existed between the Gender and Study type groups. A paired t-test was utilized to determine the existence of a significant difference between the Location groups and the Curing Method group respectively and two sample t-tests were used to compare the Study Type group. A chi-square test examined the existence of a significant difference of the ARI scores between the Curing Methods and an independent t-test was utilized to determine if a correlation exists between the mean bond strength within the ARI score groups and the actual ARI scores.

2.3 Results

Of the 92 teeth included in the *in vivo* part of the study, one measurement could not be taken because of technical difficulties (cable disconnected during debonding

45

procedure). The measurement was removed from the data set, resulting in a reduced sample size for the *in vivo* maxillary AL group (22 instead of 23 measurements).

No premature bond failure occurred in the 14 days trial period.

2.3.1 Bond Strength Testing

Twenty-nine female (*in vivo*: 12; *in vitro*: 17) and eighteen male (*in vivo*: 10; *in vitro*: 8) subjects participated in the study. Four *in vivo* groups (MX AL/ MX CCL/ MN AL/ MN CCL) with 23 measurements each (except MX AL with 22) and four *in vitro* groups (MX AL/ MX CCL/ MN AL/ MN CCL) with 25 measurements each were compared. Descriptive statistics for bond strength according to Curing Method, Study Type, and Gender are provided in Table 2.1 & Table 2.2.

No statistically significant difference was determined between the Gender, but a significant difference (P = 0.006) according to the Study Type was identified (Table 2.3). Results of female and male subjects were therefore combined. No significant difference was determined between the Location (Table 2.4), the maxillary and mandibular teeth were therefore united. Analysis of the Curing Method (AL/CCL) presented no significant difference (Table 2.5). The difference between the *in vivo* and *in vitro* results (Study Type) were significantly different for the AL (P = 0.000) and CCL (P = 0.000) group (Table 2.6).

In summary, the only statistically significant difference was found between the Study Types. *In vivo* results were significantly (P = 0.000) lower than *in vitro* results for both Curing Methods.

2.3.2 ARI Scoring & Enamel Fracture

The ARI scoring system was used as a means of defining the site of bond failure

46

between the enamel, the adhesive and the bracket base. The distributions of scores and the average mean bond strength within the scores are listed in Table 2.7 for the AL group and Table 2.8 for the CCL group. The highest amount of scores for the AL group was found in score 1 group (49.47 %) and in the score 2 group (42.11 %), followed by score 0 group (6.32 %) and score 3 group (2.11 %). The distribution of scores in the CCL group presented the highest amount of score in the score 1 group (67.70 %) followed by 2 (15,63 %), 0 (10.34 %), and 3 (4.17 %) (Table 2.8). The lowest score 0 occurred more frequently (1:2) in the CCL group, indicating none of the adhesive remains on the tooth. Score 1 had more counts in the CCL group (3:4), meaning a combination of failures at the adhesive/bracket and enamel/adhesive interface with the emphasis on the enamel/adhesive interface. The score 2 had more counts in the AL group (1:3). The bond failure site is again a combination with the emphasis on the adhesive/bracket interface. The highest score 3 occurred more frequently (1:2) in the AL group, indicating a greater trend for all adhesive remaining on the enamel at debonding. The site of failure is found on the adhesive/bracket interface. Statistical analysis using chi-square test for homogeneity showed no significant difference (P = 0.001) of the ARI scores between the Curing Methods (Table 2.9). No significant difference was found between the mean bond strength within the ARI groups and the ARI scores (Table 2.10) with a mean difference of 2.14 MPa in the AL group and 2.76 in the CCL group.

Enamel fractures occurred on two of the maxillary premolars used in the *in vitro* part of the study. One of the premolars belonged to the AL, the other one to the CCL group. Both fractures were limited to the enamel, located at the bonded area. No enamel fracture was found on the teeth tested *in vivo*.

2.4. Discussion

2.4.1 Bond Strength Testing

To date little has been reported on the clinical performance of AL for orthodontic bracket bonding, but numerous *in vitro* studies have been published.

James et al.[8] presented *in vitro* mean shear bond strength results using the APC brackets for the AL (238.1 mW/cm², 10s) of 4.2 MPa +/- 1.0 compared to the CCL (771.9 mW/cm², 20s) of 5.3 MPa +/- 1.0 MPa. 37% phosphoric acid and Transbond XT primer was used instead of the Self Etching Primer. *James et al.*[8] reported bond strengths which were lower than the mean bond strength results seen in the present study. The combined AL (250 mW/cm², 10s) *in vitro* reading in the present study was 12.25 MPa +/- 2.89 MPa and the combined CCL (480 mW/cm², 40s) was 12.06 MPa +/- 2.15 MPa. This difference could be due to the fact that *James et al.*[8] used a different AL system (ILT systems, Salt Lake City, UT), shorter curing time and a higher energy density was noted on their CCL unit.

The mean shear bond strengths of both groups in the present study were lower than those reported by *Talbot et al.*[2] for AL (230mW/cm², 10s) 14.55 MPa +/- 4.52 MPa and for the CCL (40s) 15.79 MPa +/- 4.76 MPa. Their study used the same adhesive system as *James et al.*[8] but longer CCL cure time. *Lalani et al.*[3] presented mean shear bond strengths (n=37) that were similar to the ones in the present study. Using a higher intensity AL (approximately 800 mW/cm², 10s) system (ILT systems, Salt Lake City, UT) the authors demonstrated 11.32 MPa +/- 5.06 MPa. They reported similar bond strength (11.95 MPa +/- 3.71 MPa) with their CCL (approximately 400 mW/cm², 40s)

48

group. The energy density was not measured during the study, noted values were copied from the introduction section of the paper. A different bracket system was used (022 Roth Rx metal micromesh, "A" Company, San Diego, Calif) with 37% phosphoric acid and Transbond XT primer instead of the Self Etching Primer.

The present study was conducted under the assumption that the debonding force applied by the debonding pliers consists exclusively of shear force. The universal testing machine used in the other *in vitro* studies is a stable and rigid device capable of possibly producing pure shear debonding forces, whereas the debonding device used in the present study may be a combination of debonding forces, eg shear, peel, bending and tensile forces. In addition, the rate of loading for the universal testing machine is constant, whereas the rate of loading for the debonding device is not standardized or constant due to its clinical application. The blinded investigator (DS) was instructed to standardize the debonding procedure as much as possible under the clinical condition. No adjustments can be made on the wire-sling or pliers that could imitate an adjustment to the crosshead speed. However, the similarity between the mean bond strength recorded in *Pickett's study*[10] using the debonding device *in vitro* (11.02 MPa +/- 4.49 MPa) and the mean bond strength recorded using the universal testing machine (12.82 MPa +/- 3.05 MPa) suggests that a debonding device may be a useful tool for measuring bond strengths *in vivo*.[10]

Although the mean bond strengths measured in each *in vitro* study vary, the reported bond strengths are similar for brackets cured with the AL compared to the CCL. Both the AL group and the CCL control produced bond strengths which exceeded the suggested minimum bond strength (2.8 MPa) for clinical orthodontic treatment.[9]

The bond strengths recorded *in vivo* following orthodontic treatment were

significantly lower (P = 0.000) than the bond strengths recorded *in vitro* for both Curing Methods. Possible reasons for the lower bond strengths recorded *in vivo* could be the oral environment, exposing the bonded brackets to acid, saliva, patient abuse, and masticatory forces.[11] Biodegradation is the result of a combination of disintegration and dissolution in saliva, chemical and physical degradation, wear caused by chewing food, erosion by the food itself, and bacterial activity.[12] Biodegradation of the adhesive can contribute to the failure of the bond between the bracket and the tooth.[13] *Murray et al.*[14] proposed the following explanations for *in vitro* versus *in vivo* bond strengths:

1. Un-reacted composite acrylic leaches from the composite when it is immersed in water.

2. Water can hydrolyze the acrylic and this process is enhanced in saliva.

3. Composite degrades in the presence of food stimulants such as ethanol.

4. Nonspecific porcine liver esterases enhance degradation because of enzymatic hydrolysis.

5. Composite degrades in natural saliva *in vitro*, probably as a combination of hydrolysis and enzymatic hydrolysis.

6. Certain bacteria can consume composite using it as a source of carbon.

Oilo et al.[12] also reviewed the degradation process of composite materials in the mouth and stated that it is such a complex interaction of process that it cannot be reproduced *in vitro*. They concluded that the correlation between tests *in vitro* and the clinical situation has not been established and that there is a need to develop standardized *in vitro* and *in vivo* tests. The *in vivo* bond strengths reported in the present study would seem to be a more valid representation of the clinical performance of AL and CCL than

50

previous *in vitro* studies.

The output power of different curing devices seems to have an important role in the outcome of bond strength results. *Blankenau's*[15] results demonstrated that more output power is not better. Most of these differences can be explained by examining the chemistry of photo-initiated composites: The science of the curing process of photo-initiated composites involves free radical polymerization of a monomer. The benchmark monomer in dentistry is Bis-GMA which is chemically classified as an 'olgimer' rather than a monomer. The reactive groups of interest on Bis-GMA are the carbon to carbon double bonded 'ethene' groups on either end. In photo-initiated dental composites, light is the initiator and the accelerator is almost always camphorquinone.

The reaction site on camphorquinone is either of the two ketone groups. The first step in this polymerization reaction is the initiation step, photo-reduction of camphorquinone. The usable wavelengths (around 488 nm) are absorbed by camphorquinone, which provides the specific energy to generate a triplet state free radical. Once a stable free radical is formed it will react with the monomer and begin polymerization.

This sequence in polymerization is termed the propagation step. The reaction repeats itself over and over. The more it is repeated, the longer the chain. Longer chains have stronger physical properties than do shorter chains. This propagation step continues until two free radicals collide. In this event the two free radical electrons form a bond that terminates the polymerization sequence. This step is aptly termed the termination step. The rate at which this termination reaction happens is critical. If the termination reaction was to occur after 'polymerizing' only one Bis-GMA molecule, the chain would be very short and the cured composite would be very weak. The rate of

51

termination must be slow enough to allow propagation and thereby polymerization to continue long enough to make very large chains which, in turn, will produce the strongest possible physical properties for the composite.

Two major factors play a role in the rate of termination. The first is a constant that takes into account such variables as molar concentration of the monomer and the diffusion rate of the molecules through the solvent. When this constant is calculated one critical variable is commonly held constant and that is temperature. As the temperature increases, motion through the solvent increases. This has the positive effect of increasing the rate of the propagation, however, it also increases the rate of the termination. *Pradhan* et al.[16] confirmed that under similar conditions, the AL resulted in a lower temperature rise in the composite than the CCL.

It is in this rate constant that the unwanted and unneeded wavelengths discussed earlier could play a role in decreasing the physical strengths of the composite by increasing the termination rate. The second major factor in the kinetics of this reaction is the concentration of the free radical. If the composite is exposed to high power levels (more photons) of the correct wavelength (430-500 nm) virtually all of the camphorquinone will be turned into free radicals very quickly. With such a high concentration of the free radical present the termination rate will be extremely fast and the composite will contain, almost exclusively, the shorter and thereby weaker polymers. This will result in poor physical properties for the post-cured composite.

In summary previous research suggests that using the AL to cure composite bonding material results in a much shorter curing time compared to CCL with the advantage of having enhanced post-cure physical performance. Longer chains can be

52

formed due to less free radicals to initiate the termination phase pre-maturely. There are fewer free radicals because of the reduced power output (CCL: 400-800 mW; AL: 200-300 mW), the amount of unwanted and unneeded wavelengths, less curing time, and less temperature increase within the composite by usage of the AL.[16]

Another interesting aspect is based on the observation that the reported enhancement of physical properties achieved by laser polymerization may become less significant with aging of the cured resin.[17]When diametral tensile strength values for a hybrid resin were compared over time, AL activation resulted in higher early values than CCL curing, but these differences essentially disappeared at 20 days. Because the reaction of polymerization continues after initiation, the samples cured with the CCL units increased in strength over the 20-day period.[17]

Kelsey et al.[32] conducted a carefully controlled laboratory study to determine the optimum power setting and polymerization cycle time to cure four commercially available composite resins with an AL. Most effective resin polymerization was achieved when Prisma APH was polymerized (310 mW) for 7 seconds, when Herculite was polymerized (160 mW) for 12 seconds, when P-50 was polymerized (525 mW) for 13 seconds and when Silux Plus was polymerized (270 mW) for 13 seconds. The authors concluded that the exact parameters of laser power and exposure time seem to be material specific, with greater variation being noted in power setting than in exposure time. *Talbot et al.*[2] could see a significant difference ($P<0.001$) between bond strength values at 3 different laser energies (200, 230, and 300 mW). Therefore it seems that the power setting is a major factor in the outcome of bond strength values. No literature could be found addressing the optimal power setting for Transbond XT adhesive used for the APC

brackets.

The exposure time of 10 seconds was chosen based on two reasons. First, the Lasermed AL used in this study has an audible signal after 5 seconds of curing, which makes precise 10 seconds curing time easy to achieve for each specimen. Secondly, *Featheringham's*[33] study reported that AL curing at 4 seconds resulted in mean shear bond strength *in vitro* that were significantly lower than when cured for 6, 8, or 10 seconds.

2.4.2 ARI & Enamel Fracture

In this study the ARI was used to characterize the site of bond failure. The failure sites for metal brackets has been identified as the adhesive/bracket interface.[18] No correlation could be found in the present study indicating that a particular site of bond failure is related to a high or low bond strength values. For both AL and CCL groups the failure sites for the majority of brackets were a combination of both the adhesive/bracket and enamel/bracket interface with more adhesive remaining on the base of the bracket than the tooth.

In contrast to the findings of the present study, *James et al*[8] reported more adhesive remaining on the tooth surface in the AL group than their CCL group. The bond failure site in their CCL group was similar to the present study's CCL group. *Ireland et al.*[19] found less bond strength with the Self Etching Primer and therefore concluded that, it might be expected that the locus of the bond failure would more likely be at the adhesive/enamel interface, with less adhesive remaining on the enamel surface at debonding. The present study supports this theory in terms of the location of adhesive remnants in part because most of the failure sites were found at the enamel interface with

54

less than half of the adhesive on the enamel surface (score 1), but the second highest score was reached by score 2 and not 0.

2.4.3 Tooth selection

Previously published studies suggest the failure rates of brackets on premolar teeth are higher than on incisors or canines.[20] The reason for choosing premolar teeth for the present study was based on the fact that these teeth are the most likely to be extracted during orthodontic treatment and could therefore be evaluated intra- and extra-orally. No failure occurred on any of the premolar teeth used in the present study.

Mattick et al.[22] summarized the theories that explain the different failure rates in relation to the different teeth and location: The prismless enamel tends to be more common, and to a greater depth, on posterior teeth.[23] During etching the bonding areas of posterior teeth are thought more likely to become contaminated with salivary proteins,[24] or to be adversely affected by higher levels of humidity.[25] The bracket bases of posterior teeth may have poorer adaptation to tooth surface.[26] Molar regions are exposed to greater masticatory forces[27] and there may be a difference in the etch pattern of anterior and posterior teeth.[28] *Hobson et al.'s*[29] study showed indeed that there is a significant difference in the quantities and definition of etch pattern between the 12 human tooth types. They made clear that researches studying the bonding of brackets should no longer assume that any one tooth type is representative of the dentition as a whole. As suggested by *Hobson* the potential difference in bond strength for different teeth was taken into account in the present study and only one tooth type was used. The present study did not identify any bond strength difference between maxillary and mandibular premolars.

Previous research has demonstrated bond strengths of younger permanent teeth

55

are less than those of older permanent teeth.[30] To avoid age as a confounding variable the inclusion criteria for the present study was adolescent permanent teeth.

2.5.4 Storage solution and time span

The time span between bonding and debonding was set at 14 days for organizational reasons and a report[17] stating that tensile strength of composite resins cured with AL was more variable at one day after curing than 20 days after curing. The authors concluded that composite resin testing protocols should be lengthened to control time dependant variations.

Storage solution is used in *in vitro* experimental studies to prevent dehydration of teeth collected immediately after extraction and to prevent bacterial and fungal growth in the storage media. The chemical nature of the storing agent may affect the tooth structure and material properties at the tested interface. *Ziskind et al.*[34] evaluated the use of 0.1% cetylpyridinium chloride (CPC) as a new storage solution and to assess the possible effect of 0.1% thymol on microleakage and bond strength. Forty extracted human teeth were collected from 10 different dental clinics. Immediately after extraction, the teeth were randomly divided and immersed in four different storage solutions. Two test solutions of 0.1% CPC and 0.1% thymol were compared with phosphate-buffered saline and to 3% H_2O_2. Bond strength test and dye penetration evaluation were then carried out. The findings suggest that the use of 0.1% CPC as storage solution does not affect bond strength to enamel. The effect of 0.1% thymol on shear bond strength and dye penetration is similar to the effect of phosphate-buffered saline which was used as a positive control sample.

The present study chose the thermal cycling process of 1000 cycles. Most samples

56

in previous studies of orthodontic adhesive were not thermal cycled. Studies in restorative dentistry have shown that thermal cycling can decrease bond strength by 20 – 70%.[35] *Buonocore*[36] advised thermal cycling of the specimens to assess the durability of the bond. Otherwise, he warned, that "such results may not be indicative of the effect on the bond strength of long-term immersions under oral moisture conditions."

2.4.5 Bracket and Bonding material selection

Self-etching primers (SEP) have been introduced to simplify the orthodontic bonding process. The new self-etch primer systems combine conditioning and priming agents into a single application, making the procedure more cost-effective.[37] SEP was utilized in this study to achieve a more consistent bonding procedure.

Grubisa et al.[38] compared the *in vitro* shear bond strength of Transbond Self Etching Primer (SEP) (3M Unitek, Monrovia, CAL) and Transbond XT with 35% phosphoric acid (PA) and Transbond XT beside others. They reported lower bond strengths with SEP than conventional PA etching protocols, but both approaches provided clinically adequate bond strengths. *Ireland et al.*[19] compared the effectiveness of the same SEP (Transbond Self Etching Primer, 3M Unitek, Monrovia, CAL) with conventional etching (37% phosphoric acid (15-30s)) and priming with (Transbond XT Primer, 3M Unitek, Monrovia, CAL) *in vivo*. This study produced weak evidence to suggest that bond failures with a SEP will be higher than those with conventional etching and priming.

Pre-coated metal brackets (Victory series APC brackets, 3M, Monrovia, CAL) were utilized because no mixing and application of the adhesive to the bracket base is necessary. This likely results in less opportunity to contaminate the base, less variation

57

between the bonding material application process, and more consistent bond strength results compared to studies using non pre-coated metal brackets. [8]Kula et al.[20] concluded that the APC Mini Twin bracket system and Transbond XT adhesive are equally effective in maintaining brackets clinically. In contrast, Bishara et al.[41] demonstrated that uncoated metal brackets bonded with Transbond XT had significantly higher bond strength than brackets pre-coated (APC) with Transbond. The explanation was thought to be found in the adhesive used on the pre-coated brackets which is generally speaking similar in composition to that used for bonding uncoated brackets. The dissimilarity is based on the difference in percentages of the various ingredients incorporated in the material. According to the manufacturers, the Transbond XT and the APC Transbond XT include approximately 77% and 80% quartz (silica) filler, respectively.[8]

58

2.5 Conclusions

1. No statistically significant difference was found between the bond strength of argon laser cured (10s) brackets and the conventional light cured (40s) brackets.

2. *In vivo* bond strengths results are significant (P = 0.000) lower than *in vitro* bond strengths results.

3. No significant difference exists in bond strength between mandibular versus maxillary premolar teeth.

4. No significant difference was determined in bond strength between premolars originating from male versus female subjects.

5. There is a significant (P = 0.001) difference of the ARI scores between the curing methods and no significant correlation between the mean bond strengths and ARI scores.

6. The same minimal amount of enamel fracture was found between the curing methods.

59
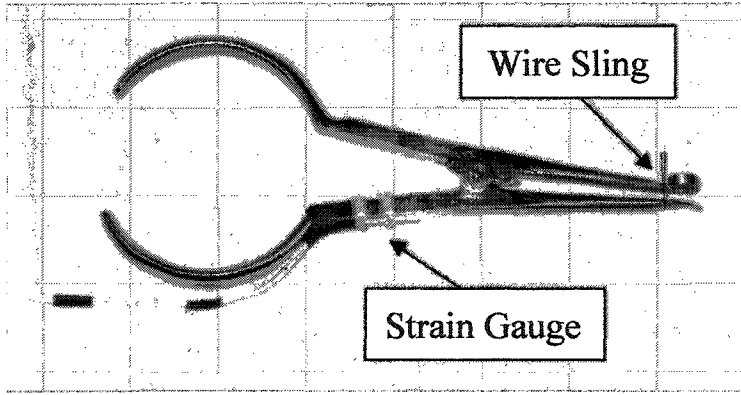
Figure 2.1 **Debonding Pliers with Strain Gauge**

60
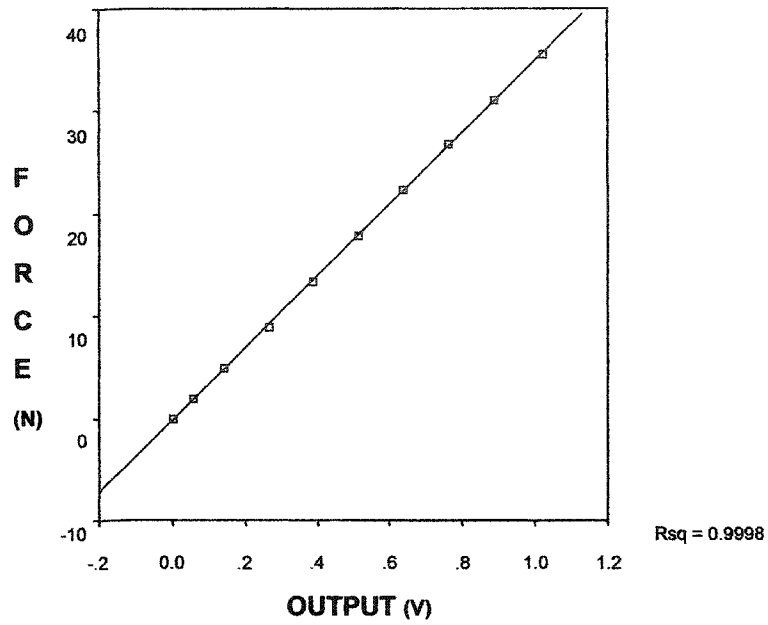
Figure 2.2 **Calibration Graph:** A known force (N) was applied to the debonding pliers on the wire sling and the output of a strain gauge circuit was measured (V). Least squares regression analysis was performed and the following equation was determined:

Force (N) = 35.113 x (V) – 0.158
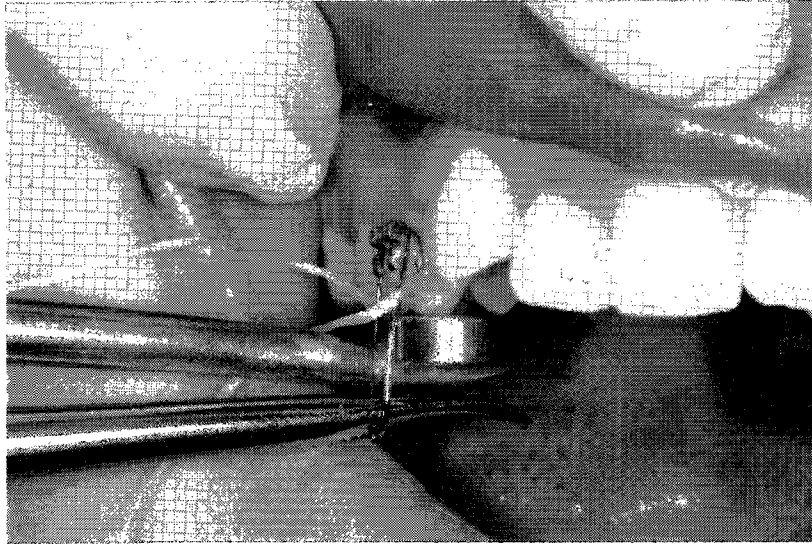
Figure 2.3   Debonding pliers during *in vivo* study: The wire sling is looped around the gingival tie wings of the bracket and the occlusal surface of the premolar is contacting the platform. The wire sling is positioned parallel to the long axis of the tooth and the pliers' arms are placed perpendicular to the long axis of the tooth. A steadily increasing force is applied to the pliers' handles which separates the pliers' arms and translates a force onto the bracket until it is detached. The dental floss attached to the bracket serves as a security measure to prevent loss of the bracket.
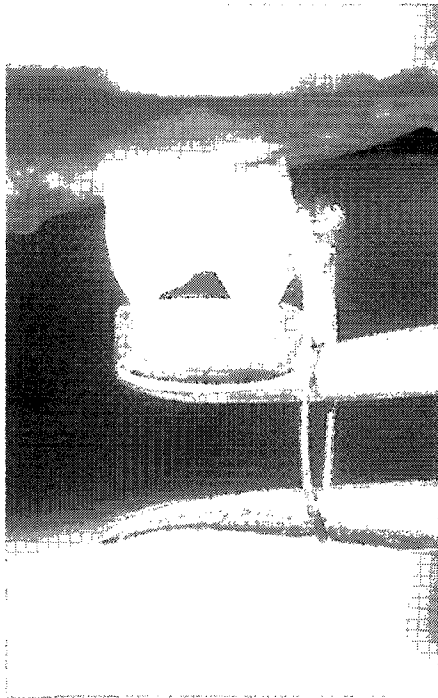
Figure 2.4   *In vitro* debonding procedure

62

Table 2.3   MANOVA for the Comparison of the Differences in
              the Gender and Study Type group

Effect	P-value
Gender	0.457
Study Type	0.006*

* P-value of less than 0.050 is considered statistically significant

Table 2.4   Pairwise comparison of the difference in Location*

Curing method	Location	Mean Bond Strength (MPa)	Standard Deviation	Range (MPa)	P-value
AL	Maxilla	11.26	3.62	3.89-17.54	0.579
AL	Mandible	10.96	2.81	5.49-15.53	0.579
CCL	Maxilla	10.60	2.92	3.76-15.35	0.313
CCL	Mandible	10.89	2.86	5.29-17.95	0.313

*Based on 48 measurements for each of the four groups

* P-value of less than 0.050 is considered statistically significant

Table 2.5   Pairwise comparison of Curing Type (Study Type
              separately; Location combined)

Curing Method	Sample Size	Mean Bond Strength	Standard Deviation	P-value
Argon laser	50[1]	12.25	2.89	0.603
Conv. Light	50[1]	12.06	2.15	0.603
Argon laser	45[2]	10.11	2.81	0.173
Conv. Light	46[2]	9.30	2.93	0.173

P-value of less than 0.050 is considered statistically significant

[1] = in vitro; [2] = in vivo

64

Table 2.6   Pairwise comparison of the Study Type (Curing method separately)

Curing Method	Study Type	Mean Difference	P-value
Argon Laser	In vitro	2.14	0.000*
	In vivo		
Conv. Light	In vitro	2.76	0.000*
	In vivo		

* P-value of less than 0.050 is considered statistically significant

Table 2.7   Distribution of ARI Scores and Average Bond Strength within the Scores for the Argon Laser group.

ARI Score	Distribution	%	Mean Bond Strength (MPa)	Standard deviation (MPa)
0	6	6.32	10.28	3.77
1	47	49.47	11.04	3.12
2	40	42.11	11.65	2.90
3	2	2.11	10.44	2.10

0 = No adhesive on the tooth; 1 = Less than half of the adhesive on the tooth; 2 =More than half of the adhesive on the tooth ; 3 = All of the adhesive on the tooth

Table 2.8   Distribution of ARI Scores and Average Bond Strength within the Scores for the Conv. Curing Light group.

ARI Score	Distribution	%	Mean Bond Strength (MPa)	Standard deviation (MPa)
0	12	12.5	10.34	2.78
1	65	67.7	10.80	2.96
2	15	15.63	11.14	2.98
3	4	4.17	9.49	1.52

0 = No adhesive on the tooth; 1 = Less than half of the adhesive on the tooth; 2 =More than half of the adhesive on the tooth ; 3 = All of the adhesive on the tooth

Table 2.9   Chi-Square Test on ARI scoring between Study Method

	P-Value
Pearson Chi-Square	0.001*

*P-value of less than 0.050 is considered statistically significant

Table 2.10   Differences in Bond Strength among ARI

Curing Method	P-Value
Argon Laser	0.649
Conv. Curing Light	0.733

*P-value of less than 0.050 is considered statistically significant

2.6 Bibliography

1. Oesterle LJ, Newman SM, Shellhart WC: Comparative bond strength of brackets cured using a pulsed xenon curing light with 2 different light-guide sizes. Am J Orthod Dentofacial Orthop 2002 Sept.; 122:242-50

2. Talbot TQ, Blankenau RJ, Zobitz ME, Weaver AL, Lohse CM, Rebellato J: Effect of argon laser irradiation on shear bond strength of orthodontic brackets: An in vitro study. Am J Orthod Dentofacial Orthop 2000;118: 274-9

3. Lalani N, Foley TF, Voth R, Banting D, Mamandras A: Polymerization with the argon laser: curing time and shear bond strength. Angle Orthod 2000 Feb; 70(1):28-33

4. Powell GL, Anderson JR, Blankenau RJ: Laser and curing light induced in vitro pulpal temperature changes. J Clin Laser Med Surg 1999 Feb; 17(1):3-5

5. Cobb DS, Dederich DN, Gardner TV: In vitro temperature change at the dentin / pulpal interface by using conventional visible light versus argon laser. Lasers Surg Med 2000; 26(4):386-97

6. Anic I, Pavelic B, Peric B, Matsumoto K: In vitro pulp chamber temperature rises associated with the argon laser polymerization of composite resin. Lasers Surg Med 1996; 19(4):438-44

7. Renneboog-Squilbin C, Nammour S, Coomans D, Barel A, Carleer-Dourov N: Measurement of pulp temperature increase to externally applied heat (argon laser, hot water, drilling). J Biol Buccale 1989 Sep;17(3):179-86

8. James JW, Miller BH, English JD, Tadlock LP, Buschang PH.: Effects of high-speed curing devices on shear bond strength and microleakage of orthodontic brackets. Am J Orthod Dentofacial Orthop 2003(123):555-61

9. Reynolds IR: A Review of Direct Orthodontic Bonding. Br J Orthod. 1979(2):171–178

10. Pickett KL, Sadowsky PL Jacobson A, Lacefield W: Orthodontic In Vivo Bond Strength: Comparison with In Vitro Results, Angle Orthod 2001; 71(2):141-8

11. Monseau Anderson A, Kao E, Gladwin M, Benli O, Ngan P: The effect of argon laser irradiation on enamel decalcification: An in vivo study. Am J Orthod Dentofacial Orthop 2002Sept.; 122:251-9

12. Oilo G: Biodegradation of dental composite/glass ionomer cements. Adv Dent Res 1992; 6:50-4

13. Matasa CG: Microbial attack of orthodontic adhesives. Am J Orthod Dentofacial Orthop. 1995 Aug; 108(2):132-41

14. Murray SD, Hobson RS: Comparison of in vivo and in vitro shear bond strength. Am J Orthod Dentofacial Orthop 2003; 123:2-9

15. Blankenau RJ: Post-cure physical properties of a composite. Data on file at LaserMed 1995 (website: www. lasermed.com)

16. Pradhan RD, Melikechi N, Eichmiller F: The effect of irradiation wavelength bandwidth and spot size on the scraping depth and temperature rise in composite exposed to an argon laser or a conventional quartz-tungsten-halogen source. Dent Mater. 2002 May; 18(3):221-6

17. Blankenau RJ, Powell GL, Kelsey WP, Barkmeier WW: Post polymerization strength values of an argon laser cured resin. Lasers Surg Med. 1991;11(5):471-4

18. Ireland AJ, Knight H, Sheriff M: An in vivo investigation into bond failure rates with a new self-etching primer system. Am J Orthod Dentofacial Orthop 2003; 124:323-6

19. Klocke A, Korbmacher HM, Huck LG, Ghosh J, Kahl-Nieke B: Plasma arc curing of ceramic brackets: An evaluation of shear bond strength and debonding characteristics. Am J Orthod Dentofacial Orthop 2003; 124: 309-15

20. Kula K, Schreiner R, Brown J, Glaros A: Clinical bond failure of pre-coated and

operator-coated orthodontic brackets. Orthod Craniofac Res. 2002 Aug;5(3):161-5

21. Linklater RA, Gordon PH: Bond failure patterns in vivo. Am J Orthod Dentofacial Orthop. 2003 May;123(5):534-9

22. Mattick CM, Hobson RS: A Comparative Micro-topographic Study of the Buccal Enamel of Different Tooth Types. J Orthod 2000 27: 143-148

23. Whittaker DK: Structural variations in the surface zone of human tooth enamel observed by Scanning Electron Microscopy. Archives of Oral Biology 1982; 27, 383–392

24. Hormati AA, Fuller JL, Denehy GY: Effects of contamination and mechanical disturbance on the quality of acid etched enamel. Journal of the American Dental Association 1980; 100, 34–8

25. Mardaga WJ, Shannon IL: Decreasing the depth of etch for direct bonding in orthodontics. Journal of Clinical Orthodontics, 1982; 16, 130–132

26. Evans ZB, Powers JM: Factors affecting in-vitro bond strength of no mix orthodontic cements. Am J Orthod Dentofacial Orthop 1985; 87, 508–512.

27. Zachrisson BU: A post-treatment evaluation of direct bonding on Orthodontics, J Orthod Dentofacial Orthop 1977; 71: 173–189

28. Johnston CS, Hussey DL, Burden DJ: The effect of acid etch duration on the microstructure of molar enamel: an in vitro study. Am J Orthod Dentofacial Orthop 1996; 109, 521–534

29. Hobson RS, McCabe JF, Rugg-Gunn AJ: The relationship between acid-etch patterns and bond survival in vivo. Am J Orthod Dentofacial Orthop. 2002 May;121(5):502-9

30. Sheen DH, Wang WN, Tang TH: Bond strength of younger and older permanent teeth with various etching times. Angle Orthod 1993; 63:225-9

31. Fox, NA, McCabe JF, Gordon PH: Bond strengths of orthodontic bonding materials: an in vitro study. British J Orthod 1991 (18): 125–130

32. Kelsey WP, Blankenau RJ, Powell GL, Barkmeier WW, Cavel WT, Whisenant BK: Enhancement of Physical Properties of Resin Restorative Materials by Laser Polymerization. Lasers Surg Med 1989; 9:623-7

33. Featheringham DA: Comparison of three curing light systems for polymerization of orthodontic adhesive: an in vivo study. AJODO 2001; 120(3): 331-2

34. Ziskind D, Gleitman J, Rotstein I, Friedman M: Evaluation of cetylpyridinium chloride for infection control in storage solution. J Oral Rehabil. 2003 May;30(5):477-81

35. Diaz-Arnold AM, Aquilino SA: An evaluation of the bond strengths of four organosilane materials in response to thermal stress. J Prosthet Dent 1989; 62:184-9

36. Buonocore MG: Retrospectives on bonding. Dent Clin North Am 1981(25):241-55

37. Oonsombat C, Bishara SE, Ajlouni R: The effect of blood contamination on the shear bond strength of orthodontic brackets with the use of a new self-etch primer. Am J Orthod Dentofacial Orthop. 2003 May;123(5):547-50

38. Grubisa H, Heo G, Faulkner G, Raboud D, Glover K, Major P: A Bonding Study of Orthodontic Brackets Using Self-Etching Primer. MSc thesis 2002; Edmonton, AB: University of Alberta

39. Bishara SE, Oonsombat C, Ajlouni R, Denehy G: The effect of saliva contamination on shear bond strength of orthodontic brackets when using a self-etch primer. Angle Orthod. 2002 Dec; 72(6):554-7

40. Cacciafesta V, Sfondrini MF, De Angelis M, Scribante A, Klersy C: Effect of water and saliva contamination on shear bond strength of brackets bonded with

conventional, hydrophilic, and self-etching primers. Am J Orthod Dentofacial Orthop. 2003 Jun;123(6):633-40

41. Bishara SE, Olsen M, VonWald L: Comparison of shear bond strength of precoated and uncoated brackets. Am J Orthod Dentofacial Orthop 1997; 112: 617-21

Chapter Three

Research Paper Two

X-ray Photoelectron Spectroscopy: A Preliminary Evaluation of the Chemical Characteristics of Argon Laser Irradiated Human Enamel Surface

3.1 Introduction

One of the most frequently encountered negative aspects of bracket bonding is the appearance of localized decalcification around the bracket base, referred to as "white spot" lesion.[1] These lesions are primarily caused by inadequate oral hygiene and poor diet control. Additional factors include increased susceptibility to caries due to dissolution of the highly calcified prismless enamel by acid etching[2] and by a reduction of self-cleansing activity in the area around the bracket base.[3] Despite the advances in orthodontic materials and techniques in recent years, the development of decalcifications around the brackets during orthodontic treatment continues to be a problem. Nearly 50% of orthodontic patients exhibit clinically visible white spot lesions during treatment lasting approximately 2 years.[4] These white spot lesions are due to demineralization of the enamel by organic acids produced by cariogenic bacteria.[5] Preventing these lesions during treatment is an important concern for the orthodontist, because the lesions are unaesthetic, unhealthy, and potentially irreversible.[6] The white spot lesion is the early carious lesion. Mineral content fluctuates as intraoral conditions change in respect to the development and maturation of bacterial plaques. Decalcification is an episodic process with alternating phases of demineralization and remineralization.[7] The efflux and influx of minerals is affected by several factors including the duration of time of a low oral pH, the presence of fluoride, the contents and concentration of saliva, the concentration and virulence of oral bacteria, the frequency of sucrose ingestion[8] and possibly the morphology of the enamel surface.

Mature enamel is a crystalline structure, containing up to 96% inorganic material

73

by weight and consists primarily of calcium hydroxyapatite $(Ca_{10}(PO_4)_6(OH)_2)$. The remainder of the enamel is made up of 3 % water and 1 % organic matter including proteins and lipids. Pure hydroxyapatite (Figure 3.1) does not occur on a macroscopic scale in biological systems. Enamel is instead made from a Ca-deficient and carbonate-containing apatite analogue. Carbonate can substitute for the OH groups, but this is only believed to occur on a minor scale. Instead the planar CO_3^{2-} group mainly substitutes for the PO_4^{3-}. Charge neutrality is thought to be maintained via calcium deficiency either by Ca^{2+} absences or by substitution with Na^+.[9]

Surface analysis is the use of microscopic chemical and physical probes that provide information about the surface region of a sample. The probed region may be the extreme top layer of atoms, or it may extend up to several microns beneath the sample surface, depending on the technique used. The analysis is performed to provide information about such characteristics as the chemical composition, the level of trace impurities, or the physical structure or appearance of the sampled region.

One potential tool to evaluate the chemical structure of surface enamel is X-ray photoelectron spectroscopy (XPS), also known as electron spectroscopy for chemical analysis (ESCA).[10] With XPS, samples are irradiated with monochromatic X-rays (Figure 3.2) which cause the ejection of photoelectrons from the surface atoms. The electron binding energies, as measured by a high-resolution electron spectrometer, are used to identify the elements present and, in many cases, provide information about the valence states or chemical bonding environments of the elements thus detected. The depth of the analysis, typically the outer 3 nm of the sample, is determined by the escape depth of the photoelectrons and the angle of the sample plane relative to the spectrometer.

The x-ray source beam is directed towards the enamel surface region to be analyzed and is utilized to excite electrons from the core-level orbitals of the atoms. The energy of a photon (hv) consists of the Planck constant ($h = 6.62 \times 10^{-34}$ Js) and the frequency ($v = Hz$) of the radiation. The kinetic energies (E_K) of the emitted photoelectrons are characteristic of the element and atomic orbital from which they originate, being related to the binding energy (E_B) through the relationship: $E_B = hv - E_K$ (Figure 3.3). Once they are emitted, they are collected by an electron analyzer and are quantified according to their characteristic binding energy. These electrons are counted and plotted versus the characteristic binding energy to obtain a spectrum. This spectrum serves as a survey tool to determine the areas of interest which are further examined with high resolution scans.

In summary, XPS is a dedicated surface characterization technique that provides unparalleled spectroscopic information regarding surface composition and elemental oxidation states to quantify the surface composition. An appropriate data processing leads to the specimen elemental composition.

The purpose of the present pilot project was to determine whether any chemical changes are caused by the argon laser irradiation (60s), to achieve a proof of concept.

75

3.2 Material and Method

One feature of successful analysis of the XPS analysis consists of the presence of a certain level of vacuum. The central instrumental element of the XPS techniques is the energy analyzer. Before the energies of secondary electrons can be analyzed, the electrons must be ejected from the surface. This requires excitation from X-ray photon sources and an appropriate level of vacuum in the ambient around the surface and the analyzer. In addition, the sample whose surface is to be analyzed has to be inserted into the vacuum and transferred into the correct position for analysis after it has undergone surface treatment. In this case electrons traveling from the enamel surface towards the energy analyzer should encounter as few gas molecules as possible, otherwise they will be scattered and lost from the analysis.[11]

Another important aspect of this technique consists of surface contamination. XPS has a sampling depth of only a few atomic layers and is therefore highly surface specific. When taken with elemental sensitivities of the order of 0.3% of an atomic layer, this surface specificity implies that the techniques are sensitive to surface contamination. Pressure level can help to keep contamination levels low and under the acceptable rate of contamination (no more than 0.05 atomic layers in 30 min). Such a pressure level is the regime of ultra-high vacuum.[11] The maximum chamber pressure in the present study was 1.33×10^{-6} Pa.

Two extracted maxillary human premolar teeth were cleaned of tissue debris and stored in 0.1% thymol solution for 3 weeks before they were rinsed with distilled water and the buccal portions of the crown were separated from the rest of the tooth with a diamond disc. The dentinal layer was completely removed from the specimens with a

76

football shaped diamond bur. The sample named 2A60 was exposed to AL irradiation for 60 seconds; the specimen named 1C presented the control. The specimens were stored in distilled water for 2 days. The specimens were allowed to degas under high vacuum (298 K) for 48 hours and were exposed to the incident beam (Al$K\alpha$) for alignment and signal optimization for approximately 1 minute prior to analysis. The basic elements of an X-ray photoelectron spectrometer consist of the X-ray source, the energy analyzer, the detector and the data display (Figure 3.4).

The present XPS analysis was performed with an Kratos Axis 165 spectrometer (Kratos Analytical, Manchester, UK) using the Al$K\alpha$ source (1486.6 eV). The beam size on the enamel surface consisted of 1200 μm x 800 μm and the area size analysis was 700 μm x 300 μm. The total signal accumulation time per specimen was approximately 120-363 seconds.

During the XPS analysis, photoelectrons were excited with the monochromatic Al$K\alpha$ X-ray source, typically operating at 300-375 W. True source monochomatization can be achieved through crystal dispersion of the generated X-ray (Figure 3.2). The samples were exposed to the low-energy X-ray source, which causes the emission of photoelectrons from atomic shells of the elements present on the surface. These electrons possess an energy characteristic of the element and molecular orbital from which they are emitted. The electrons are detected and counted according to the energy they possess. By counting the number of electrons detected at each energy value (KE $< h\nu$), a spectrum of peaks corresponding to the elements on the surface is generated. Each characteristic binding energy is representative of a specific element (e.g. C1s - 284.6 eV; O1s - 532.5 eV). The peak area of each photoemission band is proportional to the number of atoms

77

being present in the studied element.

Quantitative data can be obtained from peak height or peak areas. Identification of chemical states often can be made from exact measurements of peak positions and separations, as well as from certain spectral features. For insulating samples the coaxial charge neutralizer was used. In such cases, the spectra were charge corrected to C 1s hydrocarbon component at 285.0 eV binding energy. A survey scan and high resolution scans were performed for the elements: Oxygen, Carbon, Calcium, Phosphorus, and Nitrogen for each sample.

The analysis methods used were:

- Peak shape and background method: Following a linear-type background subtraction, the individual photoemission features were fitted with representative Gaussian distributions using least-squares optimization. The peak positions, amplitudes, and full width at half maximum parameters were obtained from the Gaussian distribution analysis. The peak areas correspond to the area with respect to the background subtraction.

- Quantization method: The atomic concentrations were calculated using the algorithm and sensitivity factors contained in Kratos Analytical Software.

3.3 Results

In the spectroscopic nomenclature the number stated behind the element is the principal quantum number (0,1,2,3,...) followed by the electronic quantum number (s,p,d,f,...). It is conventional to identify a photoelectron feature in terms of the spectroscopic name of the atomic level from which the photoelectron was ejected.

78

The Figures 3.5 and 3.6 represent the survey scan for the control and irradiated sample. The area under the peaks is a measure of the relative amounts of each element present, while the shape and position of the peaks reflect the chemical environment of each element. The y-axis of the scans were stretched or skewed to allow for a comparable scale. Visual comparison of the control surface scan with the AL irradiated surface scan reveals a decrease in peak height for Oxygen 1s and Calcium 2s and 2p, and a slight increase in Carbon 1s.

The Tables 3.1 and 3.2 present the survey scan data for the control and treated sample respectively, in terms of the determined binding energy (BE, eV), the full width at half maximum (FWHW eV), the raw area in counts per second (CPS), the radial structure functions (RSF), the atomic mass, and the atomic concentration in percentage of the following elements: Sodium, Oxygen, Nitrogen, Calcium, Carbon, Sulfur, Phosphorus, and Silicon.

The visual perception is confirmed by the atomic concentration data. The control presents 30.93 % atomic concentration for the Oxygen 1s, compared to the irradiated sample of 25.75 %. On the present samples the atomic concentration for Oxygen 1s decreased by a percentage change of 16.75 %. In terms of the Carbon 1s atomic concentration between the samples, the irradiated sample presented an atomic concentration of 57.18 % compared to the control with 49.51 %. An increase by a percentage change of 15.49 % could be determined after irradiation with the AL. Calcium demonstrated a decrease by percentage change of 28.33 %.

High-resolution scans with increased resolution were obtained for each of the elements photoemission bands to identify the chemical state of each element. A high

79

resolution scan is conducted every 1/10 increments of the binding energy (eV) for a specific area of the survey scan. The high resolution scans generally confirmed the differences seen in the survey scan and provides information about the different chemical structure and oxidation state of the chemical compounds.

The high resolution scans for the O 1s are provided in Figure 3.7 and 3.8. The data from the high resolution scan for Oxygen can be reviewed in Table 3.3 and 3.4 and presents a decrease in atomic mass concentration of 7.99% (-10.63 % change) atomic concentration for the O 1s 1 and an increase of 7.99 % atomic mass concentration for the O 1s 2 (+24.36 % change) when the control is compared to the irradiated sample.

The scans for C 1s are provided in Figure 3.9 and 3.10. The Carbon scans were charge corrected referencing the primary C 1s band to 258.0 eV for adventitious Carbon. The comparison of the high resolution scan data (Table 3.5 and 3.6) between the control and the irradiated sample for Carbon uncovers a decrease of 2.42% (-4.62 % change) atomic concentration for C 1s CC,CH; an increase of 3.67% (+11.58 % change) for C 1s CO; almost equal numbers for C 1s CO_2; and a decrease of 1.33 % atomic concentration (-31.97% change) for C1s CO_3 after argon laser irradiation.

The scans for the Ca 2p are provided in Figure 3.11 and Figure 3.12. The survey scans (Figure 3.5 & Figure 3.6) present a difference between the peak heights of the Calcium 2p region and Phosphorus 2p. The irradiated sample reports less Ca 2p and P 2p than the control, which is confirmed with the high resolution scan of this region. The scans for Ca 2p can be reviewed in Figure 3.11 and Figure 3.12. The scans for P 2p are demonstrated in Figure 3.13 and Figure 3.14.

No change was detectable between the Nitrogen peaks in the survey scans (Figure

3.15 & Figure 3.16). The high-resolution scan of the Nitrogen 1s area reveals a minor increase in Nitrogen on the irradiated sample.

In summary, the chemical surface scan showed the composition of human tooth enamel: calcium hydroxyapatite with carbonate impurities and small amounts of other trace elements and organic materials. Inspection of the irradiated enamel surface showed a slight increase of Carbon and a slight decrease of Oxygen and Calcium. The main finding in the high resolution scans was a decrease of Carbonate.

3.4 Discussion

The intensities of signals observed in the XPS spectra depend upon the amount of material present, the efficiency of absorption of the exciting X-rays by the sample material, and the electron mean free path (MFP) in the sample material. The MFP is a function of sample composition and of the kinetic energy of the escaping electrons. Thus, the effective sample thickness may not be exactly the same for photoelectron peaks observed at different points in the spectrum. If these factors are understood or if good standards are available, quantitative analysis can be performed using XPS.[12]

Chemical shifts describe the systematic shifts in peak positions resulting from changes in the chemical structure and oxidation state of chemical compounds. The high-resolution scan of Carbon reveals that there are four fundamentally different kinds of Carbon (CC, CH; -CO; $-CO_2$; $-CO_3$). Each of these Carbons is in a different chemical environment and therefore exhibits a different chemical shift. Carbon in the most electronegative environment ($-CO_3$) appears at the highest binding energy (289 eV), because the electronegative Oxygen atoms withdraw electron density from the valence

81

and bonding orbitals of the Carbon atom. This reduces the screening of the core electrons from the nuclear charge and increasing their binding energy.[13] The survey scans demonstrate very minor increase in the height of the $C1s$ peak. The high-resolution scans of this area show differences between the two samples. A slight increase of Carbon in the second least electronegative environment (CO) is presented, which is suggested to arise from slightly different amounts of CO contamination from atmospheric exposure, rather than a significant increase due to sample treatment. However a chemical shift between CO, CO_2 and CO_3 is present. The ratio between CO and CO_3 in the control is approximately 7:1 (28.02 %:4.16%) and in the irradiated sample approximately 10:1 (31.69 %:2.83 %). The ratio between CO_2 and CO_3 in the control is approximately 4:1 (15.44 %:4.16%) and in the irradiated sample approximately 5:1 (15.53%:2.86%). Both ratios show a decrease in CO_3 and/or increase in CO and CO_2.

Carbonate is one of the main impurities found in calcium hydroxyapatite,[12] with an average content of 4% (range 2.7 – 5%) The results of the high resolution Carbon spectra revealed that the AL causes a slight chemical change in the composition of the enamel surface. The enamel surface temperature increase induced by the laser irradiation seems to cause alterations in the CO_3^{2-} content (Atomic Conc% = 2.86) compared to the control (Atomic Conc %= 4.16). *Holcomb et al.*[14] conducted a temperature change study on human enamel in the temperature range of 25-1000° C. Quantitative infrared spectroscopic, lattice parameter, and thermogravimetric measures were used. Loss of the CO_3^{2-} components begins at approximately 100 °C which has implications for treatments *in vitro* and possibly *in vivo*. Structural OH- content increases approximately 70 % to a maximum near 400 °C. Structurally incorporated water is lost continuously up to

82

approximately 800 °C. A "sudden" lattice parameter contraction, approximately 0.014 Å, occurs at a kinetics-dependent temperature in the 250-300 °C range and is accompanied by reordering and the "sharp" loss of approximately one third of the structurally incorporated H_2O.[13] It could be concluded that the temperature change caused by the AL on the enamel surface in the present study is likely around or slightly above 100°C, due to the fact that there is a minor loss of CO_3^{2-}. Thermal treatment shifts the apparent solubility distribution profile of human enamel toward lower apparent solubilities, paralleling the observed increased in crystal structural order and the decrease in initial dissolution rates.[15]

Fowler et al.[16] reviewed the changes in heated and in laser-irradiated human tooth enamel and their probable effects on solubility. Since the laser-induced changes are expected to primarily arise from localized heating, previously reported thermally induced changes in tooth enamel on heating in conventional furnaces were utilized to infer corollary changes along the gradient in laser-irradiated tooth enamel. These thermally inferred changes which resulted in modifications in the tooth enamel apatite and/or newly formed phases were correlated with their probable effects on altering solubility. A temperature gradient range from 100-1600 °C was considered with subdivisions as follows: I: 100-650 °C, II: 650-1100 °C, and III: greater than 1100 °C. Modifications in tooth enamel apatite affected in range I, which is the most likely range achieved by the AL irradiation in the present study, are expected to decrease its solubility. The formation of pyrophosphate in this range may have a substantial effect on reducing the solubility rate.[16]

The detected minor amount of Silicion found in the present study, which is

83

usually not detectable on the human enamel surface, is likely to originate from the specimen preparation stage. The specimens were rinsed with distilled water while resting in a sieve that was previously used to store silicon squares used for the fabrication of composite tooth holders. These were utilized in the shear bond strength testing part of the present study.

The examined surface enamel seems to be a carbonate-containing form of calcium hydroxyapatite since a relatively high amount of Carbon could be detected; one possible explanation could be based on Jones' statement, that human "enamel is made up from a Ca-deficient and carbonate-containing apatite analogue".[7]

Hydrogen is the only element present in enamel which can not be detected by XPS.[12] It is not known if the decrease in Oxygen is related to mainly the loss of CO_3^{2-} due to the heat generated by the argon laser irradiation or if an additional change in the superficial OH group concentration (Figure 3.1) takes place. The fact that "carbonate can substitute for the OH groups"[7] could explain the decrease in Oxygen and relative increase in Carbon. The ratios between O1s1 and O1s2 are 3:1 (75.19% : 24.81%) in the control and 2:1 (67.20% : 32.80%) in the irradiated sample. Either a decrease in O1s1 or an increase in O1s2 takes place due to the irradiation. It is possible but not conclusive that the O1s1 originates from the apatite structure, with O1s2 arising from the surface OH groups. If carbonate substitutes for OH groups an increase in O1s2 would not be present.

The question about origin of the additional carbon should be raised, if a true increase in Carbon exists, as well as the question about the fate of the decreased elements in particular Calcium. Changes in Carbon could arise from different amounts of contamination. During atmospheric exposure, CO and CO_2 can adsorb on the specimen

84

surface, depending on adsorption strength and degassing conditions. Adsorption is defined as the accumulation of molecules of a gas to form a thin film on the surface of a solid (surface assimilation).

One has to keep in mind that minor differences could be attributed to the samples itself. The samples are two different teeth, although they originate from the same patient and location (maxillary premolar), just on opposite sides (left / right).

3.5 Conclusion

Minimal changes in chemical composition appear to be present comparing the enamel surface exposed to argon laser irradiation for 60 s and the control. The change in chemical composition is not likely clinically relevant.

85
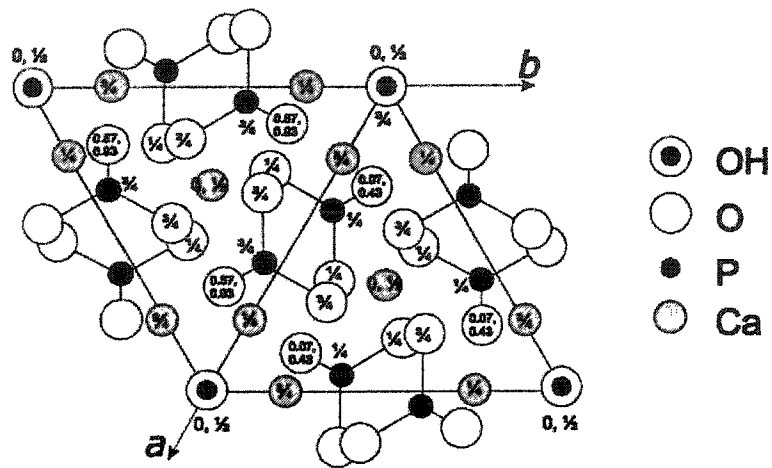
Figure 3.1 **The idealized crystal structure of hydroxyapatite, viewed along the c-axis.** Hydroxyapatite adopts the hexagonal structure with the OH groups ordered along the c-axis and Ca^{2+} occupying two different sites: positions on the corner of two 60° rotated triangles close in to the c-axis and positions at the corner of a hexagonal at a further distance from the c-axis. Pure Hydroxyapatite does not occur on a macroscopic scale in human enamel, instead made up from a Ca-deficient and carbonate containing apatite analogue. Carbonate can substitute for the OH groups, but this is only believed to occur on a minor scale. Instead, the planar CO_3^{2-} group mainly substitutes for the tetrahedral PO_4^{3-} (Jones FH. Surface Science Reports, 2001:86).

86
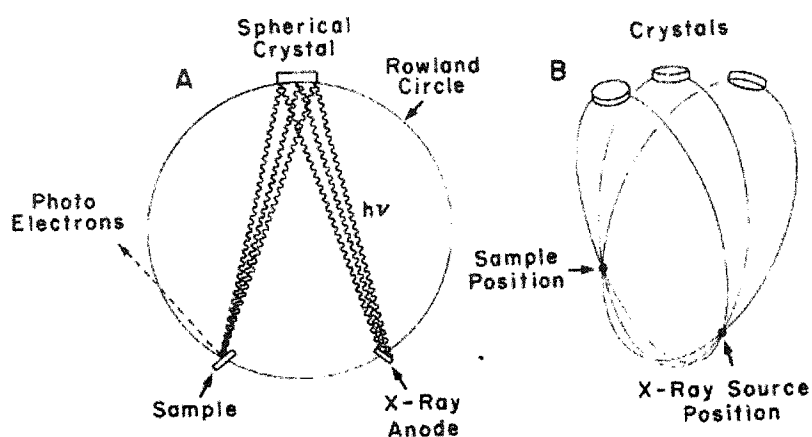
Figure 3.2 **Monochomatizing the X-ray source. (a) The basic elements of a crystal monochomator; (b) the three-crystal geometry utilized in a commercial application of this technique.** One of the objectives of instrument design is to effectively monochomatize the excitiation source. If its energy width can be reduced, a corresponding reduction in the line width of the resulting photoelectron peak will be obtained (Riggs WM, Parker MJ. Surface Analysis by X-ray Photoelectron Spectroscopy. Book: Methods of Surface Analysis. Elsevier Scientific Publishing Company, 1975: 128).

87

Photo Electrons

hν-E_b

hν
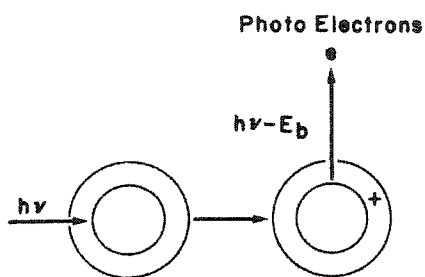
Figure 3.3 **X-ray Absorption.** X-ray photons ($h\nu$) from a nearly monoenergetic beam are directed onto the sample. The photons are absorbed by sample atoms with each absorption event resulting in the prompt emission of an electron. Electrons from all orbitals of the atom with a binding energy (E_b) less than the x-ray energy are excited, though not with equal probability. Thus, some peaks are more intense in the spectra than others. Since energy is conserved, the kinetic energy (K_E) of the electron plus the energy required to remove it from its orbital to the spectrometer vacuum must equal the X-ray energy. If the X-ray energy is known and the kinetic energy is measured with the electron spectrometer, the binding energy of the electron in the atomic orbital can be obtained.

$$E_b = h\nu - K_E$$

(Riggs WM, Parker MJ. Surface Analysis by X-ray Photoelectron Spectroscopy. Book: Methods of Surface Analysis. Elsevier Scientific Publishing Company, 1975: 107)

88
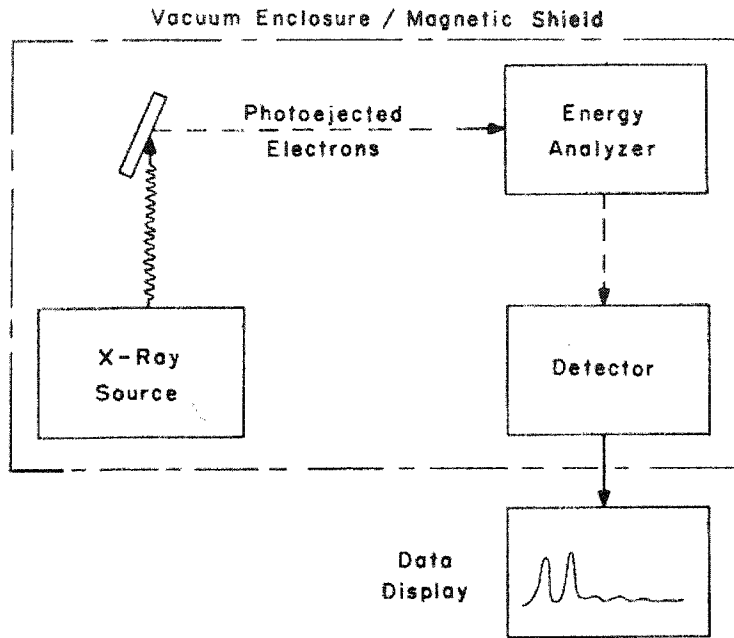
Figure 3.4   The basic elements of an X-ray photoelectron spectrometer. The function of the spectrometer is to produce intense x-ray radiation, irradiate the sample to eject photoelectrons, introduce the ejected electrons into an energy analyzer, detect the energy-analyzed electrons, and provide a suitable output of signal intensity as a function of electron binding energy (Riggs WM, Parker MJ. Surface Analysis by X-ray Photoelectron Spectroscopy. Book: Methods of Surface Analysis. Elsevier Scientific Publishing Company, 1975: 123).

89
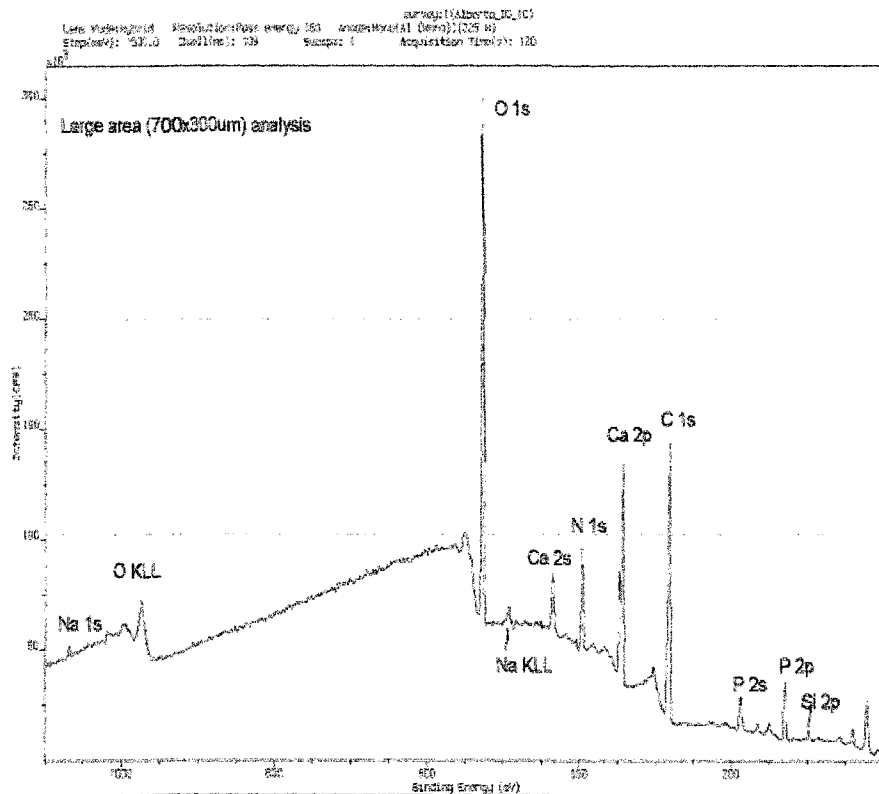
**Figure 3.5   Electron count plot versus Energy (energy spectrum)
of Sample 1C: Survey Scan**
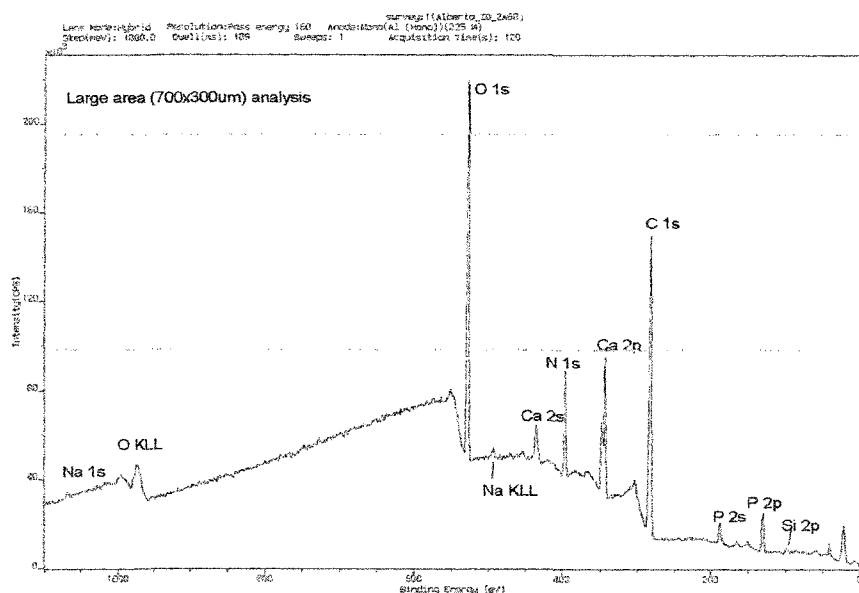
**Figure 3.6   Electron count plot versus Energy (energy spectrum)
of Sample 2A60: Survey Scan**

90
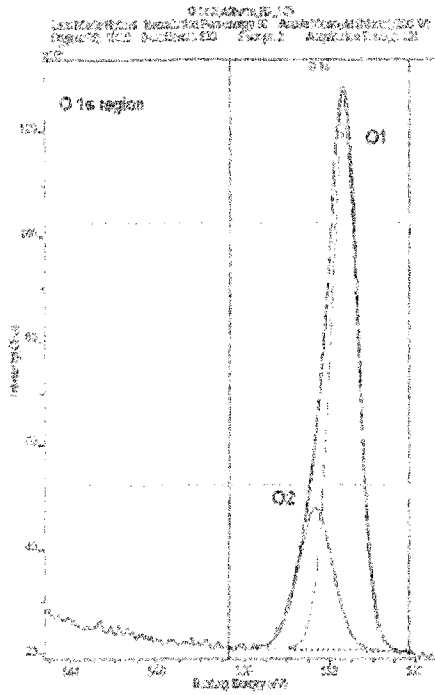
Figure 3.7   Electron count plot versus Energy (energy spectrum):
High resolution Scan of Oxygen for Sample 1C (Control)
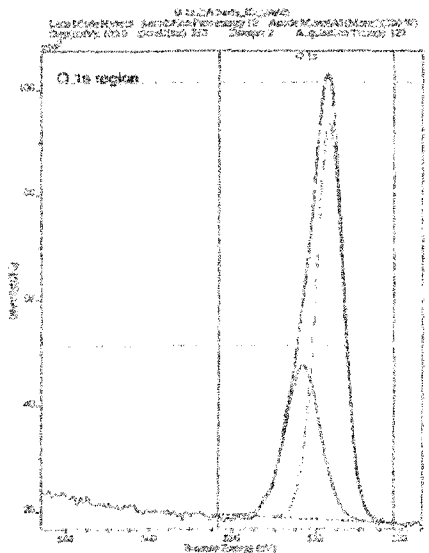
Figure 3.8   Electron count plot versus Energy (energy spectrum):
High resolution Scan of Oxygen for Sample 2A60 (AL 60s)

91
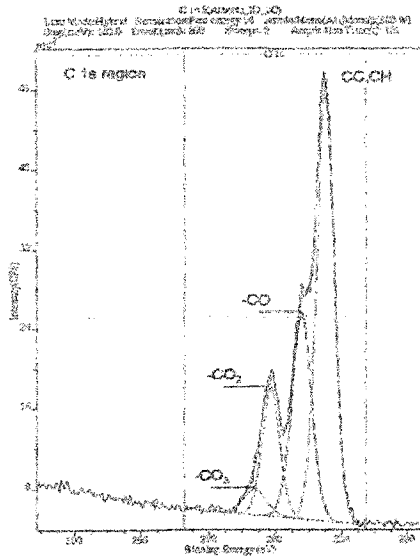
Figure 3.9 Electron count plot versus Energy (energy spectrum): High resolution Scan of Carbon for Sample 1C (Control)
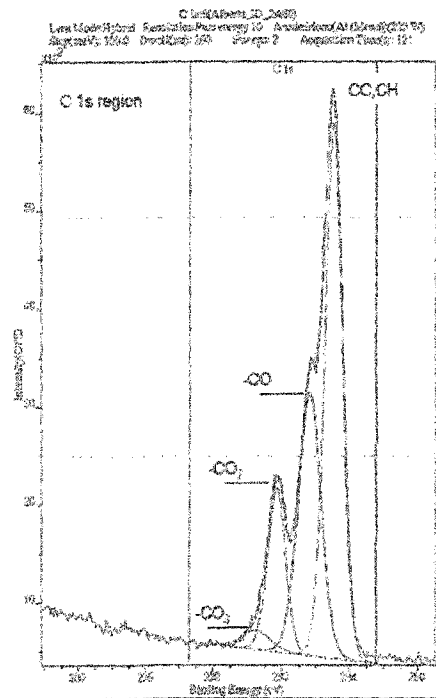
Figure 3.10 Electron count plot versus Energy (energy spectrum). High resolution Scan of Carbon for Sample 2A60 (AL 60s)

92
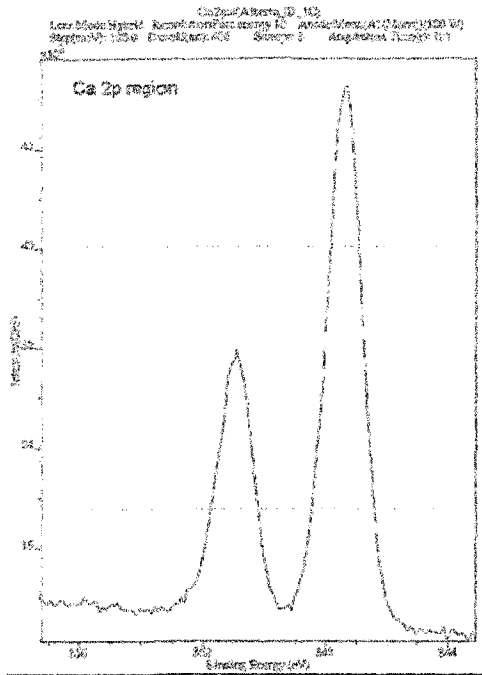
Figure 3.11   Electron count plot versus Energy (energy spectrum): High resolution Scan of Calcium 2p for Sample 1C (Control)
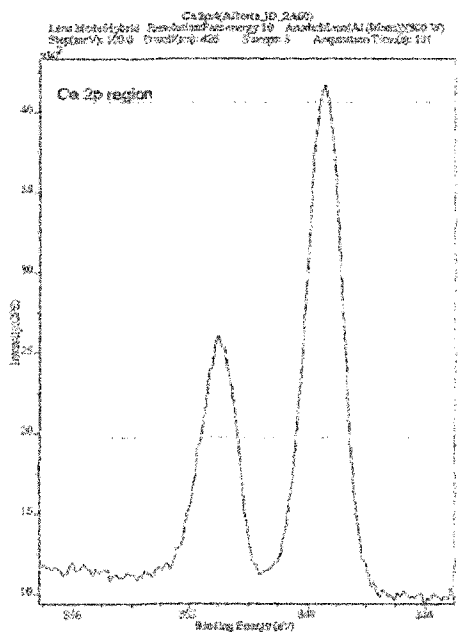
Figure 3.12   Electron count plot versus Energy (energy spectrum): High resolution Scan of Calcium 2p for Sample 2A60 (AL 60s)

93
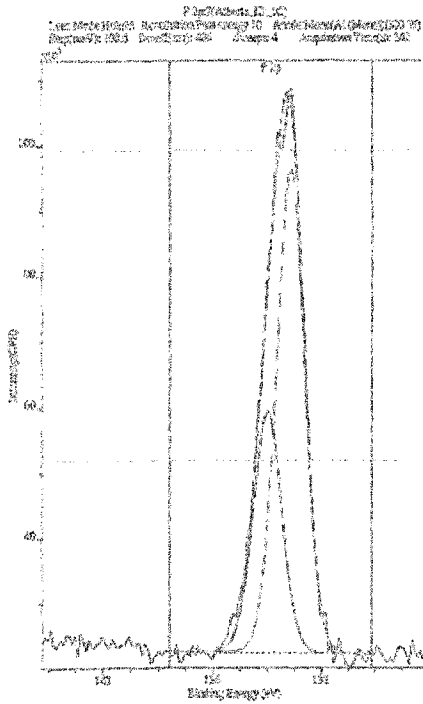
Figure 3.13   Electron count plot versus Energy (energy spectrum):
High resolution Scan of Phosphorus 2p for Sample 1C (Control)
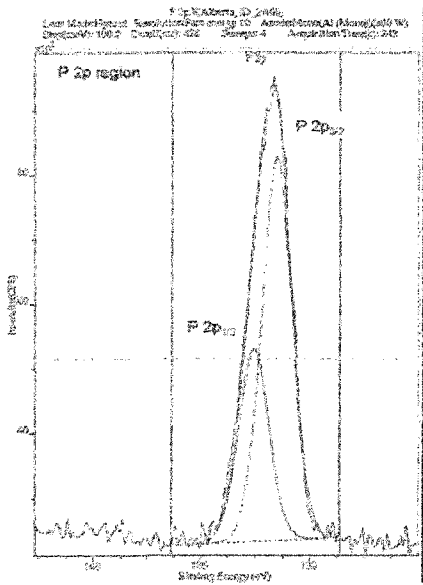
Figure 3.14   Electron count plot versus Energy (energy spectrum):
High resolution Scan of Phosphorus 2p for Sample 2A60 (AL 60s)

94
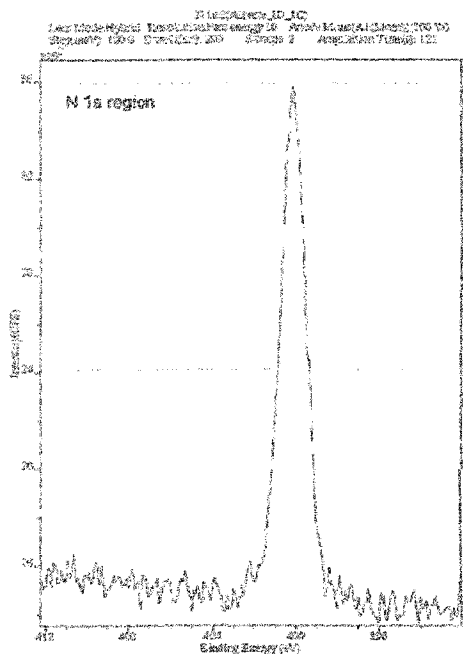
Figure 3.15   Electron count plot versus Energy (energy spectrum): High resolution Scan of Nitrogen 1s for Sample 1C (Control)
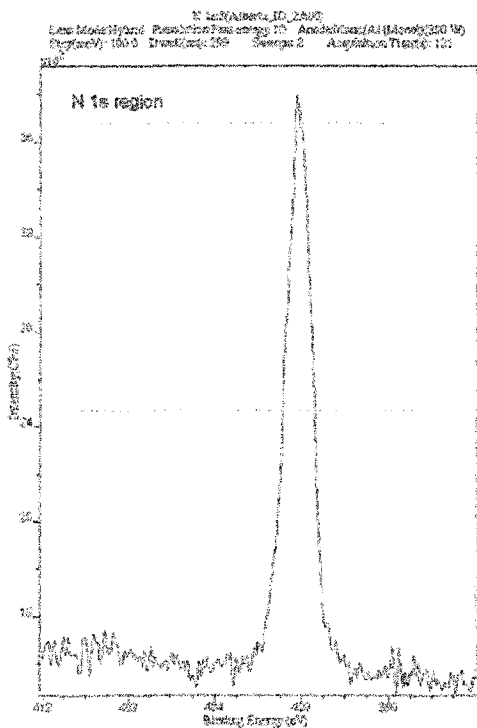
Figure 3.16   Electron count plot versus Energy (energy spectrum): High resolution Scan of Nitrogen 1s for Sample 2A60 (AL 60s)

95

Table 3.1   Quantification from Survey Scan for Sample 1C (Control)

Peak	Position BE (eV)	FWHM (eV)	Raw Area (CPS)	RSF	Atomic Mass	Atomic Conc%
Na 1s	1071	2.98	16238	1.69	23.0	0.52
O 1s	531	2.88	730139	0.78	16.0	30.93
N 1s	400	2.56	118505	0.48	14.0	7.74
Ca 2p	347	2.46	362843	1.83	40.1	6.00
C 1s	285	3.30	467994	0.28	12.0	49.51
S 2p	169	3.14	15106	0.67	32.1	0.64
P 2p	133	2.57	67675	0.49	31.0	3.87
Si 2p	101	2.38	9512	0.33	28.1	0.79

Table 3.2   Quantification from Survey Scan for Sample 2A60 (Argon Laser Irradiation for 60s)

Peak	Position BE (eV)	FWHM (eV)	Raw Area (CPS)	RSF	Atomic Mass	Atomic Conc%
Na 1s	1069	4.51	11858	1.69	23.0	0.41
O 1s	529	3.11	564567	0.78	16.0	25.75
N 1s	397	2.54	120687	0.48	14.0	8.48
Ca 2p	344	2.55	241458	1.83	40.1	4.30
C 1s	282	3.40	502320	0.28	12.0	57.18
S 2p	165	3.88	11081	0.67	32.1	0.51
P 2p	130	2.55	44472	0.49	31.0	2.74
Si 2p	99	2.36	7240	0.33	28.1	0.64

96

Table 3.3   Quantification from Components fitted to High
             Resolution Scans of Oxygen for Sample 1C (Control)

Peak	Position BE (eV)	FWHM (eV)	Raw Area (CPS)	Atomic Conc%
0 1s 1	531.4	1.48	16392	75.19
0 1s 2	532.7	1.82	5413	24.81

Table 3.4   Quantification from Components fitted to High
             Resolution Scans of Oxygen for Sample
             2A60 (Argon Laser Irradiation for 60s)

Peak	Position BE (eV)	FWHM (eV)	Raw Area (CPS)	Atomic Conc%
0 1s 1	531.4	1.47	12197	67.20
0 1s 2	532.7	1.87	5957	32.80

97

Table 3.5   Quantification from Components fitted to High
             Resolution Scans of Carbon for Sample 1C (Control)

Peak	Position BE (eV)	FWHM (eV)	Raw Area (CPS)	Atomic Conc%
C 1s CC,CH	285.0	1.21	5804	52.37
C 1s C-O	286.5	1.37	3107	28.02
C 1s O-C=O	288.3	1.20	1712	15.44
C 1s $-CO_3$	289.2	1.62	461	4.16

Table 3.6   Quantification from Components fitted to High
             Resolution Scans of Carbon for Sample
             2A60 (Argon Laser Irradiation for 60s)

Peak	Position BE (eV)	FWHM (eV)	Raw Area (CPS)	Atomic Conc%
C 1s CC,CH	285.0	1.28	7090	49.95
C 1s C-O	286.4	1.51	4499	31.69
C 1s O-C=O	288.3	1.20	2206	15.53
C 1s $-CO_3$	289.5	1.87	402	2.83

3.6 Bibliography

1. Gorelick L, Geiger A, Gwinnett AJ, Griswold PG. The effect of a fluoride program on white spot formation during orthodontic treatment. Am J Orthod 1982;(2):93-98

2. Fitzpatrick DA, Way DC. The effects of wear, acid etching, and bond removal on human enamel. Am J Orthod. 1977 Dec;72(6):671-8

3. Miwa H, Miyazawa K, Goto S, Kondo T, Hasegawa A. A resin veneer for enamel protection during orthodontic treatment Eur J Orthod. 2001 Dec;23(6):759-67

4. Basdra EK, Huber H, Komposch G. Fluoride released from orthodontic bonding agents alters the enamel surface and inhibits enamel demineralization in vitro. Am J Orthod Dentofacial Orthop. 1996 May;109(5):466-72

5. Gorton J, Featherstone JD. In vivo inhibition of demineralization around orthodontic brackets. Am J Orthod Dentofacial Orthop. 2003 Jan;123(1):10-4.

6. Ogaard B. Prevalence of white spot lesions in 19 year olds: A study on untreated and orthodontically treated persons 5 years after treatment. Am J Orthod Dentofacial Orthop 1989; 96: 423-7

7. Sturdevant C, Roberson T, Heymann H, Sturdevant J. The Art and Science of Operative Dentistry. Mosby Year Book Inc St. Louis 1995

8. Van Palenstein Helderman WH Matee MI, Denehy GE. SEM comparison of acid etched, CO_2, laser irradiated and combined treatment of dentin surfaces. JDent Res; 1996 (75): 535-45

9. Jones FH. Teeth and bones: Applications of surface science to dental materials and related biomaterials. Surface science reports 2001 (42): 75-205

10. Yoshida Y, Van Meerbeek B, Nakayama Y, Snauwaert J, Hellemans L, Lambrechts P, Vanherle G, Wakasa K. Evidence of chemical bonding at

99

biomaterial-hard tissue interfaces. J Dent Res. 2000 Feb;79(2):709-14.

11. Riviere JC: Instrumentation. Practical Surface Analysis (Second Edition) Volume 1. Auger and X-ray Photoelectron Spectroscopy. Edited by D.Briggs and M.P. Seah 1990 John Wiley & Sons Ltd

12. Riggs WM, Parker MJ. Surface Analysis by X-ray photoelectron spectroscopy. Book: Methods of Surface Analysis. Elsevier Scientific Publishing Company, 1975: 123

13. Finke M, Jandt KD, Parker DM. The Early Stages of Native Enamel Dissolution Studied with Atomic Force Microscopy. J Colloid Interface Sci. 2000 Dec 1;232(1):156-164.

14. Holcomb DW, Young RA. Thermal decomposition of human tooth enamel. Calcif Tissue Int. 1980;31(3):189-201

15. Hsu J, Fox JL, Higuchi WI, Otsuka M, Yu D, Powell GL. Heat-treatment-induced reduction in the apparent solubility of human dental enamel. J Dent Res. 1994 Dec;73(12):1848-53

16. Fowler BO, Kuroda S. Changes in heated and in laser-irradiated human tooth enamel and their probable effects on solubility. Calcified Tissue International 1986 Apr;38(4):197-208

Chapter Four

Research Paper Three

Atomic Force Microscopy: A Preliminary Evaluation of the Morphological Characteristics of Argon Laser Irradiated Human Enamel Surface

4.1 Introduction

Enamel is secreted by cells known as ameloblasts, which differentiate at the enamel dentine junction and migrate outward towards what becomes the surface of the enamel. The tracks left by these individual cells are known as enamel prisms. The position of the advancing front of forming enamel is preserved as long-period incremental structures termed striae of Retzius. In the lateral and cervical enamel, Retzius lines contact the enamel surface, forming circumferential rings known as perikymata. The region between two perikymatae is referred to as imbricational enamel.[1] The distance between the perikymatae is measured between 4 and 150 μm.[2] 70% of permanent teeth enamel surfaces are prismless. The thickness of prismless enamel is often found to be around 30 μm[1] and the area and location varies.[3] An atomic force microscope is designed for measuring surface features that are extremely small and is capable of imaging features as small as a carbon atom (0.25 nm) and as large as 80 μm (80 000 nm).[4] The scan size of the present study consisted of 10 μm.

Atomic force microscopy (AFM) is a variation on a method of imaging surfaces with atomic or near-atomic resolution, collectively called scanning probe microscopy (SPM). A small tip is scanned across the surface of a sample in order to construct a 3D image of the surface. Fine control of the scan is accomplished using piezoelectrically-induced motions. Any type of surface can be probed by the molecular forces exerted by the surface against the tip.

Applications of the AFM method in dental research have been reviewed.[4] This technique was utilized to observe the human enamel features from individual crystals up to prisms. Smaller scale images allowed the individual enamel crystals to be resolved.

102

Height differences between individual faces create the roughness of enamel surface.[5]Large scale images of human tooth enamel show arrangements of the prisms, imaged as deep holes with protrusions of interprismatic enamel in between.[4]These studies confirm the applicability of AFM for studying the human enamel surface.[5]

The Nanoscope (Digital Instruments, Santa Barbara, California) performs scanning probe microscopy techniques to measure surface characteristics, including topography, and images of samples. The Nanoscope image analysis and presentation software contains powerful algorithms for the measurement and presentation of surface topography results in the X, Y and Z planes. Images can be viewed in the two- or three dimensional representations, with a variety of color schemes.

The purpose of the AFM scan part of the study was to attain more information on surface morphology changes after AL irradiation (60s) in comparison to the untreated sample (control).

4.2 Material and Method

The surface morphology of human enamel was examined with an atomic force microscope. The same two upper premolar teeth, which were used in the XPS surface scan method were used for the AFM scan. The specimens were extracted, cleaned of tissue debris, and stored in 0.1% thymol solution for 3 weeks before they were rinsed with distilled water. The buccal enamel surface was separated from the rest of the tooth with a diamond disc. The dentinal layer was completely removed from the specimens with a football shaped diamond bur. The sample named 2A60 was exposed to AL irradiation for 60 seconds and the specimen named 1C served as the control. The

103

specimens were stored in distilled water for 5 days prior to the scan.

An atomic force microscope (Nanoscope III, Digital Instruments, Santa Barbara, California) was used to study the surface morphology of the non-exposed enamel specimen in comparison with the specimen exposed to the AL beam for sixty seconds. In AFM, the interaction of a stylus probe and sample surface is quantified and mapped across the sample. The probe or "tip" is of nanometer-scale sharpness, and the standard image is 3D surface topography at resolution approaching the atomic or molecular scale. The tip is attached to a micro-fabricated cantilever of low spring constant. The scan rate used was 1.97 Hz. Both samples were scanned 512 times to obtain a 10x10 μm image with a data scale of 250 nm. The length scale X measured 2 μm/div and in the direction Z consisted of 250 nm / div. The differences in color indicate the differences in height / depth in the top 250 nm layer of the enamel surface. Dark red means 0 nm (deepest point of scan range), orange around 125 nm and yellow a maximum of 250 nm (peak tip on superior border of scan range).

4.3 Results

The information obtained from the AFM images is qualitative and present no major changes in the morphology of the enamel surface after laser irradiation. Visual inspection seems to present a slightly higher occurrence of red colored surfaces in the AL irradiates (Figure 4.2 & Figure 4.4) samples than in the control (Figure 4.1 & Figure 4.3). The peaks of the AL treated specimen appear mildly rounded and therefore the surface appears slightly smoother.

104

4.4 Discussion

Only one study was found describing the "normal" enamel surface of a permanent tooth using the AFM technique. Their sample was derived from the third molar from a male patient, 25 years old, with no abnormalities. The same size tooth surface area as in the present study of 10 x 10 μm was evaluated with the same kind of nanoscope (Nanoscope III, Digital Instruments, Santa Barbara, California). The scan rate was 1 Hz, almost half as fast as the scan rate of the present study. The enamel surface presented by the AFM images were reported to consist of two kinds of grain: small ones (average diameter from 0.2 to 0.5 μm) which are somewhat incorporated in/associated with large grains with an average diameter of 2-4 μm.[3] *Batina et al.*[3] did not discern any order of grain alignment, however they reported that the grains were closely touching each other.[3] The 2D images of the present study of the control and the irradiated sample demonstrate different sized converged grains on an uneven surface, differentiated by the color scheme.

The difference in the amount of red colored surface identified in the present study, could just be an indicator for different location closer to imbricational enamel. The peaks and ridges might be a sign for differential termination of ameloblast activity or due to environmental influences. The type of AL used in the present study (2.5 mW/cm²) is not known to cause destructive alterations on the enamel surface. It is however possible that heat created by the AL on the enamel surface could have caused the slightly rounded appearance of the peaks and ridges in the 2A60 samples.

AFM was used by *Farina et al.*[6] to compare the pattern of particle distribution in the outermost layer of the tooth surfaces in human and animals. The authors reported that AFM gives high-contrast, high-resolution images and is an important tool as a source of

105

complementary and/or new structural information. They confirmed the observation that human enamel (permanent teeth) demonstrates particles tightly packed in the outer surface. This further supports the hypothesis that the greater depth projection might just be imbricational enamel[6] and might not related to the AL irradiation.

It is likely that temperature changes on the enamel surface, induced by the AL irradiation, are the main reason for the mild surface alterations. Currently, there appears to be no information on the actual temperature increase on the enamel surface during AL irradiation. *Kuroda et al.* [7] examined laser induced changes in high temperature regions. X-ray diffraction and infrared spectroscopy were used to identify changes in enamel of extracted intact human teeth subjected to high energy density (10,000 J/cm^2) 10.6 microns wavelength carbon dioxide laser irradiance. The laser irradiance melted the enamel apatite. Much smaller energies were used in the present study (15 J/cm2).

Heating enamel in the temperature range 200 - 600 ° C not induced by laser resulted in poor crystal packing due to void formation, permanent change in the sign of its birefringence (from negative to positive) in some areas, and an altered crystal morphology. *Palamara et al.*[8] reported that transmission electron microscopy of enamel heated in the temperature range 200 ° C to 400 ° C revealed increasing volume of intra- and inter-crystalline voids and a significant increase in void volume at 400 °C.[8] It is therefore likely that the temperature increase caused by AL irradiation in the present study (15 J/cm^2) was much lower than the values used in the *Palamara et al.*[8] study. The temperature increase on enamel with the AL might cause an initial melting effect that "seals" the surface rather than exposing it through void formation observed at much higher temperatures.

106

One explanation of why this effect could provide a certain degree of demineralization protection was presented by *Hicks et al.* [9] stating that an alteration in the enamel pore structure of enamel takes place, which entraps and reprecipitates the mineral phases released during demineralization. Superficial heat development created by the AL irradiation could seal the pores. The retention of these minerals in these pores could inhibit the demineralization process.

4.5 Conclusion

Argon laser irradiation (60 s, 15 J/cm²) seems to cause only minor morphological change on the enamel surface. The alterations might consist in a sealing effect resulting in a slight decrease in surface roughness.

107
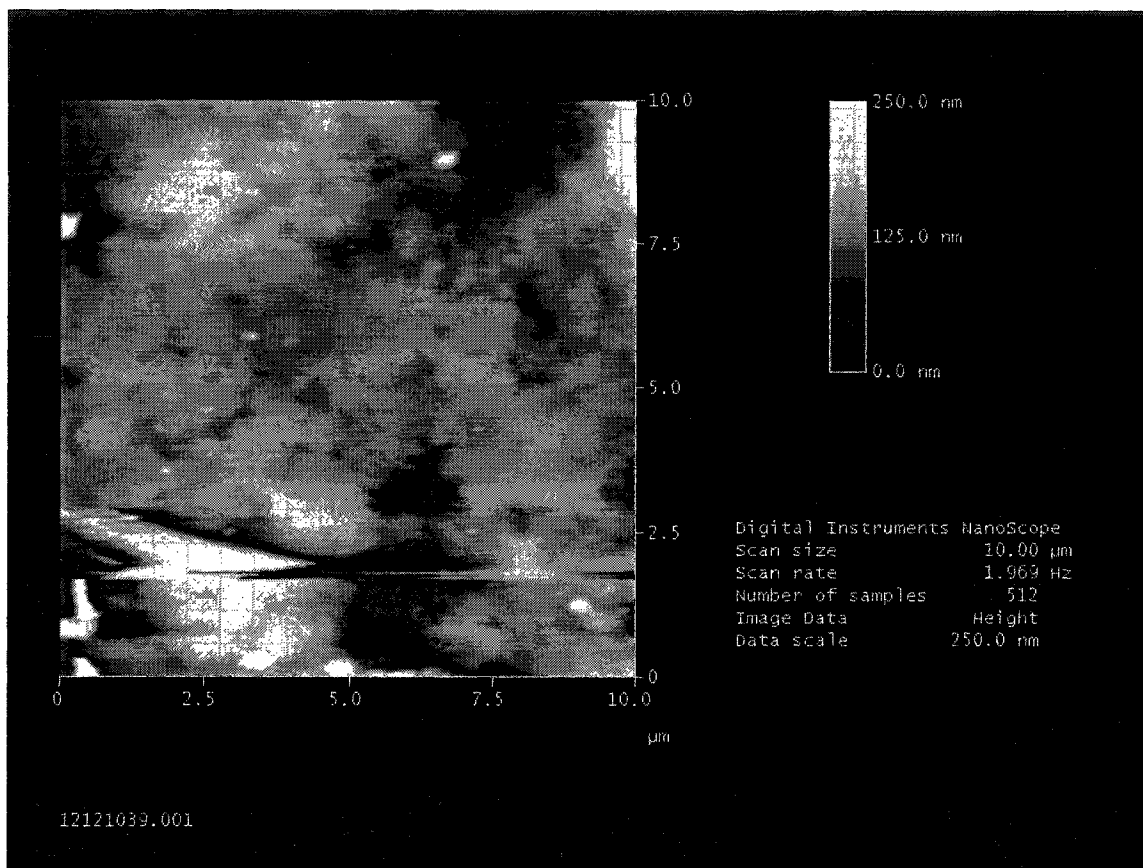
Figure 4.1 Example of the AFM images for Sample 1C (2D)

108
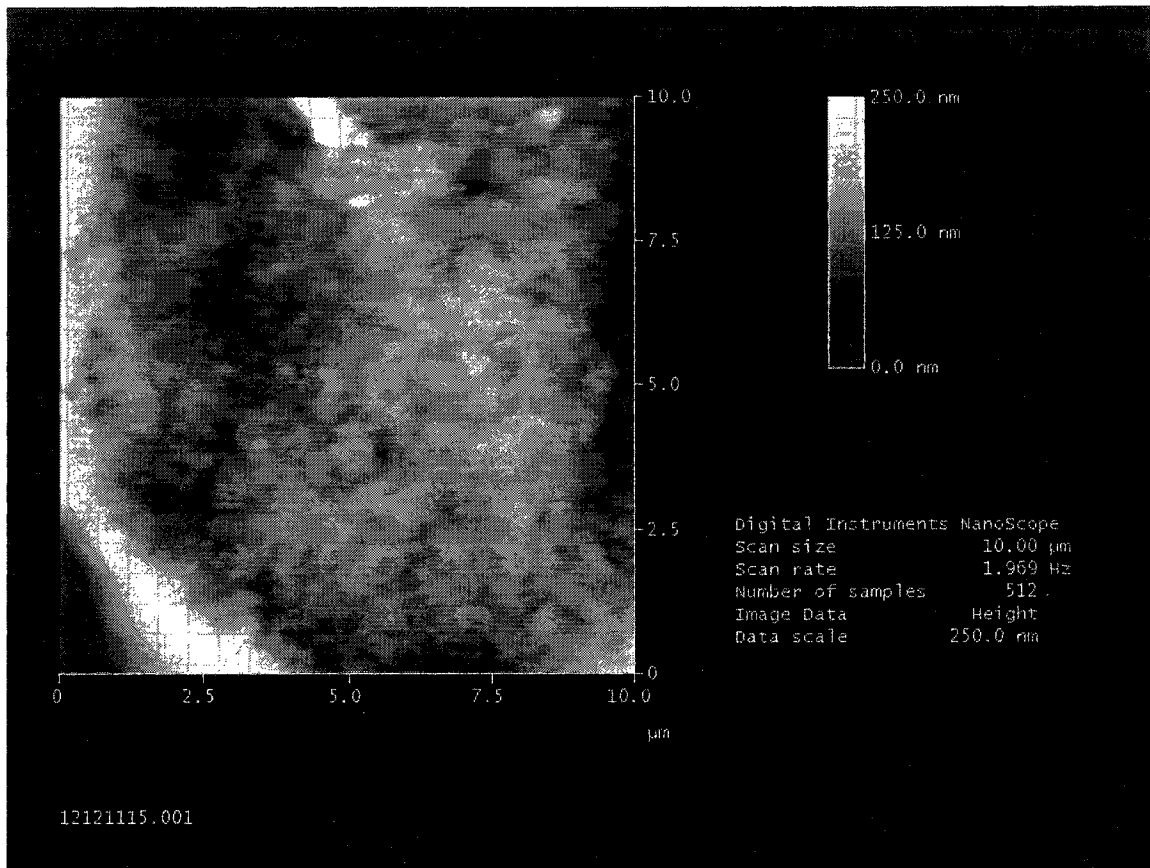
Figure 4.2 Example of the AFM images for Sample A60 (2D)

109
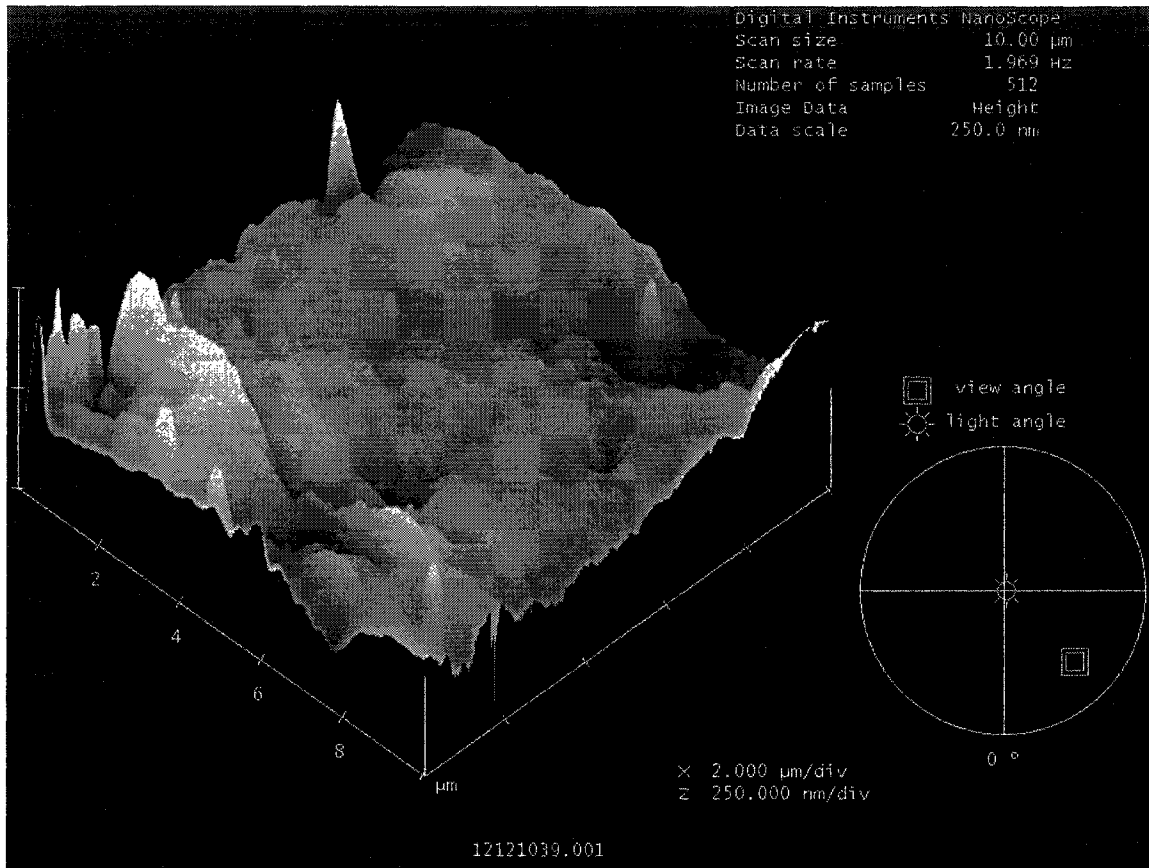
Figure 4.3 Example of the AFM images for Sample 1C (3D)

110
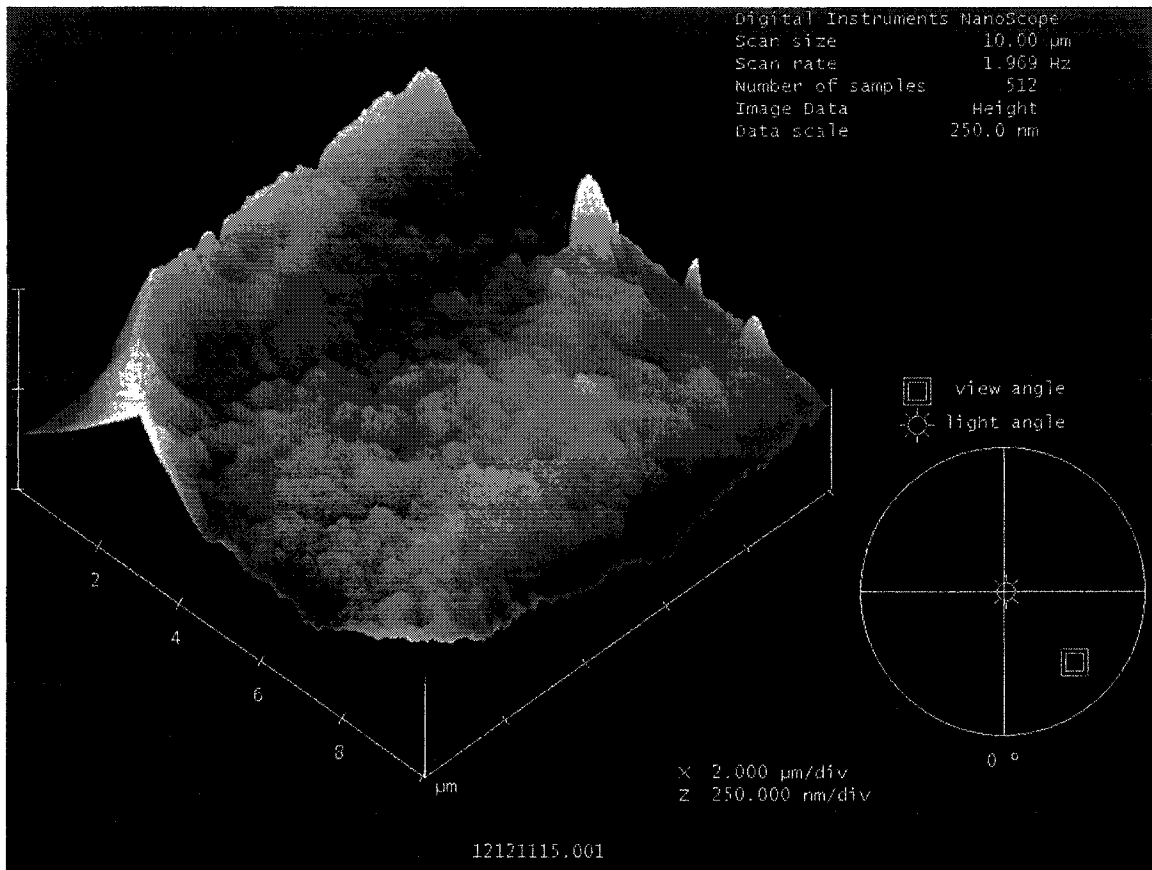
Figure 4.4 Example of the AFM images for Sample A60 (3D)

4.6 Bibliography

1. Schroeder HE: Orale Strukturbiologie. Georg Thieme Verlag 1982; 2.unveraenderte Auflage: 87-92

2. Osborn JW. A relationship between the striae of Retzius and prism directions in the transverse plane of the human tooth. Arch Oral Biol 1971; 16: 1061

3. Batina N, Renugopalakrishnan V, Lavin PN, Hernandez Guerrero JC, Morales M, Garduno-Juarez R.An atomic force microscopic study of the ultrastructure of dental enamel afflicted with amelogenesis imperfecta. J Biomater Sci Polym Ed. 2002;13(3):337-48

4. Jones FH. Teeth and bones: Applications of surface science to dental materials and related biomaterials. Surface science reports 2001 (42): 75-205

5. Schaad P, Paris E, Cuisinier FJ, Voegel JC: Atomic force microscopy study of human tooth enamel surfaces. Scanning Microsc. 1993 Dec;7(4):1149-52.

6. Farina M, Schemmel A, Weissmüller G, Cruz R, Kachar B, Bisch PM: Atomic force microscopy study of tooth surfaces. J Struct Biol. 1999 Mar;125(1):39-49.

7. Kuroda S, Fowler BO: Compositional, structural, and phase changes in in vitro laser-irradiated human tooth enamel. Calcif Tissue Int. 1984 Jul;36(4):361-9

8. Palamara J, Phakey PP, Rachinger WA, Orams HJ: The ultrastructure of human dental enamel heat-treated in the temperature range 200 degrees C to 600 degrees C. J Dent Res. 1987 Dec; 66(12): 1742-7

9. Hicks MJ, Flaitz CM, Westerman GH, Blankenau RJ, Powell GL, Berg JH. Caries-like lesion initiation and progression around laser-cured sealants. Am J Dent. 1993 Aug;6(4):176-80 and ASDC J Dent Child. 1993 May-Jun;60(3):201-6.

Chapter Five

Research Paper Four

Nanoindentation: A Preliminary Evaluation of the Hardness and Roughness Characteristics of Argon Laser Irradiated Human Enamel Surface

5.1 Introduction

Most of the enamel prisms do not end at the enamel surface but 30 μm below it. 70% of enamel surface in the permanent dentition consists of prismless enamel, which is harder and denser mineralized and less soluble in acid than the enamel prisms below. It consists of densely packed crystallites, whose longitudinal axes are positioned perpendicular to the enamel surface. This layer is able to store fluoride to a greater extent and is more resistant to cariogenic attacks.[1]

It has been shown that nanoindentation is a useful tool in measuring enamel surface changes.[2] The goal of nanoindentation tests is to extract elastic modules and hardness of the specimen material from load displacement measurements. Conventional indentation hardness tests involve the measurement of the size of the residual plastic impression in the specimen as a function of the indenter load. In nanoindentation testing, the size of the residual impression is often only a few microns, hence it is very difficult to obtain a direct measure using optical techniques. Therefore the depth of the penetration beneath the specimen surface is measured as the load is applied to the indenter. The known geometry of the indenter allows for the modulus of the specimen material to be obtained from a measurement of "stiffness" of the contact, which is the rate of change of load and depth.[3]

The Berkovich indenter is generally used in small scale indentation studies. It is constructed with a face angle of 65.3° and it has the same projected area-to-depth ratio as the Vickers indenter. The tip radius for a typical Berkovich indenter is in the order of 50-100 nm.[3]

The Hysitron TriboIndenter® (Hysitron Inc., Minneapolis, MN) is a high-

114

resolution nanomechanical test instrument capable of performing both nanoindentation (NI) and scratch testing. It can also provide *in situ* images. In indentation mode, the instrument is a load-controlled displacement-sensing device. An indenter tip is driven into a sample and then withdrawn by decreasing the applied force. The applied load (P) and depth of penetration (h_c) into the sample are continuously monitored. A load versus depth curve can then be generated from the collected data. Figure 5.1 depicts an example of a load versus depth curve in which the load is increased at a constant rate to some peak value (loading), held at that value for a set amount of time and then decreased to zero (unloading) at the same rate as loading. The reduced elastic modulus (E_r) and hardness (H) can then be calculated from the load versus depth curve. The 'reduced elastic modulus' (E_r) is the amount a material deforms when a load is placed on it.

Images of the tested surface can also be generated immediately before and after the indentation or scratch when the instrument is operated in SPM mode, which operates a Scanning Probe Microscopy (SPM) technique in which a fine tip is brought into atomically close contact with a sample surface without actually touching the surface. This is done by sensing the repulsive force between the probe tip and the surface. The forces are extremely small (about 1 nanonewton). The tip is then moved back and forth over the sample surface and can measure the topography with almost atomic resolution. These images provide useful information on sample tests and surface morphologies of the sample. The regular shapes of the indents and/or scratches assured good contacts between the indenter and sample surface. Further, meaningful information on the morphological features of the sample surface, e.g., particle size, shape and distribution, can be extracted from these images. The usual method for displaying the data is to use a color mapping for

115

height. The differences in color demonstrate the roughness of the sample surfaces. Finally, because the images are created *in-situ*, scanned with the same tip as the indenter tip, the combination of the imaging and indenting/scratching capability is very powerful in positioning the tip and investigating the interesting features. Another advantage of this technique consists of the fact that probing molecular-scale interaction is possible without demanding an ultrahigh vacuum environment. [3]

A second round of tests was performed with a different nanoindentation instrument. A MultiRange Nanoprobe® (Hysitron Inc., Minneapolis, MN) is a "high-load" indentation tool that is designed for use with the TriboIndenter. It augments the capabilities of the TriboIndenter by allowing indentations to be performed at much higher loads and displacements than the three-plate capacitive transducer that is standard on the TriboIndenter. The maximum displacement available is 80 μm. The maximum force can be as large as 2 N. It can be operated in load or displacement control mode. It also generates a load versus depth curve that can be analyzed with the same techniques as the data taken with the standard three-plate capacitive transducer.

The following nanoindentation (NI) and scanning probe microscopy (SPM) surface tests and images were performed and collected to measure the hardness and roughness of the enamel surface after argon laser (AL) irradiation.

5.2 Material and Method

Two extracted human upper premolar teeth from a healthy young (13 years old) female orthodontic patient were cleaned of tissue debris, stored in 0.1% thymol solution for 3 weeks and then rinsed with distilled water. The buccal portion of the crown was

116

separated from the rest of the tooth with a diamond disc. The dentinal layer was completely removed from the specimens with a football shaped diamond bur. The sample named A60 was exposed to AL irradiation for 60 seconds to achieve a more obvious change if present; the specimen named 1C presented the control. The prepared specimens were stored in distilled water for 2 days. The operator of the indenter was not aware of the treatment performed on sample A60. Both samples were tested in the center of the buccal surface. Fifteen indentation tests were performed on each of the two samples, which came from the same patient. The tip of the indenter is a standard three-sided diamond pyramid (Berkovich indenter tip). A trapezoidal load function consisting of a 5 seconds loading segment, a 2 seconds holding segment, and a 5 seconds unloading segment. A maximum normal load of 8000 μN was used for each test, determined by the Annex B of the Standard which provides schematic representation of load and depth control. Images were also taken of the sample surface to measure the surface roughness of each of the samples. For this calculation a 10 μm scan size was chosen. Using Hysitron's (Hysitron Inc., Minneapolis, MN) image analysis software a surface roughness value was calculated.

A second round of tests was performed using a different Nanoprobe (Hystron's Multi-Range Nanoprobe, Hysitron Inc., Minneapolis, MN) to circumvent any roughness effects in the data. Ten indentation tests were performed on each of the two samples using the Multi-Range Nanoprobe, a Berkovich diamond indenter tip, and a trapezoidal load function consisting of a 10 second loading segment, a 5 second holding segment, and a 10 second unloading segment. A maximum normal load of 240 mN was used for each test. This load was chosen so as to achieve a contact depth of greater than 1.5 μm

117

hoping to overcome any errors caused by roughness. Higher loads were not used due to the fact that the focus is on the enamel surface, which is approximately 30 microns deep; performing indentation at higher depths may result in the tests being affected by the underlying 'untreated' enamel zone.

Independent t-test was performed to compare the argon laser irradiated sample with the control regarding the hardness and reduced elastic modulus.

5.3 Results

The hardness (H) and the reduced elastic modulus (E_r) are determined from the partial unload portions of the load/depth curve (Figure 5.1) together with the tip contact area versus contact depth function. For a better understanding traditional analyses of load-depth data are presented in Figure 5.2, Figure 5.3 and Figure 5.4. The selection of location for the tests was performed with an optical microscope to find a 'flat' location on the samples (Figure 5.5). Table 5.1 provides descriptive data from the indentation tests with a load of 8000 μN. The reduced elastic modulus (E_r), hardness (H), and contact depth (h_c) means, standard deviation and ranges are provided. Samples 1C and A60 showed average reduced elastic modulus values (E_r) of 102.3 GPa +/- 7.6 and 97.7 GPa +/- 5.1, and with average hardness values (H) of 4.09 GPa +/- 0.45 and 4.79 GPa +/- 0.39 respectively. The irradiated sample showed a significant (P = 0.000) increase in hardness (H) and a decrease in the reduced elastic modulus (P = 0.060) with a load of 8000 μN (Table 5.2). Table 5.3 presents the descriptive data of the nanoindentation tests performed with a load of 240 mN. The control sample demonstrated an average reduced elastic modulus value of 100.7 GPa +/- 4.7 GPa and an average hardness value of 4.17

118

GPa +/- 0.4 GPa. The average reduced elastic modulus value for the irradiated sample consisted of 98.3 GPa +/- 4.5 GPa and for the hardness of 4.17 GPa +/- 0.3 GPa. No significant difference was found in hardness nor reduced elastic modulus between the samples (Table 5.4). Figures 5.6 and 5.7 are plots of reduced elastic modulus (E_r) versus contact depth (h_c) and hardness (H) versus contact depth (h_c) respectively for the two samples with a load of 8000 μN and Figure 5.8 and Figure 5.9 for the load of 240 mN. The irradiated sample demonstrates a lower reduced elastic modulus (E_r) and less contact depth for both rounds of tests with a more obvious difference with a load of 8000 μN. Increased hardness (H) and a decrease in the contact depth (h_c) are present on the irradiated sample with a load of 8000 μN.

Figures 5.10 and 5.11 are representative *in-situ* images of single indents on samples 1C and A60 respectively. Visual inspection of the images demonstrates an obvious decrease in particle (grain) size and less change in color on the irradiated sample. Table 5.5 contains the RMS roughness values for 1C and A60 calculated from the 10μm topography images (Figure 5.12 & Figure 5.13)

5.4 Discussion

Enamel is the hardest component of the body (260-360 KHN (Knoop hardness number), 300-400 VH (Vickers hardness number)).[1] Most of the hardness measurements in the literature have been obtained using microindentation techniques such as Vickers and Knoop hardness tests. Comparison between microindentation and nanoindentation hardness data and the ones obtain with NI is not straightforward. In case of Knoop or Vickers tests, hardness is defined as the resistance to plastic deformation, whereas NI

119

takes the resistance to plastic and elastic deformation into account. Therefore the values of the hardness obtained with the conventional microindentation technique are higher.[2] Samples 1C and A60 show different average values for the reduced elastic modulus (E_r) and hardness (H), though the difference is not greater than that of the standard deviation. Accordingly, a comparison of the hardness values obtained for untreated enamel of the buccal surface of the premolar in the present study are higher (4.09 GPa+/- 0.27 GPa) than the values for the untreated enamel of the buccal surface of an unerupted third molar reported by *Finke et al.*[2] (3.51 GPa +/- 0.90 GPa)[2] and lower than the values reported by *Lippert et al.*[4] (4.85 GPa +/- 0.28 GPa) of untreated (polished) premolar enamel (location on tooth surface not specified).

Cuy et al.[5] used NI to map out the properties of enamel over the axial cross-section of a maxillary second molar. Local variations in mechanical characteristics were correlated with changes in chemical content and microstructure across the entire depth and span of a sample. The range of hardness (H) observed over an individual tooth was found to be far greater than previously reported. These variations corresponded to the changes in chemistry, microstructure, and prism alignment but showed the strongest correlations with changes in the average chemistry of enamel. For example, the concentrations of the constituents of hydroxyapatite (P_2O_5 and CaO) were highest at the hard occlusal surface and decreased on moving toward the softer enamel-dentine junction. The mechanical properties of the enamel were also found to differ from the lingual to the buccal side of the molar. At the occlusal surface the enamel was harder and stiffer on the lingual side than on the buccal side. The indents in the present study were taken on the midpoint of the buccal surface of the crown of the maxillary premolar. The

120

higher values (>6GPa) reported by *Cuy et al.*[4] may represent differences between enamel surface hardness of a mandibular second molar and a maxillary first premolar.

The large amount of standard deviation in the contact depth (h_c), reduced elastic modulus (E_r) and hardness (H) values can be attributed to the large surface roughness. The latter is very important in nanoindentation, since the contact area is measured indirectly from the depth of penetration. The natural roughness of real surfaces can cause errors in the determination of the area of contact between the indenter and the specimen.[3] The enamel sample surfaces used have rough striations ('ripples' or 'ridges') on the surface. The equations used to calculate reduced modulus and hardness assume that the sample surface is perfectly perpendicular to the diamond indenter. If a test is taken on the tilted side of a striation coming from a high point, the data will be affected. Also the theory assumes that the sample surface is an infinite half space (infinitely flat). If the top of a striation or the bottom between high points is indented, the modulus / hardness will appear artificially low or high respectively, depending on the ratio of the indentation size versus the curvature of the sample. These factors will increase the standard deviation of the tests. The present study results of Round 1 and Round 2 show lower values for the standard deviation during hardness testing of the AL irradiated sample, which may indicate a reduced roughness value.

Second testing with larger loading (240 mN) was conducted to overcome the measurement error which could result from the surface roughness. The increased maximum load might have overcome this problem but was probably not as sensitive in detecting the changes caused by the argon laser irradiation in the top 1-10 μm surface layer. Further testing is necessary to determine the ideal load for hardness testing

121

minimizing the error caused by the surface roughness while maintaining depth of interest.

There are no previously published studies to the author's knowledge, which examined the hardness and roughness of the human enamel surface after AL irradiation.

5.5 Conclusion

This pilot study suggests that argon laser irradiation results in possible reduced enamel surface roughness. A correlation between decrease in roughness and a significant increase in hardness could be detected on the lased enamel (AL: 15 J/cm^2, 60s) compared to the untreated control when a maximum load of 8000 μN was used. Higher maximum load of 240 mN did not confirm any significant changes.

122

Table 5.1   Descriptive data of the Nanoindentation tests (load: 8000 μN)

	Sample* Type	Mean	Standard Deviation	Range
Er(GPa)	1C	102.3	7.59	92.9 - 117.8
	A60	97.7	5.11	88.2 - 106.0
H(GPa)	1C	4.09	0.45	3.48 - 5.21
	A60	4.79	0.39	4.18 - 5.29
hc(nm)	1C	257.1	14.30	224.7 - 279.1
	A60	235.5	10.56	222.8 - 252.7

*15 indents per group

Table 5.2   Independent t-test: Reduced Elastic Modulus (E_r) and Hardness (H) (load: 8000 μN)

	Mean Difference	Standard Error Difference	P-value*
E_r(GPa)	4.63	2.36	0.060
H(GPa)	-0.71	0.15	0.000*

*P value of less than 0.05 is statistically significant

Table 5.3   Descriptive data of the Nanoindentation tests (load: 240 mN)

	Sample* Type	Mean	Standard Deviation	Range
Er(GPa)	1C	100.7	4.70	93.5 – 108.5
	A60	98.3	4.50	89.7 – 105.9
H(GPa)	1C	4.17	0.44	3.72 – 5.05
	A60	4.17	0.30	3.74 – 4.57
hc(nm)	1C	1538	77	1392 - 1624
	A60	1557	55	1464 - 1618

*10 indents per group

Table 5.4   Independent t-test: Reduced Elastic Modulus (E_r) and Hardness (H) (load: 240 mN)

	Mean Difference	Standard Error Difference	P-value*
E_r(GPa)	2.43	2.05	0.252
H(GPa)	0.10	0.21	0.640

*P value of less than 0.05 is statistically significant

Table 5.5   RMS roughness values from 10 µm surface scans

	1C	A60
RMS Roughness	38.04nm	19.38nm

124
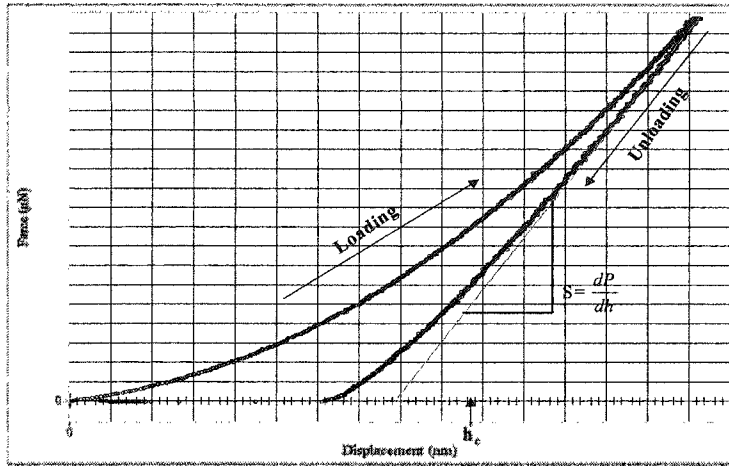
Figure 5.1   Example of a Load vs. Depth Curve for an elastic plastic Solid

(Sample Analysis Report Document NRL-X-381, Hysitron Inc., 10025 Valley View Rd, MN). Load (Force (μN)) and depth of penetration (Displacement (nm)) are recorded at each load increment, ultimately providing a measure of modulus and hardness as a function of depth beneath the surface. Following the attainment of the maximum load, the load is steadily removed and the penetration depth recorded. The loading part of the indentation cycle may consist of an initial elastic contact, followed by plastic yield within the specimen at higher loads. Upon unloading, if yield has occurred, the load displacement data follow a different path until at zero applied load; a residual impression is left in the specimens surface. The maximum depth of penetration for a particular load, together with the slope of the unloading curve measured at the tangent to the data point at maximum load (red line), lead to a measure of reduced elastic modulus (E_r) and hardness (H) of the specimen material.

125
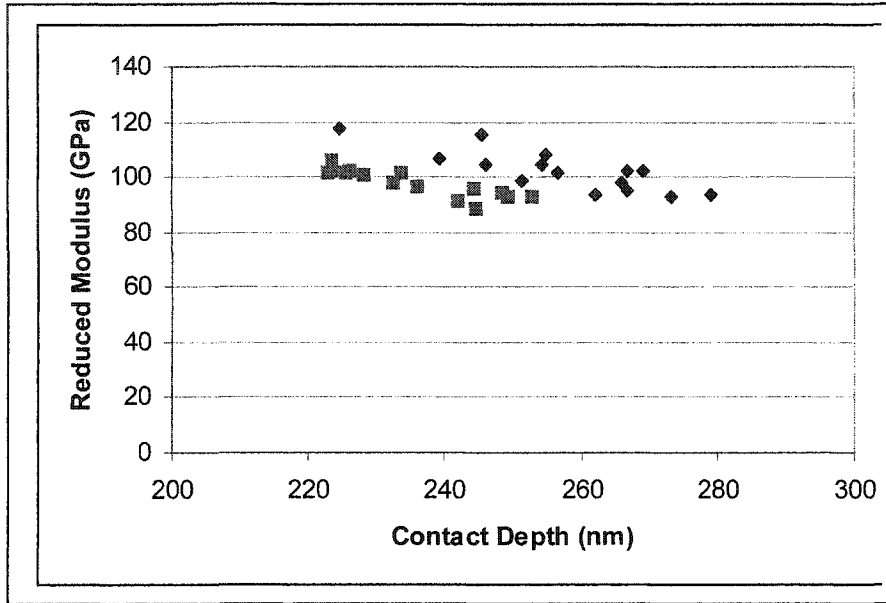
Figure 5.2   **Example of a plot of reduced elastic modulus (E_r) versus contact depth (h_c)** (Sample Analysis Report Document NRL-X-381, Hysitron Inc., 10025 Valley View Rd, MN). The reduced elastic modulus is defined by the following equation, $E_r = S \dfrac{\sqrt{\pi}}{2\sqrt{A}}$, where S is the unloading stiffness $\left(\dfrac{dP}{dh}\right)$ and A is the projected contact area. The reduced elastic modulus is related to the modulus of elasticity (E) through the following equation, $\dfrac{1}{E_r} = \dfrac{(1-v_1^2)}{E_1} + \dfrac{(1-v_2^2)}{E_2}$, where E_1 corresponds to the indenter material (diamond = 1140 GPa), E_2 refers to the indented material (enamel), and v is poisson's ratio (0.07). Poisson's ratio varies between 0 and $\frac{1}{2}$ for most materials. The unloading stiffness (S) is calculated by fitting the unloading curve to the power law relation, $P = A(h - h_f)^m$, where A, h_f, and m are arbitrary fitting parameters. The stiffness can be calculated from the derivative of the preceding equation:

$$S = \frac{dP}{dh}(h_{max}) = mA(h_{max} - h_f)^{m-1}.$$

126
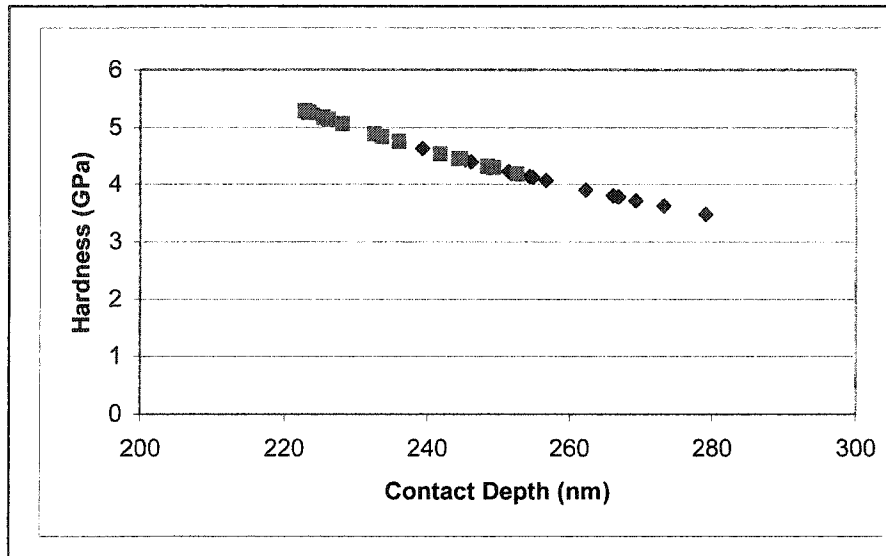
Figure 5.3   **Example of a plot of hardness (H) versus contact depth (h$_c$)** (Sample Analysis Report Document NRL-X-381, Hysitron Inc., 10025 Valley View Rd, MN). The hardness is defined by the ratio of the maximum load to the projected contact area:

$$H = \frac{P_{\max}}{A}.$$
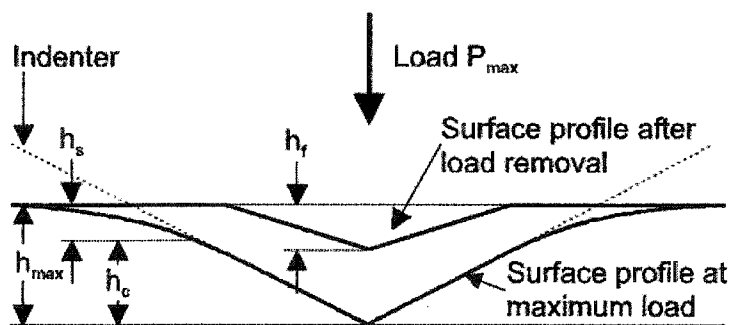
Figure 5.4   **Illustration of the indentation geometry at maximum load and after unloading** (http://www.tu-harburg.de/gk/Research/Claussen/tbs.html). The contact area is determined from a tip calibration function A (h$_c$) where the contact depth (h$_c$), is found by using the following equation: $h_c = h_{\max} - \varepsilon \frac{P_{\max}}{S}$. To account for edge effects, the deflection of the surface at the contact perimeter is estimated by taking the geometric constant ε as 0.75.

127
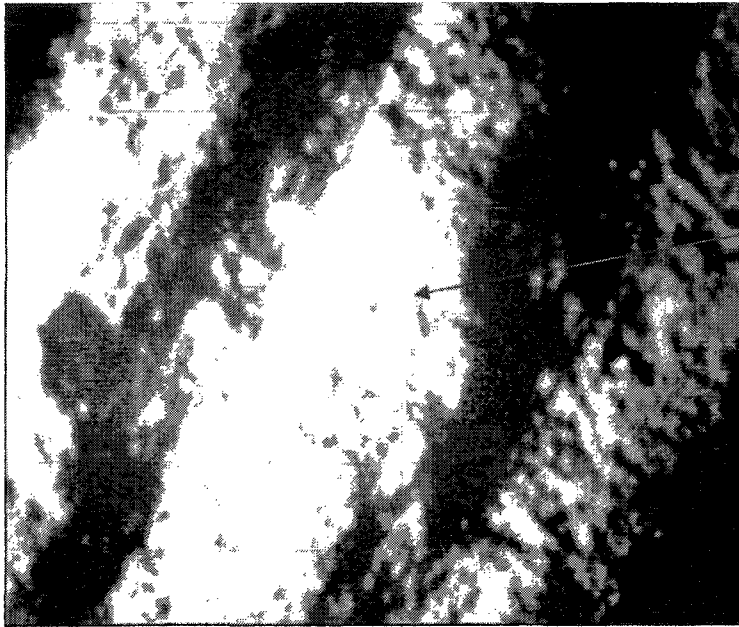
240 mN
Indentation

Figure 5.5   **Image (optical microscope) of surface of Sample A60** showing striations with high and low points. For the indentations, smooth areas were selected (image size: 470um x 550um) to decrease the negative influence of the surface roughness on the hardness testing.

128
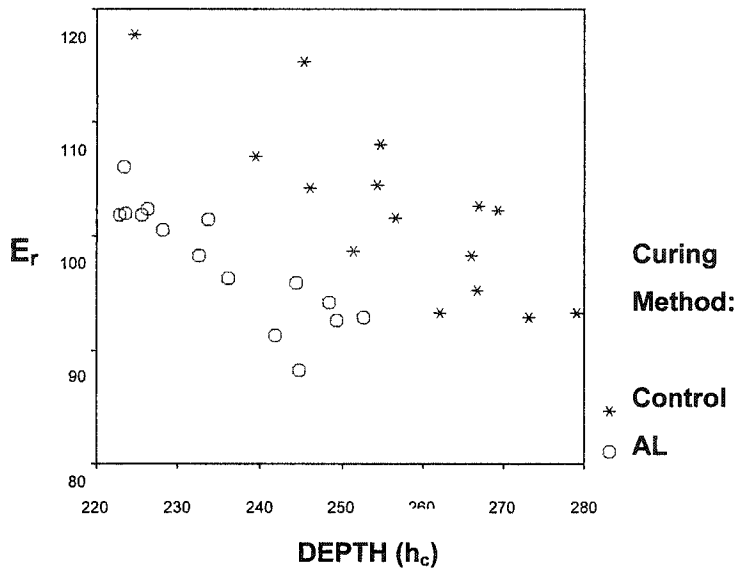
Figure 5.6   Plot of reduced elastic modulus (E_r) versus contact depth (h_c) for the 8000μN indentations tests : Samples 1C / A60.
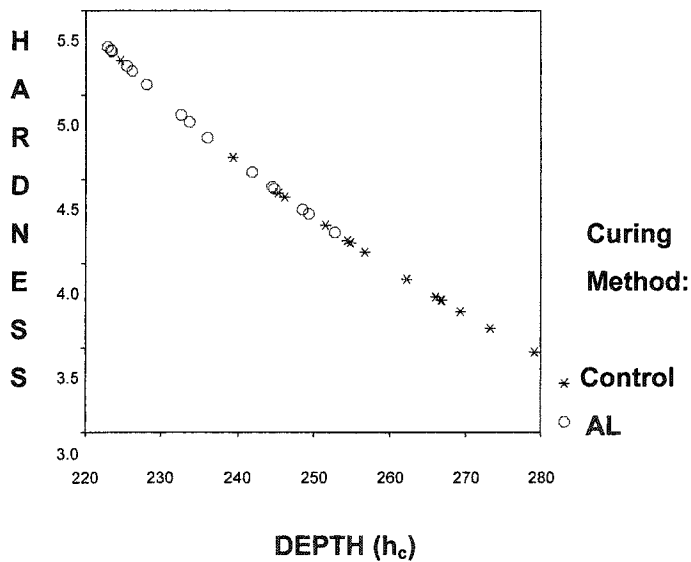
Figure 5.7   Plot of hardness (H) versus contact depth (h_c) for the 8000μN indentation tests : Samples 1C / A60.

129
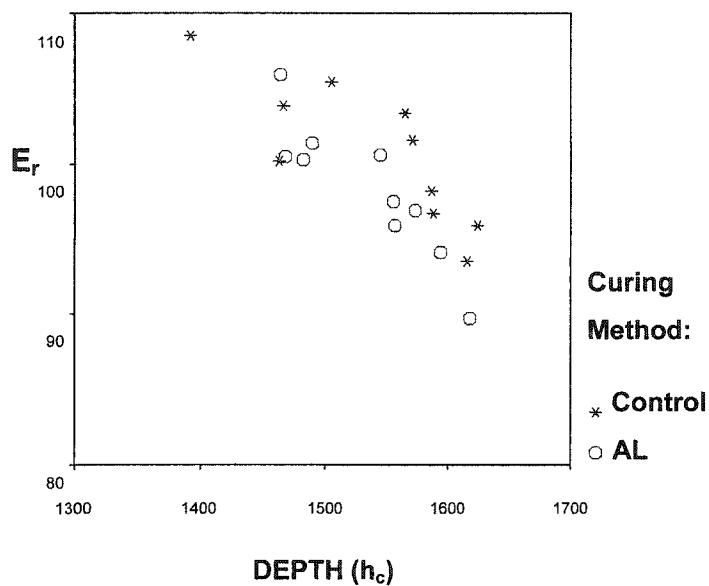
**Figure 5.8   Plots of reduced elastic modulus versus contact depth
for the 240 mN indentation tests: Samples 1C / A60.**
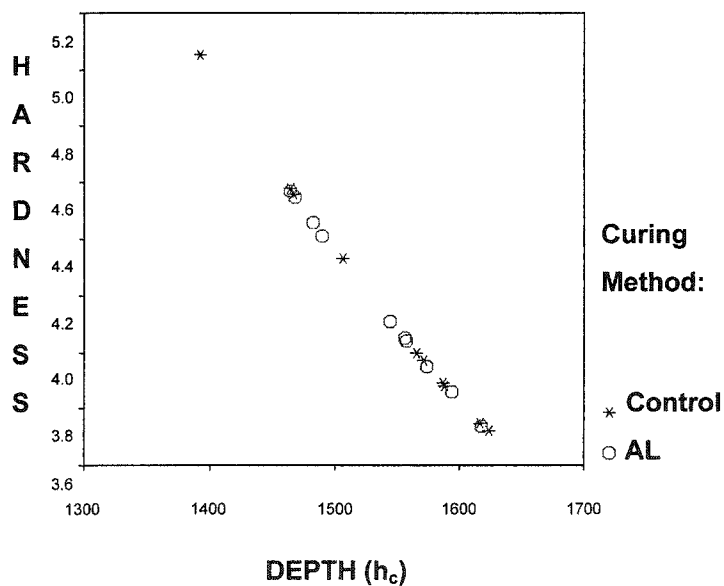
**Figure 5.9   Plots of hardness versus contact depth for the 240 mN
indentation tests: Samples 1C / A60.**

130
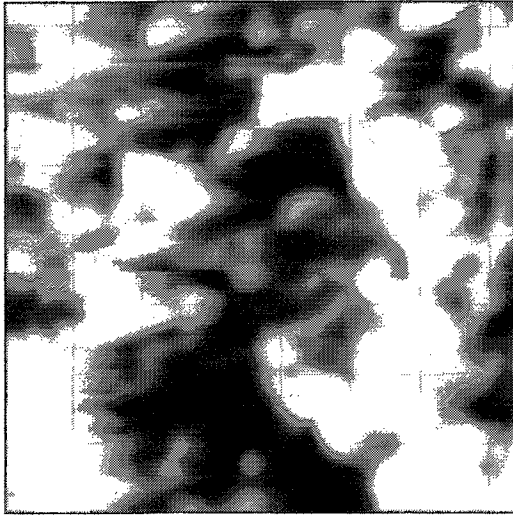
Figure 5.12   10 μm scan for roughness calculation on sample 1C
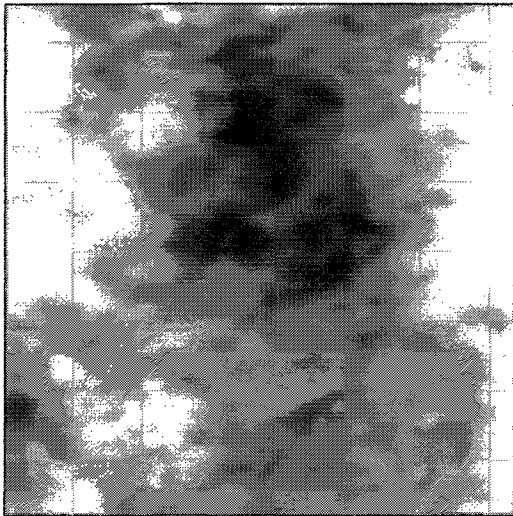
Figure 5.13   10 μm scan for roughness calculation on sample A60

132

5.6 Bibliography

1. Schroeder HE: Orale Strukturbiologie. Georg Thieme Verlag 1982; 2.unveraenderte Auflage: 87-92

2. Finke M, Hughes JA, Parker DM, Jandt KD. Mechanical properties of in situ demineralised human enamel measured by AFM nanoindentation. Surface Science 2001;491(3): 456-67

3. Fischer-Cripps AC. Nanoindentation. 2002 Springer Verlag: 20-135

4. Lippert F, Jandt KD, Parker DM. Nanomechanical Properties of Deciduous and Permanent Enamel Investigated Using AFM Nanoindentation . IADR Goteborg 2003; 0514 (Website:iadr.confex.com/iadr/2003Goteborg/techprogram/abstract_29008.htm)

5. Cuy JL, Mann AB, Livi KJ, Teaford MF, Weihs TP: Nanoindentation mapping of the mechanical properties of human molar tooth enamel. Arch Oral Biol. 2002 Apr;47(4):281-91

133

Chapter Six

Discussion

And

Recommendations

6.1 Focus of the project

The focus of the project was to evaluate the bond strength characteristics of AL curing compared to CCL. The secondary objective was to gain information regarding AL related changes in the enamel surface microstructure and properties. Gaining more information on how and why AL irradiation changes the enamel surface and confers protection against demineralization is necessary for this technology to be adopted into clinical practice. The well-organized and efficient office will resist an extra step in the bonding process. Therefore it is important to determine if the AL could be used to replace the CCL, rather than just creating another step for demineralization prevention, provided that AL irradiation is beneficial in increasing the acid resistance of the enamel surface.

The curing time of 60 seconds, instead of the clinical curing time of 10 seconds, was used, in the three chapters examining surface characteristics after AL irradiation, to increase the apparant changes, since the current literature does not reflect what kind and to what extent changes are to be expected. Once it is known on what kind of findings to focus on, ten seconds can be utilized after specifying the instrument settings and utilizing the full potential of the highly sensitive surface science instrumentation.

6.2 How will it affect the profession?

As dental technology continues to evolve, new methods for performing certain dental procedures will continue to replace those once considered the pinnacle. The AL may be one such example. Its use in polymerizing composite resins incorporates an equal degree of polymerization as is obtained with CCL units. It might even be initially enhanced in the first days after bonding,[1] which would be reflected in the resultant

135

improvement in physical properties and bond strengths. Although this enhancement may be temporary,[1] it may nonetheless have important clinical implications in preventing early bond failures.

The reduction in polymerization times provided by the AL and other high speed curing devices (XPAC, LED) is beneficial in reducing chair-side time and achieving patient satisfaction, especially with restless children. It could also be helpful in situations where maintenance of a dry field for any length of time is difficult. The laser beam offers the advantage of no loss of power over distance, as is suffered by the CCL unit.[2] The distance of the handpiece up to 6 mm does not affect the tensile bond strength.[3] The laser's narrow fiber optic tip and easy-to-handle handpiece may facilitate access to critical hard to reach areas (second molars).

Although the size, weight and portability of newer AL curing units have improved greatly at approximately 20 pounds, the unit is still fairly cumbersome and occupies considerably more space than a CCL unit. The laser can generate a substantial amount of heat, the cooling fans tend to be noisy, and there is a 30-second time lag between turning the unit on and actual light emission. These drawbacks can in part be overcome with current units that can be installed centrally, with curing wands radiating into individual operatories.[2] The additional cost for fiber optic lines would be far less than the purchase of multiple argon laser units. The central location would be an important factor since the fiber optic cables should not grossly exceed 6 m to prevent significant loss of intensity.

Because the AL technology is still new in the dental office, cost remains a deterrent to its acquisition. Depending on the manufacturer, portable ALs range from $ US 12,000 to $US 20,000, and central installation may incur additional expenses. Added

to the cost consideration, is the fear of becoming obsolete in an arena of rapid technological change.[2] Although the price has dropped to about $US 6000 in recent years, it is still a substantial investment if multiple curing units are required.

In summary, if AL irradiation could substitute the curing process with the CCL in an effective and efficient way and significantly reduce the risk of decalcifications during orthodontic treatment substantially, the additional expenditure could be justified.

The present findings support that the AL cures orthodontic brackets as effective as the CCL in one-fourth the curing time. The present study demonstrates occurrence of minor changes in the chemical composition, and obvious changes in the roughness and the hardness (load used: 8000 μm) of the enamel surface. The altered surface might be less prone to acid attack but a specifically designed study would have to examine this aspect.

Extensive further research has to be conducted to give further insight into the potential benefits of the AL, since it might help to eliminate the unsightly presence of white spot lesions which compromise an orthodontic end result causing dissatisfaction to both the orthodontist and the patient. A "demineralization-free" orthodontic practice would certainly act as a good marketing tool.

6.3 Summarized conclusions

The exact mechanism of increased acid resistance in lased enamel has not been fully clarified. It is difficult to compare the numerous reports of laser irradiation effects on human dental enamel because of the variety of lasers used, their differing energy densities, laser wavelengths, and variation in exposure time. Several theories are

137

presented including the creation of a microsieve network[4], which suggests that an alteration in the enamel pore structure takes place, which entraps and reprecipitates the mineral phases released during demineralization. [5] [6] In other words, the retention of minerals in these pores prevents them from being released from the enamel surface into the surrounding solution thus inhibiting the demineralization process. The fine microporosities with the confluent globular surface coating, found in the *Westerman et al.*[6] SEM study, may provide a reservoir for mineral phases during a cariogenic attack. In general terms, if the surface layer has an increased fluoride content in comparison with the underlying enamel, demineralization may be lessened, and remineralization of the enamel surface by mineral phases acquired from the surface coatings, oral fluids and other exogenous sources may be facilitated.[6] The findings of the present study could support the microsieve theory, but no content of fluoride was detected in the XPS scan. Possible reasons could consist in the fact that quantities below 1 % might not be detected and that the fluoride could be located below the XPS scanned enamel layer.

The decreased surface roughness could originate from the heat produced by the laser irradiation on the enamel surface which could produce local melting of the superficial (2-5 μm) enamel layer and seal the micropores[7] and their content without changing the chemical composition. The enamel surface would therefore be less permeable for diffusion of ions into and out of enamel during demineralization. [8] [9]

The decrease in roughness caused by AL irradiation (60s) observed in the SPM images could raise concern about reduction in bond strength. The present bond strength study demonstrated no alteration in bond strength after argon laser curing (10s). Another study conducted by *Talbot et al.*[10] evaluated the effect of AL irradiation (10s) at three

138

unique time points (before, during, and after bracket placement). No affect on bond strength was found regardless of the time point of application.

The increase in hardness after AL irradiation could be demonstrated with the comparison to a snow layer that superficially melts and turns into a harder, smoother and less porous ice crust. Altering the enamel surface morphology without changing the ability to effective cure the orthodontic bracket in shorter time compared to the CCL could be a promising future approach to work efficient and preventive.

6.4 Major conclusions

The preliminary surface scan results from the present study show that AL irradiation seems to produce minimal chemical change, a significant increase in hardness (load used: 8000 μm) and decrease in roughness. The bond strength testing part of the study demonstrated *in vivo* and *in vitro,* that potential alterations on the enamel surface due to AL irradiation are not affecting bond strength.

In conclusion, the use of low energy density AL irradiation (2.5 - 15 J/cm^2) could be a valuable tool to cure orthodontic resin efficiently, and to possibly transform the superficial enamel into a more demineralization resistant tooth surface.

6.5 Limitations associated with the project

The two week *in vivo* clinical trial does not represent a valid representation of the complete length of an orthodontic treatment. However, it does give an idea of the difference between the *in vivo* results and *in vitro* results, and questions the validity of the innumerable *in vitro* results used to assess curing materials and sources. The thermal

139

cycling process was included in an effort to imitate the thermal changes in the oral cavity, but this study did not take into account that oral fluid composition may have a major impact on the bond strength. Study participants will have varied oral flora, and dietary and oral hygiene habits making it impossible to get a consistent comparison between *in vivo* groups. Behavioral differences will also have an impact on the amount of load experienced on an orthodontic bracket and this will vary according to selection and processing of food. Patient compliance is another frequently unavoidable factor in *in vivo* studies. Participants may not follow oral hygiene and diet instructions thus altering the study outcome.

The enamel surface scans in this study were used as a utensil to screen the enamel surface for changes caused by the AL irradiations. Final conclusions cannot be drawn from the small sample size used, but it does provide a general idea on which level the enamel alteration might take place.

6.6 Suggestions for future studies

A split-mouth *in vivo* clinical trial conducted over the complete length of the orthodontic treatment, with a well selected and large enough sample size would be the next step in studying the potential benefits of AL use in orthodontics.

Further research into changes caused by the AL at the molecular level would require a representative number of samples. It would be useful to use the same exposure time (10s) for bonding studies and surface characteristics studies. The surface characteristics of the enamel areas under the brackets and around the brackets of extracted teeth should be examined, that were previously cured with the AL and remained

140

in the mouth for a sufficient amount of time to determine a potential effect on demineralization prevention. Another approach would be a simulated decalcification study in acid baths that could determine *in vitro* effects of AL. The simulated decalcification sites could be evaluated using SPM (AFM) to underline the potential smoothing effect and NI to evaluate the hardness difference, which might be more affected by the amount of acid attack than AL effect. XPS could demonstrate the changes at the chemical level caused by the acid attack with or without AL irradiation. Since only the NI is a destructive procedure, the same teeth could be evaluated by all three surface science methods. Furthermore it would be interesting to examine the irradiation time requires to reduce the roughness on the enamel surface and to determine their relationship.

The present study can be seen as an initial step for further research to answer the questions of how AL irradiation alters the human enamel surface, conferring some protection against demineralization.

6.7 Bibliography

1. Blankenau RJ, Powell GL, Kelsey WP, Barkmeier WW: Post polymerization strength values of an argon laser cured resin. Lasers Surg Med 1991; 11:471-4

2. Fleming MG, Maillet WA: Photopolymerization of Composite Resin Using the Argon Laser. J Can Dent Assoc 1999; 65:447-50

3. Lloret PR, Rode K, Turbino ML, Eduardo CP: Comparison of the tensile bond strengths of composite resin cured with an Argon Laser using two different distances of the handpiece. LELO- Experimental Laboratory of Lasers in Dentistry, University of São Paulo- School of Dentistry 1999; FAPESP- Projeto N ° 99/08433-4 (website)

4. Monseau Anderson A, Kao E, Gladwin M, Benli O, Ngan P: The effect of argon laser irradiation on enamel decalcification: An in vivo study. Am J Orthod Dentofacial Orthop 2002 Sept.; 122:251-9

5. Hicks MJ, Flaitz CM, Westerman GH, Blankenau RJ, Powell GL, Berg JH: Caries-like lesion initiation and progression around laser-cured sealants. Am J Dent. 1993 Aug;6(4):176-80 and ASDC J Dent Child. 1993 May-Jun;60(3):201-6.

6. Westerman GH, Hicks MJ, Flaitz CM, Powell GL, Blankenau RJ.: Surface morphology of sound enamel after argon laser irradiation: an in vitro scanning electron microscopic study. J Clin Pediatr Dent. 1996 Fall; 21(1):55-9

7. Chew A, Sykes DE, Waddilove AE: Surface Characteristics of Laser Modified Human Tooth Enamel Using Laser Microprobe Mass Spectrometry and Scanning Electron Microscopy. J Anal Atomic Spec 1997; 12 (10): 1101-3

8. Lenz P, Glide H, Walz R: Studies on enamel sealing with CO_2 laser. Dt zahnaerztl Z 1982; 37:469-78

9. Sato K: Relation between acid dissolution and histological alteration of heated tooth enamel. Caries Res 1983; 17: 490-95

10. Talbot TQ, Blankenau RJ, Zobitz ME, Weaver AL, Lohse CM, Rebellato J. Effect of argon laser irradiation on shear bond strength of orthodontic brackets: an in vitro study. Am J Orthod Dentofacial Orthop. 2000 Sep;118(3):274-9

Appendix A

UNIVERSITY OF ALBERTA HEALTH SCIENCES FACULTIES,
CAPITAL HEALTH AUTHORITY AND CARITAS HEALTH GROUP

HEALTH RESEARCH ETHICS APPROVAL

Date:	December 2002

Name of Applicant:	Nadja Hildebrand
Organization:	University of Alberta
Department:	Dentistry

Project Title:	**Argon Laser versus Conventional Visible Light cured Orthodontic Bracket Bonding: in vivo study.**

The Health Research Ethics Board (HREB) has reviewed the protocol for this project and found it to be acceptable within the limitations of human experimentation. The HREB has also reviewed and approved the subject information letter and consent form.

The approval for the study as presented is valid for one year. It may be extended following completion of the yearly report form. Any proposed changes to the study must be submitted to the Health Research Ethics Board for approval. Written notification must be sent to the HREB when the project is complete or terminated.

for _(signature)_

Dr. Sharon Warren
Chair of the Health Research Ethics Board (B: Health Research)

File number: B-031102-DENT

University of Alberta   Capital Health   CARITAS HEALTH GROUP
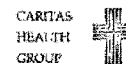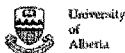
PARENTAL INFORMATION FORM

RISKS AND DISCOMFORT

Other than routine risks and discomforts associated with orthodontic treatment and extractions, which have been explained to me, there are no known or expected additional risks from participating in this study. Soft tissue burn from the laser is possible but very unlikely. The risk can be minimized by careful handling of the laser instrument. Patients will have one or two additional appointment(s) aside from their normal orthodontic visit, depending if the extractions will be performed at the University of Alberta or in private practice. The appointment will include the placement and removal of the brackets on the four teeth which will be extracted soon after. Placement of these brackets will not affect my orthodontic treatment. Participation in this study will not affect my orthodontic treatment plan.

FINANCIAL CONSIDERATIONS

Other than the normal and customary fee for orthodontic treatment and extractions, there is no additional cost associated with participation in this study.

VOLUNTARY COMPENSATION

If I am injured as a result of this research, treatment will be available. Compensation for the injuries will not voluntarily be provided by the investigator, sponsor, University of Alberta, or other associated affiliates.

ALTERNATIVES

Nonparticipation in this study will not affect my orthodontic treatment.

CONTACT PERSON

For more information about this research, I can contact Dr. Nadja Hildebrand or Dr. Paul Major at 780 492 4469. For more information regarding my rights as a research subject, I may contact the Administative Assistant Karen Turpin of the Panel B – Health Research at 780 492 0839.

----------------------------   ----------------

Initial of Participant   Date

----------------------------   ----------------

Initial of Guardian   Date

145

CONFIDENTIALITY

I understand that all information obtained as a result of my participation in this research will be held confidential (or private), except when professional codes of ethics or legislation (or the law) requires reporting. The information you provide will be kept for at least five years after the study is done. The information will be kept in a secure area (i.e. locked filing cabinet)). Your name or any other identifying information will not be attached to the information you gave. Your name will also never be used in any presentations or publications of the study results.

The information gathered for this study may be looked at again in the future to help us answer other study questions. If so, the ethics board will first review the study to ensure the information is used ethically.

VOLUNTARY PARTICIPATION

Participation in this study is voluntary. I understand that I may withdraw from the study at any time. Early withdrawal from this study will result in forfeiture of the moneys offered for participation, but will involve no penalty or loss of benefits for me. I have been given the opportunity to ask questions about the research, and have received answers concerning areas I did not understand. Upon signing this form, I will receive a copy, I willingly consent to participation in this study.

---------------------------   ----------------
Signature of Participant   Date

---------------------------   ----------------
Signature of Guardian   Date

---------------------------   ----------------
Signature of Investigator   Date

Appendix C

PATIENT INFORMATION FORM

Argon Laser versus Conventional Visible Light cured Orthodontic Bracket Bonding: an in vivo study.

I, _____, have been asked to participate in this study. Nadja has explained the study to me. This study will be performed at the University of Alberta, Department of Orthodontics and will be conducted by Dr. Paul Major, Dr. Daron Stevens and Dr. Nadja Hildebrand.

What is the study for?

The purpose of this study is to find out if the glue between the braces and my teeth works as well or better if they use a different light machine to harden the glue.

Why did they choose me?

They are looking for patients between 13 and 16 years of age who are in the orthodontic program as a patient and who need to have four teeth taken out during their orthodontic treatment.

What is going to happen?

Four braces will be glued on four of my teeth, the ones which will be taken out by my dentist at a later point in time. One of the two bonded teeth in the upper and lower jaw will be hardened with the conventional light for 40 seconds and the other one with the new and faster light for 10 seconds. The new light is already in use in other orthodontic offices and is called an argon laser. Putting the braces on my teeth will be a boring but easy procedure. After two weeks, shortly before my teeth will be taken out by your dentist, the brackets will be taken off with special debonding pliers, I will feel some pressure on my teeth for a few seconds.

Why should I participate?

For participation in this study I will receive $50 reward after my teeth have been taken out by my dentist. If I should decide not to participate in the study before its completion, I will not receive any gift. I understand that the results of this study will not be a benefit to me, other than getting a preview of some of the future procedures during my orthodontic treatment, but it might help future patients to have shorter and more efficient bonding appointments.

----------------------------   ------------------
Patient   Date

147

Appendix D
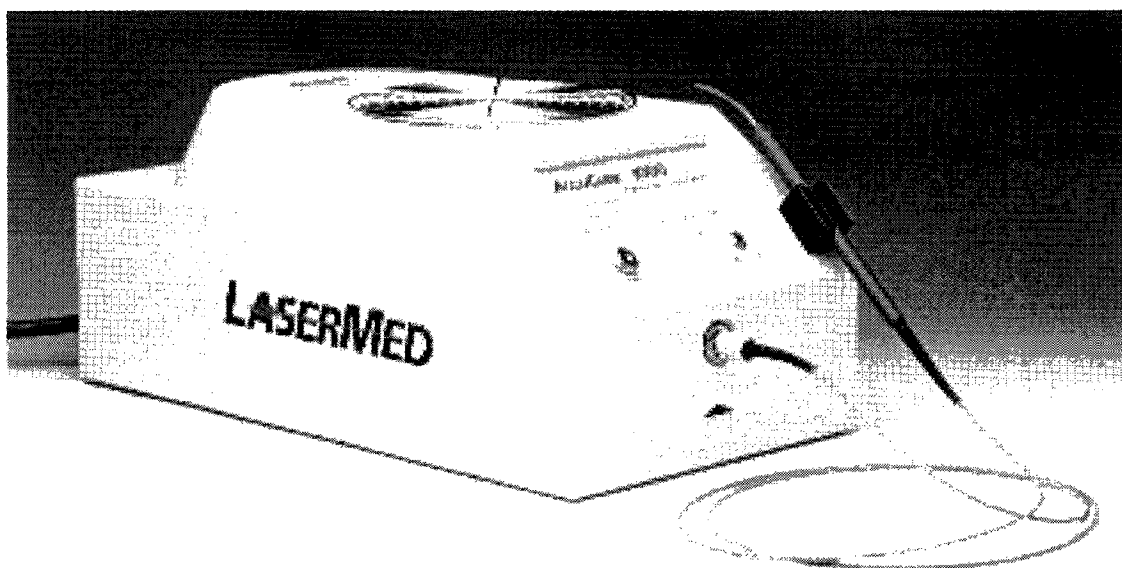
Figure 2.1   Argon Laser (AccuCure 1000, Salt Lake City, UT)

Technical Specifications:

Laser Type:	Argon Ion Air Cooled
Laser Tube Type:	Internal Mirror, Ceramic/Metal
Wavelength:	457nm – 502 nm
Delivery System:	Fused Silica Fiber Optic UltrLite ABS Plastic Handpiece
Power Control Selectable:	150 mW – 250mW in 50mW increments
Laser Tube Average Life:	2000 Hours
Voltage:	120 VAC
Current:	20 amp
Unit Dimensions:	20.4 cm X 40.7 cm X 17.8 cm
Unit Weight:	8.2 kg

Registration Certificate

UNIVERSITY OF ALBERTA

for

Radiation Equipment

Equipment Type: Class 3b Laser

Manufacturer: Lasermed

Model: Accucure 1000

Serial Number: 151201

Facility Type: Research

Location: 1048 DenPhar

Applicant: Dr. Paul Major

Department: Dentistry

Certificate Number: L - 084

Date of Issue: 5 Feb 03

Expiry Date: 28 Feb 05

Chairman, Radiation Control Committee

Appendix F

Sample size calculation

1-Sample t Test

```
Testing mean = null (versus not = null)
Calculating power for mean = null + difference
Alpha = 0.05  Sigma = 0.8
```

Difference	Sample Size	Target Power	Actual Power
0.12	469	0.9000	0.9000
0.12	401	0.8500	0.8500
0.12	**351**	**0.8000**	**0.8003**
0.12	311	0.7500	0.7508
0.20	171	0.9000	0.9016
0.20	146	0.8500	0.8510
0.20	**128**	**0.8000**	**0.8015**
0.20	113	0.7500	0.7501
0.30	77	0.9000	0.9013
0.30	66	0.8500	0.8511
0.30	**58**	**0.8000**	0.8017
0.30	52	0.7500	0.7558
0.40	44	0.9000	0.9000
0.40	38	0.8500	0.8511
0.40	34	0.8000	0.8078
0.40	30	0.7500	0.7540
0.50	29	0.9000	0.9012
0.50	25	0.8500	0.8503
0.50	**23**	**0.8000**	0.8171
0.50	20	0.7500	0.7554

Pilot study

The following is the results of paired t-tests:
1. Argon-max and CCL-max
2. Argon-mand and CCL-mand

Paired Samples Statistics

		Mean	N	Std. Deviation	Std. Error Mean
Pair 1	ARGONMX	4.4316	19	1.05449	.24192
	CCLMX	4.3184	19	.80194	.18398
Pair 2	ARGONMN	4.1932	19	.84287	.19337
	CCLMN	4.2089	19	.72385	.16606

Paired Samples Correlations

		N	Correlation	Sig.
Pair 1	ARGONMX & CCLMX	19	.678	.001
Pair 2	ARGONMN & CCLMN	19	.522	.022

Paired Samples Test

		Paired Differences							
					95% Confidence Interval of the Difference				
		Mean	Std. Deviation	Std. Error Mean	Lower	Upper	t	df	Sig. (2-tailed)
Pair 1	ARGONMX - CCLM	.1132	.78046	.17905	-.2630	.4893	.632	18	.535
Pair 2	ARGONMN - CCLM	-.0158	.77308	.17736	-.3884	.3568	-.089	18	.930

151

Appendix G

Raw data

Initial measurement in vivo (V):

patient	BSVALmx	BSVCCLmx	BSVALmn	BSVCCLmn	gender	age	BSVtype
PW	3.81	4.13	3.19	3.51	F	16	vivo
AS	3.65	4.33	2.9	4.18	F	16	vivo
JA	4.25	3.87	3.99	3.92	F	13	vivo
VZ	2.94	2.4	3.13	2.84	M	16	vivo
SM	4.69	2.54	3.38	2.48	F	12	vivo
AK	3.12	3.08	3.23	3.25	M	13	vivo
JK	2.83	3.18	3.81	2.37	M	13	vivo
MP	3.69	3.88	2.99	4.07	F	12	vivo
RN	3.48	3.89	5.32	3.35	F	15	vivo
AW	3.11	2.41	1.97	2.93	F	13	vivo
AC	0	3.34	3.31	3.5	M	14	vivo
RS	2.06	2.09	3.56	1.84	F	12	vivo
DP	3.85	2.6	4.52	2.34	M	12	vivo
BJ	2.9	1.91	2.46	1.8	M	12	vivo
AY	3.1	3.47	2.27	5.15	F	12	vivo
CF	3.12	1.51	4.25	2.73	F	12	vivo
MH	4.96	2.26	5.31	3.33	M	16	vivo
RA	3.29	4.69	3.48	6.23	M	16	vivo
JM	2.9	2.58	4.34	2.76	M	14	vivo
MC	5.32	5.12	1.31	4.01	M	12	vivo
SW	5.23	2.34	2.31	2	F	13	vivo
JP	2.11	2.55	2.74	4.36	M	13	vivo
NB	4.93	3.81	4.49	3.92	F	12	vivo

*second
premolar

0=technical
difficulties

152

Initial Measurements in vitro (V):

SM	2.41	2.46	2.36	2.64	F	14	vitro
WP	4.82	5.11	4.19	4.56	F	15	vitro
NK	2.11	3.02	2.84	3.26	M	15	vitro
SA	4.68	5.39	3.95	5.33	F	16	vitro
MM	5.35	4.61	3.63	5.26	M	13	vitro
AJ	5.27	4.81	5.22	4.97	F	13	vitro
KS	5.19	4.28	5.1	4.38	F	14	vitro
ZV	3.99	3.46	4.14	3.49	M	16	vitro
WB	5.32	4.52	3.46	4.16	M	15	vitro
MS	5.66	4.43	4.93	4.44	F	12	vitro
LS	3.62	5.36	3.99	4.38	F	32	vitro
KA	4.18	4.04	4.21	4.26	M	13	vitro
RG	2.91	3.85	3.31	3.95	F	17	vitro
KJ	3.89	4.14	4.88	3.37	M	13	vitro
CH	4.31	3.98	3.62	3.44	F	15	vitro
SH	4.67	3.56	4.96	3.96	F	14	vitro
PP	5.55	5.01	5.39	5.07	F	39	vitro
GH	5.32	4.96	4.68	4.47	F	13	vitro
PM	4.95	5.06	4.81	4.58	F	14	vitro
KS	6.09	4.78	4.99	5.47	F	11	vitro
TM	2.99	4.08	3.33	3.94	F	17	vitro
KK	4.59	4.11	3.98	3.25	M	19	vitro
SH	4.91	3.28	3.88	3.93	F	15	vitro
NS	3.74	3.99	4.67	4.33	F	11	vitro
KB	4.11	2.97	4.06	3.57	M	21	vitro

*second
premolar

153

Converted into MPa (in vivo):

patient	BSMALmx	BSMCCLmx	BSMALmn	BSMCCLmn	gender	age	BSMtype
PW	10.97	11.89	9.18	10.11	F	16	vivo
AS	10.51	12.46	8.35	12.04	F	16	vivo
JA	12.24	11.14	11.49	11.29	F	13	vivo
VZ	8.46	6.91	9.01	8.17	M	16	vivo
SM	13.51	7.31	9.73	7.18	F	12	vivo
AK	8.97	8.87	9.3	9.36	M	13	vivo
JK	8.23	9.15	10.97	6.82	M	13	vivo
MP	10.62	10.63	8.61	11.72	F	12	vivo
RN	10.92	11.2	15.32	9.64	F	15	vivo
AW	8.95	6.93	5.67	8.43	F	13	vivo
AC	0	9.62	9.53	10.08	M	14	vivo
RS	5.93	6.01	10.25	5.29	F	12	vivo
DP	11.09	7.48	13.02	6.73	M	12	vivo
BJ	8.35	5.49	7.09	5.18	M	12	vivo
AY	8.92	9.99	6.53	14.83	F	12	vivo
CF	8.98	4.34	12.24	7.86	F	12	vivo
MH	14.29	6.51	15.29	9.59	M	16	vivo
RA	9.47	13.51	10.02	17.95	M	16	vivo
JM	8.35	7.42	12.5	7.94	M	14	vivo
MC	15.32	14.75	3.76	11.55	M	12	vivo
SW	15.06	6.73	6.65	5.75	F	13	vivo
JP	6.07	7.34	7.89	12.56	M	13	vivo
NB	14.2	10.97	12.93	11.29	F	12	vivo

*second
premolar

0=technical
difficulties;
no reading

154

Converted into MPa (in vitro):

SM	6.93	7.08	6.79	7.6	F	14	vitro
WP	13.88	14.72	12.07	13.13	F	15	vitro
NK	6.07	8.69	8.17	9.39	M	15	vitro
SA	13.48	15.53	11.37	15.35	F	16	vitro
MM	15.41	13.28	10.45	15.15	M	13	vitro
AJ	15.18	13.85	15.04	14.31	F	13	vitro
KS	14.95	12.33	14.69	12.61	F	14	vitro
ZV	11.49	9.96	11.92	10.05	M	16	vitro
WB	15.32	13.02	9.96	11.98	M	15	vitro
MS	16.3	12.76	14.2	12.79	F	12	vitro
LS	10.42	15.44	11.49	12.61	F	32	vitro
KA	12.04	11.63	12.12	12.27	M	13	vitro
RG	8.38	11.06	9.53	11.37	F	17	vitro
KJ	3.89	11.2	14.06	9.7	M	13	vitro
CH	12.41	11.46	10.42	9.9	F	15	vitro
SH	13.45	10.25	14.29	11.4	F	14	vitro
PP	15.99	14.43	15.53	14.6	F	39	vitro
GH	15.32	14.29	13.48	12.87	F	13	vitro
PM	14.26	14.57	13.85	13.19	F	14	vitro
KS	17.54	13.77	14.37	15.76	F	11	vitro
TM	8.61	11.75	9.59	11.35	F	17	vitro
KK	13.22	11.84	11.46	9.36	M	19	vitro
SH	14.14	9.44	11.17	11.32	F	15	vitro
NS	10.77	11.49	13.45	12.47	F	11	vitro
KB	11.84	8.55	11.69	10.28	M	21	vitro

*second
premolar

155

ARI results (in vivo):

Subject	ALmx	CCLmx	ALmn	CCLmn	Study Type
PW	2	0	1	1	vivo
AS	2	2	0	1	vivo
JA	1	1	2	1	vivo
VZ	2	1	2	1	vivo
SM	1	2	2	2	vivo
AK	2	1	2	1	vivo
JK	1	1	1	1	vivo
MP	1	0	1	2	vivo
RN	1	2	2	3	vivo
AW	3	1	1	1	vivo
AC	1	1	1	0	vivo
RS	1	1	1	1	vivo
DP	1	2	2	1	vivo
BJ	1	1	1	1	vivo
AY	2	1	1	1	vivo
CF	1	0	2	2	vivo
MH	1	0	2	0	vivo
RA	2	1	2	1	vivo
JM	2	1	2	2	vivo
MC	1	1	1	1	vivo
SW	0	1	0	1	vivo
JP	0	1	1	2	vivo
NB	1	2	1	1	vivo

156

ARI results (in vitro):

SM	1	1	2	3	vitro
WP	1	1	0	1	vitro
NK	1	1	2	3	vitro
SA	1	2	2	1	vitro
MM	1	1	1	1	vitro
AJ	2	1	2	1	vitro
KS	1	1	2	1	vitro
ZV	2	1	3	1	vitro
WB	2	2	1	1	vitro
MS	1	1	1	1	vitro
LS	2	0	1	1	vitro
KA	2	1	1	1	vitro
RG	1	0	1	0	vitro
KJ	2	1	2	1	vitro
CH	1	0	2	0	vitro
SH	2	1	2	1	vitro
PP	1	2	2	1	vitro
GH	2	1	0	1	vitro
PM	1	1	1	1	vitro
KS	2	1	2	2	vitro
TM	1	2	2	1	vitro
KK	1	0	2	1	vitro
SH	1	1	2	3	vitro
NS	2	1	1	1	vitro
KB	1	1	1	1	vitro

*enamel
fracture

157

Summary of results from the 8000μN indentation tests

	Indent #	Er(GPa)	H(GPa)	hc(nm)
Sample 1-C	1	93.246	3.909	262.184
	2	92.863	3.619	273.234
	3	104.473	4.137	254.304
	4	98.282	3.803	266.055
	5	106.955	4.631	239.293
	6	117.774	5.205	224.666
	7	93.267	3.478	279.115
	8	101.593	4.067	256.642
	9	102.605	3.782	266.862
	10	95.191	3.785	266.728
	11	104.272	4.398	246.081
	12	98.677	4.226	251.422
	13	115.315	4.422	245.318
	14	102.190	3.719	269.282
	15	108.119	4.123	254.782
	Average	102.32	4.09	257.06
	St. Dev.	7.59	0.45	14.30
Sample A-60	1	88.184	4.445	244.661
	2	101.470	4.841	233.668
	3	94.172	4.321	248.435
	4	91.279	4.544	241.795
	5	96.236	4.749	236.122
	6	98.224	4.881	232.611
	7	92.562	4.294	249.293
	8	92.785	4.187	252.680
	9	95.944	4.454	244.403
	10	102.376	5.139	226.224
	11	106.037	5.263	223.319
	12	101.794	5.170	225.497
	13	101.987	5.258	223.426
	14	101.799	5.285	222.835
	15	100.496	5.060	228.135

158

Sample	Indentation Number	Contact Depth hc(nm)	Reduced Modulus Er(GPa)	Hardness H(GPa)
Sample 1-C	1	1571	101.6	3.97
	2	1505	105.4	4.33
	3	1587	98.2	3.89
	4	1616	93.5	3.75
	5	1588	96.7	3.88
	6	1463	100.2	4.58
	7	1624	95.9	3.72
	8	1392	108.5	5.05
	9	1466	103.8	4.56
	10	1565	103.3	4.00
	Average	1538	100.7	4.17
	St Dev	77	4.7	0.44
Sample A-60	1	1594	94.1	3.86
	2	1467	100.5	4.55
	3	1544	100.6	4.11
	4	1555	97.5	4.05
	5	1574	96.9	3.95
	6	1489	101.4	4.41
	7	1464	105.9	4.57
	8	1618	89.7	3.74
	9	1482	100.3	4.46
	10	1557	95.9	4.04
	Average	1534	98.3	4.17
	St Dev	55	4.5	0.30

159

CURRICULUM VITAE

Personal Data:

Name:	Nadja Katherina Susanne Hildebrand (maiden name: Luedtke)
Date of Birth:	Oct. 13, 1971
Address:	328 B Michener Park, Edmonton, Alberta T6H 4N1
Tel:	(780) 989 - 2861
E-mail:	nadja@ualberta.ca

Education:

1977 – 1981	Primary school (1. – 4. grade):	Cretzmar – Schule, Sulzbach, Germany
1981 – 1988	High school (5. – 10. grade):	Leibniz-Gymnasium, Frankfurt, Germany
1988 – 1991	High school (11. – 13. grade):	Eichwald-Gymnasium, Schwalbach, Germany

Aug. 1991 – Dec. 1998	Assisting in Dr. Douglas Toll's orthodontic office, Bad Soden, Germany & professional training as a Dental Assistant specialized in Orthodontics (compl. in Jan. 1994)
April 1993 – June 1999	Dental school, University of Frankfurt, Germany (Johann Wolfgang Goethe Universität) June 1999: Registered dentist in Germany
June 1997 – Oct. 2000	Completition of my doctoral thesis with Prof. Dr. Heidemann, Frankfurt, Germany ("Properties of highly-filled composite as a fissure sealant material")
Jan. 1999 – Dec. 1999	NDEB, Canada Jan. 2000: Registered dentist in Canada March 2000: Licensed dentist in Canada
Jan. 2000 – May 2001	Assisting in Dr. Alan A. Lowe's orthodontic office, Vancouver (part-time)
June 2000 – May 2001	Integrated Dental Practitioner Program, UBC, Vancouver
Since Aug. 2001	Graduate Orthodontic Resident, U of A, Edmonton

Sport activities:	Kite surfing, tennis, snowboarding, swimming, hiking, and biking

160